1-1-2005

The Silver Spring and Blackrock faults, east-central Nevada: Kinematics, timing, and role of low-angle normal faulting in the development of Railroad Valley

Tyler R Knudsen
University of Nevada, Las Vegas

THE SILVER SPRING AND BLACKROCK FAULTS, EAST-CENTRAL NEVADA: KINEMATICS, TIMING, AND ROLE OF LOW-ANGLE NORMAL FAULTING IN THE DEVELOPMENT OF RAILROAD VALLEY

by

Tyler R. Knudsen

Bachelor of Science
University of Utah
2002

A thesis submitted in partial fulfillment
of the requirements for the

Master of Science Degree in Geoscience
Department of Geoscience
College of Sciences

Graduate College
University of Nevada, Las Vegas
May 2005

UNLV
UNIVERSITY OF NEVADA LAS VEGAS

Thesis Approval

The Graduate College
University of Nevada, Las Vegas

April 20, 2005

The Thesis prepared by

Tyler R. Knudsen

Entitled

The Silver Spring and Blackrock faults, east-central Nevada:
Kinematics, timing, and role of low-angle normal faulting in
the development of Railroad Valley

is approved in partial fulfillment of the requirements for the degree of

Master of Science in Geoscience

Wanda J. Taylor
Examination Committee Chair

Dean of the Graduate College

Examination Committee Member

Examination Committee Member

Graduate College Faculty Representative

1017-53

ABSTRACT

The Silver Spring and Blackrock Faults, East-Central Nevada: Kinematics, Timing, and Role of Low-Angle Normal Faulting in the Development of Railroad Valley

By

Tyler R. Knudsen

Dr. Wanda J. Taylor, Examination Committee Chair
Professor of Geoscience
University of Nevada, Las Vegas

The structural development of Railroad Valley, a large and economically important Tertiary basin in east-central Nevada, has been the focus of much debate. This study addresses many of the points of controversy through a detailed geologic study of structures in the southwestern White Pine Range.

Detailed geologic mapping and construction of cross-sections reveal both low- and high-angle normal faults. The low-angle faults consist of three bedding-parallel faults, two top-to-the-southwest and one top-to-the-south, and two large displacement (>8 km heave) (26,000 ft) top-to-the-west detachments that denude a range-scale Mesozoic fold. Two spatially distinct groups of high-angle normal faults are present: (1) mostly synchronous faults in the hanging wall of the large-displacement detachments that developed in 3-D strain above non-planar footwalls and (2) faults within the footwalls of the large-displacement detachments that indicate a counterclockwise rotation in extension direction from east-west to northwest-southeast though time.

A structural model is proposed for the southwestern White Pine Range where extension and uplift of the range begins in the Oligocene along low-angle faults, and in the Late Miocene, shifts to high-angle normal faulting. A regional comparison of geometries, kinematics, and timing of major detachment faults suggests that Railroad Valley developed as a result of several distinct structural systems, some of which are separated by transverse faults.

TABLE OF CONTENTS

LIST OF FIGURES

LIST OF PLATES

ACKNOWLEDGEMENTS

Financial support for this thesis was provided by: the American Association of Petroleum Geologists Grants-in-Aid, grants from the University of Nevada Las Vegas Geoscience Department and Graduate Student Association, a Nevada Earthquake Safety Council grant to Dr. Wanda Taylor, and a DOE appropriation for the study of earthquakes in southern Nevada to Drs. Barbara Luke, Wanda Taylor, Catherine Snelson, and Ron Sack.

I am most grateful to my advisor, Dr. Wanda J. Taylor, for introducing me to the geology of the southern White Pine Range and for her guidance, support and endless patience. I thank my committee members, Dr. Andrew Hanson, Dr. Michael Wells, and Dr. Kathleen Robins for their critical reviews and input. Thanks are due to the faculty, staff, and graduate students of the Geoscience Department for their encouragement and support.

Without the love and support of my family, this thesis would not have been possible. A special thanks goes to my wife for her constant motivation, patience, accompanying me on many excursions, and her genuine enthusiasm for all of my interests. Finally, I am especially grateful for my newborn daughter and her smiling face. I never imagined how fun and entertaining a little baby could be.

CHAPTER 1

INTRODUCTION

The Cenozoic tectonic evolution of the northern Basin and Range province involves several distinctive types of structures including low-angle normal faults or detachments, high-angle normal faults, and transverse faults. The specific role that each of these structures played in shaping basins and the present topography remains controversial even though our understanding of the tectonic development of the province has increased greatly in the last few decades. This study focuses on establishing the structural evolution of the southern White Pine Range, one of several ranges bordering Railroad Valley, Nevada, through geometric, kinematic, and temporal analysis of extensional structures. Results of this analysis are compared to structural styles observed in nearby ranges to explore the possibility that a single mode of extension can be applied along the entire margin of Railroad Valley. This comparison reveals that Railroad Valley developed along several discrete detachment faults operating within separate structural domains.

The White Pine, Horse, and Grant ranges compose the eastern margin of Railroad Valley, a tectonically active continental basin located in east-central Nevada (Fig. 1). The 100 km long Railroad Valley is one of the widest and deepest Tertiary extensional basins in Nevada (Kleinhampl and Ziony, 1985) and contains the most prolific oil fields in the Great Basin. Due to its economic importance, a large number of studies incorporating

geologic mapping and drill-hole and seismic data, focused on the structural evolution of the basin (e.g., Lumsden, 1964; Moores et al., 1968; Effimoff and Pinezich, 1981; Fryxell, 1984; Bartley and Gleason, 1990; Lund et al., 1991; Camilleri, 1992; Grow et al., 1992; Walker et al., 1992; Liberty et al., 1994; McCutcheon and Zogg, 1994; Peterson, 1994; Langrock, 1995; Francis and Walker, 2001). These studies, typically focusing on a relatively small portion of one of the basin-bounding ranges, identified several major Tertiary detachment faults that dissect Mesozoic contractile structures. Most workers agree that low-angle normal faulting contributed to the delineation of the basin and adjacent ranges. However, many significant questions remain. (1) What is the timing of initiation of extension? (2) What is the relative contribution of high-angle normal faults versus low-angle normal faults in basin formation? (3) Can a single structural model be used along the entire length of Railroad Valley to explain its formation?

The tectonic history of east-central Nevada is complex. In the Mesozoic, miogeoclinal strata in the area were deformed in the central Nevada thrust belt (Bartley et al., 1993; Taylor et al., 1993; Taylor et al., 2000). Deformation includes mostly east-vergent thrusts with steeply dipping ramps and broad, open folds (Taylor et al., 1993; Taylor et al., 2000). In the Tertiary, these contractile structures were disrupted and deformed by several episodes of extension that varied in time, style, and direction (e.g., Bartley, 1989; Taylor et al., 1989; Taylor and Switzer, 2001). This deformation includes periods of both high- and low-angle normal faulting. Extension on some of the low-angle normal faults, or detachments, created broad range-scale extensional isostatic folds (Spencer, 1984; Buck, 1988; Wernicke and Axen, 1988; Camilleri, 1992; Lund et al., 1993) that could easily be misidentified as contractional folds (Janecke et al., 1998). The

successive overprinting of different structural styles in east-central Nevada makes it difficult to reconstruct the structural evolution of the region. Only by careful study of the relationships among these structures can the tectonic development be unraveled.

A casual comparison of the various proposed structural models reveals some similarities among structural styles documented throughout the eastern margin of Railroad Valley. Studies in the central Grant Range reveal a series of east-dipping detachments that are cut by a series of west-dipping detachments that are thought to be responsible for the modern delineation of the basin margin there (Fryxell, 1988). The northern Grant Range contains an imbricate stack of west-directed detachments that are arched about a north-trending axis (Camilleri, 1992; Lund et al., 1993). This domal structure has been attributed to isostatic footwall uplift caused by the removal of the detachment hanging-wall sheets (Camilleri, 1992). Uplift in the Horse and White Pine ranges has been largely attributed to movement on northwest- to west-dipping large-offset detachment faults, the Ragged Ridge and Blackrock faults, respectively (Lumsden, 1964; Langrock, 1995; Horton and Schmitt, 1998). Strata in the footwall of the Blackrock fault are arched about a north-trending axis similar to the arched system in the northern Grant Range (Lumsden, 1964; Moores et al., 1968; Langrock, 1995).

These similarities among documented structural styles are interpreted by some to indicate that a single structural model may be used to account for uplift and deformation along the majority of the eastern margin of the basin. For example, Francis and Walker (2001) proposed a model that attempts to correlate documented detachment faults throughout the White Pine, Horse, and Grant Ranges into a regional detachment that would be responsible for basin development from the southern Grant Range to the central

White Pine Range. A careful comparison of structural styles and kinematics documented throughout the eastern margin of Railroad Valley is critical to testing the hypothesis of a single structural model, but until now has not been done.

The goals of this study are to: (1) Unravel the structural evolution of the southwestern White Pine Range where several major structures, including a large-scale anticline and several detachment faults remain to be studied in detail. This is accomplished through a detailed geologic study including field mapping, construction of restorable cross-sections, and $^{40}Ar/^{39}Ar$ thermochronology. (2) Compare the structural style observed in the southern White Pine Range including geometric, kinematic, and temporal data with data from other structural studies along the eastern margin of Railroad Valley to determine if a single mode of extension can be applied along the entire length of the basin.

CHAPTER 2

STRATIGRAPHY

The southern White Pine Range exposes a thick sequence of Paleozoic miogeoclinal carbonate and detrital rocks (Fig. 2) unconformably overlain by Cenozoic volcanic and alluvial units (Fig. 3). Two small Tertiary plutons, in addition to numerous dikes and sills, also crop out within the study area. Mesozoic strata are not exposed in the White Pine Range, indicating either erosion or nondeposition. Detailed descriptions of mapped units are provided on Plate 1.

Paleozoic Stratigraphy

Paleozoic formation names and thicknesses of Lumsden (1964) and Lumsden et al. (2002) generally are used in this study. Some of the Cambrian units exhibit abrupt facies changes near the latitude of the White Pine and Horse Ranges (Lumsden, 1964; Rowell and Rees, 1981; Rees, 1986; Lumsden et al., 2002). Consequently, some differences in unit subdivisions were necessary. These variations are discussed below.

The Lower Cambrian Pole Canyon Limestone was originally described and divided into five members by Drewes and Palmer (1957) in the southern Snake Range, Nevada. In the White Pine Range, workers typically subdivided the unit into three members (Lumsden, 1964; Moores et al., 1968; Lumsden et al., 2002): a lower member of shale-

parted limestone, a medial member of thinly-bedded limestone, and an upper member of massive cliff-forming limestone. Detailed stratigraphic studies by Hood (1985) assigned the lower member to the Pioche Shale; designated the middle member as a new formation, the Currant Summit Limestone; and called the upper member alone the Pole Canyon Limestone. However, during fieldwork for this study, consistent differentiation of the lower and middle members was not possible. Thus, following Williams (2000), these two lower units were combined and referred to as the Lower Member of the Pole Canyon Limestone.

Along the southern margin of the White Pine Range, an 80 m (260 ft) thick massive limestone unit with large stromatoporoids crops out beneath the Cambrian Dunderberg Shale. This distinctive limestone has not been documented elsewhere and Lumsden (1964), who first recognized the unit, suggested that the ledge represents a local algal reef. The unit is tentatively designated as the Upper Lincoln Peak Formation due to its stratigraphic position beneath the Dunderberg Shale (Williams, 2000).

Lumsden (1964) describes an abrupt facies change between measured sections of the Dunderberg Shale in Plane Crash Canyon and in the Horse Range (Fig. 4). The yellow-weathering shale and limestone of the Lincoln Peak near Currant Gap strongly contrasts with the light blue-gray recrystallized limestone and phylitic shale of the Lincoln Peak near the stocks in the White Pine Range. This high variability in both the Dunderberg Shale and Lincoln Peak Formation in addition to low-grade metamorphism of the units near the intrusions make it difficult to confidently map the units separately. Therefore, following Lumsden (1964), Moores et al. (1968), and Lumsden et al. (2002) these units

were mapped as a single unit near the stocks as Undifferentiated Lincoln Peak/Dunderberg Shale.

Cenozoic Rocks

Oligocene volcanic rocks of the Garret Ranch Group are the oldest Cenozoic units exposed in the study area (Fig. 3). The source area for the Windous Butte and Shingle Pass tuffs of this Group is the Central Nevada Caldera Complex, a series of calderas located to the southwest (Best et al., 1993) (Fig. 5). The locations of source areas for the Currant Tuff and the White Pine Range Rhyolite are uncertain but are probably nearby because they are limited in areal extent (Lumsden, 1964; Langrock, 1995).

Overlying the volcanic rocks of the Garret Ranch Group are volcaniclastic, alluvial and lacustrine deposits of the Miocene Horse Camp Formation (Lumsden, 1964; Moores et al., 1968; Moores, 1968; Brown and Schmitt, 1991; Horton and Schmitt, 1996, 1998). This formation is exposed near Highway 6 in the southern part of the field area (Fig. 4; Plate 1). Horton and Schmitt (1998) suggest that the Horse Camp basin developed prior to the delineation of the White Pine, Horse, and Grant Ranges by the Railroad Valley fault. Motion along that fault uplifted and exhumed the basin's sediments.

Two biotite-bearing quartz monzonite stocks, the Railroad Valley and Silver Spring stocks, intrude Middle Cambrian carbonate and shale units in the western portion of the study area (Fig. 4; Plate 1). A small grossular garnet-bearing metamorphic contact aureole surrounds the stocks. Lumsden (1964) first described the stocks and suggested the likelihood that the smaller Silver Spring stock is an extension of the larger Railroad Valley stock. This hypothesis is supported by petrographic and compositional similarities

as well as zircon U/Pb dates. These dates of 33.8 $\pm$ 9.7 Ma and 35.1$\pm$ 5.7 Ma for the Railroad Valley and Silver Spring stocks, respectively, are within analytical uncertainty (Taylor et al., 1996). Within error of these zircon ages, K-feldspar argon data from this study yields a weighted mean age of 33.17 $\pm$ 0.18 Ma (1σ) (Appendix A), greatly improving the accuracy of the age determination of the stocks.

Several Tertiary and Quaternary consolidated and unconsolidated alluvial units unconformably overlie Paleozoic and Tertiary units. Four geomorphic surfaces of varying dissection and induration were identified. These surfaces occur at different elevations, which may indicate different episodes of relative uplift, and thus, extension.

CHAPTER 3

GEOLOGIC BACKGROUND

Paleozoic Passive Margin and Nearby Orogenesis

Throughout much of the Paleozoic, western North America was a passive margin that experienced the accumulation of thick, mostly carbonate strata with smaller amounts of detrital sediments. The thickness of Paleozoic strata in east-central Nevada is estimated to be about 7200 m (23600 ft) (e.g., Humphrey, 1960; Kellogg, 1963; Hose and Blake, 1976).

Three well-documented major tectonic events disrupted the passive margin during the Paleozoic. The late Devonian to Mississippian Antler Orogeny emplaced an upper plate of oceanic rocks, the Roberts Mountain allochthon, eastward onto the continental shelf (Fig. 5) (Roberts et al., 1958; Smith and Ketner, 1977; Speed and Sleep, 1982). Deformation from the Antler Orogeny did not reach as far east as the White Pine Range, although rocks of the Antler foredeep basin, the Mississippian Chainman Shale, Diamond Peak Formation, and the Joanna Limestone were deposited here (Miller et al., 1992; Giles and Dickinson, 1995).

Widespread east- and west-vergent thrust faults and folds that deform Antler foredeep deposits and portions of the Roberts Mountain allochthon are constrained to have developed in middle Mississippian to Permian time (Trexler et al., 2003). This

deformation centers west and southwest of Carlin, Nevada (Fig. 5) (Trexler et al., 2003) and is not known to deform rocks of the White Pine Range, but an angular unconformity of this age is exposed just to the west in the Pancake Range. Trexler et al. (2003) interpret the Mississippian to Permian event to be a late phase of the Antler orogeny or perhaps a separate orogenic event.

Oceanic strata were again emplaced over the continental margin in the late Permian to early Triassic during the Sonoman Orogeny (Fig. 5) (Speed, 1979; Miller et al., 1992). Deformation of this orogeny lies more than 100 km to the west of the White Pine Range, and unlike the Antler Orogeny, no conspicuous foredeep basin has been recognized (Speed and Sleep, 1982).

Mesozoic Contraction

In western Nevada, the Luning-Fencemaker belt most likely was active in the early to middle Jurassic (Oldow, 1984; Speed et al., 1988; Elison, 1991; Wyld et al., 2001, 2003). This orogeny resulted in the mostly east-vergent folding and thrusting of Mesozoic marine rocks (Oldow, 1984), and these effects lie well to the west of the White Pine Range.

Sometime between the Permian and Cretaceous, mostly east-vergent thrust faults and folds developed from near Eureka to Alamo, Nevada as part of the central Nevada thrust belt (Fig. 5) (Bartley et al., 1993; Taylor et al., 1993, 2000). The majority of central Nevada thrust belt deformation is interpreted to have occurred from the late Jurassic to Early Cretaceous (Taylor et al., 2000). This deformation was contemporaneous with, and within the hinterland of, the larger Mesozoic to early Tertiary Sevier fold-thrust belt that

extends from southern Idaho, through western Utah and into southern Nevada (Fig. 5) (Taylor et al., 1993). Evidence of the central Nevada thrust belt in the White Pine Range includes mostly broad, north-south-trending folds and minor thrusts (Langrock, 1995; this study).

Due to orogenesis and the resulting highlands throughout much of the Mesozoic era, sedimentary rocks of this age were either not deposited or were removed by erosion in the White Pine Range.

Tertiary Extension

Major extension of much of western North America began in the Eocene (Burchfiel et al., 1992; Sonder and Jones, 1999; Dickinson, 2002). Early extension in much of the Basin and Range is marked by the formation of metamorphic core complexes (Crittenden et al., 1980; Dickinson, 2002). These structures consist of a low-angle normal fault that separates an upper plate of brittlely deformed upper crustal rocks from a lower plate of ductilely deformed, variably metamorphosed mid- to lower crustal rocks (Coney, 1980; Davis, 1983; Lister and Davis, 1989). Many low-angle normal faults have been documented that occur completely within the brittle regime, lacking metamorphosed rocks in their footwalls. Examples are the Mormon Peak, Tule Springs and Castle Cliff detachments in southern Nevada (Axen et al., 1990; Axen, 1998), detachments in the Leppy Hills (Schneyer, 1984) and southern two-thirds of the Goshute-Toano Range (Ketner et al., 1998; Silberling and Nichols, 2002) in northwestern Nevada, and the Blackrock (Langrock, 1995) and Silver Spring (this study) faults in the White Pine Range. Several other low-angle normal faults, that mostly lack metamorphic lower plates,

have been mapped in ranges south of the White Pine Range (e.g., Fryxell, 1988; Camilleri, 1992). These faults have been interpreted to have played a critical role in the structural evolution of Railroad Valley and nearby ranges, although significant disagreement exists regarding integration of detachment faulting into the structural history of the area. An overview of these detachments and various models explaining the development of the detachments is provided in the next section.

Low-angle normal faults in the Great Basin typically are cut by younger normal faults, many of which are high-angle. High-angle normal faulting generally began in the Middle Miocene and continues to today (Burchfiel et al., 1992; Wernicke, 1992; Dickinson, 2002). This latter extension is considered to be mostly responsible for the present topography. The Railroad Valley fault, a major range-bounding normal fault along the eastern margin of Railroad Valley is considered the main contributor to the Quaternary uplift of the southern White Pine Range (Moores et al., 1968; Grabb, 1994).

To accommodate strain in three dimensions, extended terrains typically contain transverse faults, faults that strike perpendicular to the regional structural grain (Faulds and Varga, 1998). Several transverse faults that are parts of lineaments are identified in the Great Basin (Fig. 6) (Ekren et al., 1976; Rowley, 1998). These lineaments are delineated primarily by magnetic anomalies and the alignment of topographic features. Many segments of these lineaments contain transfer faults that are strike-slip or oblique-slip faults that strike subparallel to the extension direction and facilitate the transfer of strain from one extensional domain to another (Faulds and Varga, 1998). The east-west-striking Currant Summit fault has been interpreted to be an oblique-slip transfer fault (Fig. 7) with 3300 m (10,800 ft) of strike-slip offset, accommodating differential strain

between the highly extended White Pine Range and the less-extended Horse Range (Fig. 4) (Williams, 2000). The Currant Summit fault is the easternmost expression of the Prichards Station lineament that continues westward to the Paradise Range in west-central Nevada (Fig. 6) (Ekren et al., 1976).

Structural Model Review for Railroad Valley

Many geologists who have worked in and around Railroad Valley consider detachment faulting to play the major role in the uplift of ranges and subsequent down-dropping of Railroad Valley (e.g., Lund et al., 1993; Lisenbee and Kieffer Rowe, 1996; Francis and Walker, 2001; Francis and Walker, 2002a). The role of a major high-angle, west-dipping, range-bounding fault, the Railroad Valley fault, is unclear. Some workers include the Railroad Valley fault as an integral component in their structural models while others question its existence.

Structural models for the development of Railroad Valley are based mostly on studies covering a limited area of a range, documenting only a single fault or set of faults. The question arises: can a single structural model be applied for Railroad Valley along its eastern margin? Francis and Walker (2001; 2002a) recently presented a broader model that incorporates individual fault segments into a single fault that explains the entire structural development of the northern part of the valley. The following section summarizes the geometry, timing, kinematics, and proposed structural models for the major low-angle normal faults exposed along the eastern margin of Railroad Valley and their contributions to the development of the present topography.

White Pine Range

The Blackrock fault is exposed largely to the north of the map area (Fig. 8) (Lumsden, 1964; Walker et al., 1992; Langrock, 1995; Lisenbee and Kieffer Rowe, 1996). Near Blackrock Canyon, Langrock (1995) describes the Blackrock fault as non-planar, with both north- and east-striking segments, and a large corrugation. Here, the 15° to 30° west-dipping fault disrupts and denudes Mesozoic contractile folds and most likely a thrust fault at depth (Langrock, 1995). Using the geometry of the corrugation and the orientation of the intersection line between the east- and north-striking segments, among other lines of evidence, Langrock (1995) constrained the slip direction of the Blackrock fault to be west-northwest. Based on hanging-wall faults that cut 31.3 Ma volcanic rocks, the timing of movement on the Blackrock fault is considered to be Oligocene or younger (Langrock, 1995). Langrock suggests that the Blackrock fault developed with corrugations at a low angle with no significant amount of doming and <25° of later tilting.

Farther to the north and east, Lisenbee and Kieffer Rowe (1996) as well as Walker et al. (1992) show that the Blackrock fault has an anticlinal shape where the fault changes from a west dip to an east dip along a north-trending axis that approximately coincides with the ridge crest of the White Pine Range (Fig. 8). Consistent with Langrock's interpretations, Lisenbee and Kieffer Rowe (1996) suggest that movement on the Blackrock fault is generally top-to-the-west based on the geometry of west-dipping hanging-wall fault splays that sole into the main fault. Lisenbee and Kieffer Rowe (1996) conclude that in order to avoid a reverse sense of motion on the east-dipping segment of the Blackrock fault, that the fault must have been tilted eastward into its present

orientation. They favor a model where the Blackrock fault is the major structure responsible for the uplift of the White Pine Range, attaining its present geometry by footwall uplift and rotation as an isostatic response to the removal of the hanging wall.

Grant-Quinn Canyon Ranges

In the northwestern portion of the Grant Range near Beaty Canyon, a series of stacked low-angle normal faults that are arched about a north-south trending axis is documented (Fig. 8) (Camilleri, 1992; Lund et al., 1991; 1993). These faults cut older polyphase contractile structures (Lund et al., 1991; 1993). Based on fault-to-bedding angles and the geometry of fault splays that coalesce into a single fault zone on the west side of the range, the faults are interpreted to have top-to-the-west movement (Lund et al., 1991, Camilleri, 1992). Cross-cutting relationships show that each structurally higher fault is younger than the one below (Lund et al., 1991; Camilleri, 1992). Oligocene volcanic rocks share the same deformational history as the underlying Paleozoic and early Tertiary sections and $^{40}Ar/^{39}Ar$ ages from detachment-related metasomatic minerals constrain the age of detachment faulting in the northwestern Grant Range to between 31 and 20 Ma (Lund et al., 1991, 1993; Brooks and Snee, 1996).

Lund et al. (1991, 1993) and Camilleri (1992) conclude that synchronous detachment faulting and doming are the major mechanisms for extension in the northern Grant Range. Camilleri (1992) offers a kinematic model to explain the arched fan of faults that is based on the flexural rotation model by Buck (1988). Camilleri (1992) envisions the mode of extension in the northwestern Grant Range as follows: (1) formation of the earliest fault that dips west slightly steeper than the west-dipping stratigraphic section, (2) hanging wall removal causes eastward rotation of the upper portion of the fault into a

shallow geometry that no longer favors westward movement, (3) this induces the formation of a new fault at the same dip as the original fault, and (4) these steps are repeated resulting in domed structures and strata where each higher fault is younger than the one below it, bounded to the west by an active, higher-angle range-front fault. It is unclear, however, if this range-front fault dips at a high to moderate angle (Moores et al., 1968; Foster, 1979; Bortz, 1994) or if it remains at a gentle dip as it projects beneath Railroad Valley uncut by high-angle faults (Lund et al., 1991; 1993; Francis and Walker, 2001; 2002a).

To the south in the west-central Grant Range, Fryxell (1984; 1988) mapped a series of brittle low-angle normal faults (Fig. 8) that cut Mesozoic-age folds, thrust faults, metamorphic rocks, and granitic intrusions. Here, younger west-dipping detachment faults cut older east-dipping detachment faults (Fryxell, 1988). One of the earlier top-to-the-east faults, the Troy Peak fault, cuts a 27.8 Ma welded tuff, constraining the age of east-directed faulting to early late Oligocene or younger (Fryxell, 1988; Taylor et al., 1989). The Little Meadow fault, one of the later top-to-the-west faults, cuts a 14.2 Ma tuff indicating that the younger extensional period, at least in part, occurred in the middle Miocene or later (Fryxell, 1988).

This structural geometry differs from the relatively simple arched fan of detachments interpreted in the northern part of the range. Fryxell (1998) proposes that this difference in structural style between the northwestern and west-central Grant Range may be due to exposure of different structural levels. She explains that strata in much of the range are arched about an east-west-trending axis that passes through the central part of the range.

Therefore, structures that developed on the northern limb of the arch in the northwestern part of the range may have developed at shallower structural levels.

Fryxell et al. (1996) and Fryxell (1998) suggest that the younger west-directed group of faults is likely responsible for the modern topographic delineation of Railroad Valley and the central Grant Range. Similar to structural models proposed for the northern part of the Grant Range, they conclude that this later phase of extension represents a continuum of low-angle normal faulting that spans up to and includes the development of the Railroad Valley fault (Fryxell et al., 1996; Fryxell, 1998).

In the southern Grant and northern Quinn Canyon ranges, Bartley and Gleason (1990) documented the southern continuation of the Troy Peak and Little Meadow faults among other low-angle normal faults (Fig. 8). These faults consistently overprint Mesozoic contractile deformation. They show that here, the post-14 Ma Little Meadow fault has a slip direction of top-to-the-west-northwest. They also show that another major detachment, the Wadsworth Ranch fault (Fig. 8) had top-to-the-southwest movement and was active between ~32 and ~26 Ma. Based on cross-cutting relationships between these faults and related structures, Bartley and Gleason (1990) conclude that this region underwent an Oligocene southwest-directed extensional period followed by a Miocene period of northwest-directed extension.

Horse Camp Basin

The Horse Camp basin is an area of low relief bordered by the White Pine Range to the north, the Horse Range to the east and the Grant Range to the south (Fig. 8). The 3000 m (9800 ft) of sediment filling the basin includes conglomerate and sandstone with lesser amounts of mudstone, limestone, megabreccia, and tuff. These deposits are

interpreted to record an early extensional phase that is tectonically related to, but structurally distinct from Railroad Valley (Lumsden, 1964; Moores et al., 1968; Horton and Schmitt, 1998). The basin developed above a west-dipping detachment, the Ragged Ridge fault, and is bounded by two east-west-striking transverse structures: the Currant Summit fault to the north and the Ragged Ridge/Stone Cabin fault zone to the south (Fig. 8). Cross-cutting relationships with volcanic rocks as well as fossils within the basin sediments suggest that the Horse Camp basin developed mainly in the Miocene (Moores, 1968; Kleinhampl and Ziony, 1985; Horton and Schmitt, 1998). In the late Miocene, sedimentation into the basin ceased as the basin was exhumed as part of the footwall of the newly formed Railroad Valley fault (Fig. 8).

Similar to the model of Camilleri (1992) in the northwestern Grant Range, Horton and Schmitt (1998) invoke a flexural rotation model to explain the development of the Horse Camp basin and its subsequent exhumation by the Railroad Valley fault. They propose that the gently west-dipping Ragged Ridge fault is an abandoned segment of the present range-bounding Railroad Valley fault. In this model, the Ragged Ridge fault was uplifted and rotated by footwall isostatic rebound caused by the westward removal of the hanging wall of the Railroad Valley fault (Horton and Schmitt, 1998).

White Pine Detachment: A Regional Detachment System

Francis and Walker (2001) were the first to explore the possibility of a single structural model that ties all of these detachment systems together as the main contributor for the structural development of Railroad Valley. They suggest that a discontinuous but widespread regional detachment, which they call the White Pine detachment, extends from the central White Pine Range through the Horse Range and southward throughout

the Grant Range. In their model, the Railroad Valley protobasin began to form by minor attenuation on detachment faults as early as the late Eocene (Francis and Walker, 2001). In the Oligocene, Mesozoic plutons were reheated, gaining ductility, and began to rise, causing uplift, continued detachment faulting, and doming of overlying strata (Walker et al., 1992; Francis and Walker, 2001; 2002a; Walker and Francis, 2002). They attribute the development of the major topographically high areas along the eastern margin of Railroad Valley to this process. They identified five of these high areas or domes: the northern, central, and southern White Pine domes, and the Horse Range and Grant Range domes (Francis and Walker, 2001; 2002a). They conclude that these domes are cored by remobilized plutons and that major attenuation and denudation of the rising domes were accomplished primarily along the White Pine detachment that overlies the structural domes (Francis and Walker; 2001).

In their model they envision the White Pine detachment occurring predominantly within the mechanically weak Mississippian Chainman Shale, locally cutting downsection. Francis and Walker (2001, 2002a) simply place the trace of the White Pine detachment wherever post-Chainman units are juxtaposed next to pre-Chainman units. Using this criterion they identified the White Pine detachment or its equivalent in several places along the length of the White Pine and Grant Ranges. These exposures include the Blackrock Fault in the central and southern White Pine Range, and several of the detachments (Fryxell, 1988; Lund et al., 1991; Camilleri, 1992) in the northwestern and central Grant Range. They explain that in many places the White Pine detachment is now structurally higher than the range crest and is eroded away.

Summary

Previous studies investigating the structural evolution of Railroad Valley focused on a single portion of one of the ranges that bound the basin. These studies resulted in proposed models that stress the role played by low-angle normal faulting in basin development. Central to many of these models is isostatic footwall uplift and resultant doming of strata and faults within the uplifted ranges. Structural similarities among the various models led some workers to speculate on a single detachment along the eastern margin of the basin.

The main goal of this study is to document the geometries, kinematics, and temporal relationships of the Silver Spring fault and other extensional structures in the southern White Pine Range in order to develop a viable structural model for the area. Then, this model will be compared to extensional styles observed in other ranges to support or refute the hypothesis that a single extensional model can be applied regionally throughout the eastern margin of Railroad Valley.

CHAPTER 4

METHODS

Detailed mapping at 1:24,000 scale using standard geologic mapping techniques (e.g., Compton, 1985) was used to produce a geologic map of approximately 30 square kilometers in the southern White Pine Range area. The White Pine Peak and Duckwater SE USGS 7.5' topographic quadrangles served as base maps. Aerial photographs at a scale of approximately 1:24,000 were used as a mapping aid.

Deformed state cross sections were constructed from structural and stratigraphic data mapped and collected in the field. Unit thicknesses were determined from stratigraphic map patterns where possible, otherwise regional thicknesses measured from elsewhere in the White Pine Range by Lumsden (1964) and Lumsden et al. (2002) were used. Fault orientations were based on measured fault surfaces, three-point method calculations, structure contour method calculations, and/or the ability of the fault to be retrodeformed. Apparent thicknesses of bedding and fault planes were calculated using W.S. Tangier Smith's (1925) graphic solution of true dip.

Present day deformed sections were restored in a stepwise fashion following standard techniques (Dahlstrom, 1969; Crane, 1987; Groshong, 1989; White, 1992). Retrodeformed cross-sections were used to constrain fault and fold geometries at depth, calculate fault offset, and to estimate the amount of total extension across the section.

Stereonets were used to plot poles to fault surfaces, fault striations, poles to axial planes, and fold axes to analyze the geometries and kinematics of major faults. All plots were made on equal area lower hemisphere stereonets using R. Allmendinger's Stereonet for Windows v. 1.2.

$^{40}Ar/^{39}Ar$ isotopic analysis, including multi-domain thermal modeling, was performed on a sample of K-feldspar collected from the Railroad stock in hopes of deriving the thermal history of the stock. Understanding the cooling history of the sample, collected in the footwall of the Silver Spring fault, could help constrain the timing of maximum cooling of the stock which may be interpreted as the time of maximum movement on the detachment. Detailed descriptions of the thermal history analysis as well as the results are in Appendix A.

CHAPTER 5

STRUCTURAL DESCRIPTIONS

Rocks in the southern White Pine Range record a complex structural history of Cenozoic extension overprinting Mesozoic contraction. Numerous high- and low-angle normal faults occur throughout the area. Faults were documented by offset units, fault breccia and/or gouge, and fault scarps. Large-scale folds exposed in the Paleozoic section were mostly identified from the map patterns or cross-sections that geometrically require folds, because axial planes for these folds were generally not detectable in the field. Abundant small-scale and mesoscale folds occur near many of the low-angle normal faults.

Low-Angle Normal Faults

Low-angle normal faults exposed within the area are non-planar; omit, not repeat, stratigraphic section; attenuate section; and are mostly parallel to bedding. Most of these faults crop out within Lower Cambrian carbonate and shale units. They consistently occur with an upper plate of very thick-bedded, cliff-forming limestone of the Upper Pole Canyon Limestone, Upper Lincoln Peak or Windfall formations and a lower plate of shale and/or thin-bedded limestone of the Lower Pole Canyon Limestone, Lincoln Peak, and/or Dunderberg Shale formations. Bedding-parallel faults were recognized by fault

breccia, omission of section, truncation of footwall bedding, and abundant outcrop-scale drag folds near the fault surface in the lower plate.

The Silver Spring Fault

The Silver Spring fault is the most widely exposed low-angle fault in the area (Figs. 4 and 9; Plate 1). It occurs between cliffs of the Cambrian Windfall Formation and the underlying Dunderberg Shale and/or Lincoln Peak Formation. The fault also cuts and exposes the Silver Spring and Railroad stocks in its footwall (Fig. 4, Plate 1). Dikes, probably associated with the stocks, also are cut at the fault surface. The fault can be traced beyond the mapped area for about 1 km to the north along the western margin of the White Pine Range where it may be cut by the Blackrock fault (Fig. 4) (Lumsden, 1964; Moores et al., 1968). To the east, the Silver Spring fault can be traced for a very short distance until it is cut by a series of high-angle normal faults (Fig. 4).

Two groups of high-angle normal faults are present: (1) numerous minor offset (<2 m) hanging-wall faults that end at the Silver Spring fault and (2) moderate to large offset (>10 m) faults that cut the Silver Spring fault. The smaller hanging-wall faults are seemingly ubiquitous and were not mapped because the offset is too small to show at the map scale.

Several measurements of the fault surfaces were taken on the Silver Spring fault. Most dipped to the southwest, although locally the fault dips to the east (Figs. 10 and 11). The average strike and dip of all measured surfaces on the Silver Spring fault are 142°, 15° SW (Fig. 10). Also, a single set of fault striations was measured to have a plunge and trend of 18°, 241°.

The Silver Spring fault is nearly bedding-parallel with bedding-to-fault angles typically being 0° -15°. Locally, a larger discordance exists where small pre- and\or syn-fault folds are cut by the Silver Spring fault creating local bedding-to-fault angles up to ~25° in the footwall. This near concordance of bedding and the fault creates a lack of offset elements, making it difficult to determine sense of motion and the amount of offset on the fault. However, at least moderate amounts of section appear to be absent in the southern White Pine Range. The reported regional thickness for the combined Cambrian Dunderberg Shale and Lincoln Peak Formations is about 1050 m (3400 ft) (Moores et al., 1968). The actual maximum thickness of these formations near the fault is 700 m (2300 ft). Therefore, movement on the Silver Spring fault resulted in up to 350 m (1150 ft) of attenuation of the Middle Cambrian section.

The Silver Spring fault is non-planar at map-scale and commonly undulates in outcrop-scale exposures. Generally, the fault conforms to the shape of a major south-southeast-plunging anticline, the White Pine anticline (Plate 1, Plates 2a and 2b) (Lumsden, 1964). A structure contour map of the Silver Spring fault shows the broad, irregular domal shape of the fault surface (Fig. 11). This map shows a north-striking segment on the west flank of the range connecting to a northwest-striking segment across a fault bend. At the southern tip of the range the northwestern-striking segment transitions into a west-striking segment across another fault bend (Fig. 11).

A small, south-plunging, synclinal-shaped groove in the Silver Spring fault surface occurs just west of the easternmost canyon along the southern range front (Fig. 11; Plate 2b). The axis of the small corrugation trends to the north-northeast for about 1 km from the southern range front. The western limb of the corrugation has a strike and dip of

045°, 15° SE. The eastern limb strikes and dips 031°, 13° SW. Both the Cambrian Windfall Formation and Dunderberg Shale that compose the hanging wall and footwall, respectively, are folded about a similar axis (fold C on Figure 9; see also Fig. 4; Plate 1). However, the limbs of the folded strata dip more steeply at orientations of 050°, 21° SE for the western limb and 026°, 16° SW for the eastern limb. Consequently, the fault surface does cut across bedding here.

Bristlecone Fault

In the west end of the map area near the intrusions, a structurally lower bedding-parallel fault occurs about 90-180 m (300-600 ft) below the Silver Spring fault (Fig. 4; Plates 1 and 2a, 2b). The fault appears between the massive algal cliffs of the Upper Lincoln Peak Formation and the thinly-bedded limestone and argillite of the lower Lincoln Peak Formation (Fig. 4; Plate 1). This previously unrecognized fault is here called the Bristlecone fault. Five measurements of the exposed fault surface yielded an average strike of 122° and dip of 15° SW (Fig. 10). Contouring the fault surface reveals an average orientation of 151° and 18° SW.

Near Plane Crash Canyon, the Upper Lincoln Peak Formation and the Bristlecone fault are absent (Fig. 4; Plate 1). East of Plane Crash Canyon, the Upper Lincoln Peak crops out again although it is unclear if a fault serves as its lower contact because the base of the unit is not exposed.

Currant Gap Fault

At Currant Gap, a low-angle normal fault separates the massive cliffs of the Upper Pole Canyon Limestone from the underlying Lower Member (Figs. 4 and 9; Plate 1). This fault is a segment of the first of five low-angle fault sheets described by Lumsden

(1964). He also includes the Silver Spring fault as an equivalent to the fault at Currant Gap. Because it is unclear if these fault s are the same fault, I describe them separately, referring to the fault near Currant Gap as the Currant Gap fault.

The Currant Gap fault mostly parallels bedding, but locally cuts across bedding at a small angle in various directions. Both the bedding and fault surface are gently warped into an antiform that trends generally north-south, similar to the Silver Spring fault. The attitudes of several exposed fault surfaces were measured ranging from 062°, 8° SE to 147°, 9° SW. The average orientation is 097°, 11° S (Fig. 10).

Near Highway 6, the fault occurs as two sub-parallel strands, one at the base of the Upper Pole Canyon Limestone and the other between 10 and 30 m (33 and 100 ft) above within the Upper Pole Canyon Limestone (Plate 1). On the northern and eastern sides of Currant Gap, the two strands merge into a single strand (Plates 1 and 2c). Exposures of the Currant Gap fault are limited to the immediate area around the Gap because it is cut and offset by nearby surrounding high-angle faults (Figs. 4 and 9; Plate 1).

Blackrock Fault

The trace of the Blackrock fault has been mapped for several kilometers along the western flank of the White Pine Range from the Blackrock Canyon area to just west of the Railroad Stock (Fig. 8) (Lumsden, 1964; Moores et al., 1968). The fault separates an upper plate of upper Paleozoic sedimentary and Tertiary volcanic rocks from a lower plate of Cambrian through Mississsippian rocks (Langrock, 1995).

A similar fault crops out along the extreme southwestern margin of the White Pine Range. Small faulted blocks of Pennsylvanian Ely and the Mississippian Joanna, Diamond Peak, and Chainman formations are separated from the Cambrian Windfall

Formation by a low-angle fault surface (Fig. 4, Plate 1). This fault is locally silicified and unlike the other detachments, has significant stratigraphic omission. The hanging-wall blocks are complexly faulted and incorporate small slivers of Tertiary Windous Butte Formation. The hanging-wall faults appear to terminate at the detachment surface. Six well-exposed fault surfaces were measured and have an average attitude of 123°, 21° SW (Fig. 10). The easternmost trace of this fault is about 1 km east of the mouth of Plane Crash Canyon (Figs. 4a and 9; Plate 1).

Ragged Ridge Fault

Although the trace of the Ragged Ridge fault is not exposed in the map area, it is thought to be responsible for the juxtaposition of Tertiary Windous Butte Formation and Horse Camp Basin deposits next to lower Cambrian rocks west of Currant Gap (Fig. 4a, Plate 1). The 30° west-dipping Ragged Ridge fault is locally exposed to the south where it defines the eastern boundary of the Miocene Horse Camp Basin (Horton and Schmitt, 1998). Over 3000 m (9800 ft) of sediments and volcanic rocks were deposited in that basin (see Chapter 3) (Moores et al., 1968; Horton and Schmitt, 1998).

High-Angle Normal Faults

Seventy-four high-angle normal faults were mapped and divided into distinct sets. These sets were defined based on timing relationships, where possible, and geometric similarities. In order to describe and compare the timing and spatial relationships among the different high-angle normal fault sets, the mapped area was divided into two separate domains. Domain 1 includes the Middle to Lower Cambrian rocks and Tertiary intrusions that compose the main part of the range front and the area near Currant Gap (Fig. 9).

Forty faults that occur within domain 1 were separated into three temporally distinct timing sets (Fig. 12). From youngest to oldest these are: north- to northwest-striking faults, northeast-striking faults, and east-striking faults. Domain 2 is defined as the middle to upper Paleozoic section and Tertiary volcanic rocks that compose the hanging walls of the Blackrock and Ragged Ridge faults (Fig. 9). Thirty-three high-angle faults in domain 2 exhibit inconsistent timing relationships and are divided into four sets based only on their strikes: north-south, east-west, northwest-southeast, and northeast-southwest (Fig. 12).

The relative timing of high-angle normal faulting is loosely constrained by cross-cutting relationships (Fig. 12). High-angle faults cut both the Paleozoic and Tertiary sections where exposed. They also cut across folds and the Silver Spring, Bristlecone, and Currant Gap faults. No faults from either domain were observed to cut across the Blackrock or Ragged Ridge faults into the other domain (Fig. 9; Plate 1). However, this is likely due to a lack of exposure making timing relationships between high-angle normal faults and the large-displacement detachment faults unclear. All faults, but one are covered by Tertiary-Quaternary alluvial fan deposits.

Domain 1 High-Angle Fault Sets

Twenty-two faults that strike north to northwest consistently cut northeast- and east-striking fault sets (Fig. 12; Plate 1). These faults are mostly planar and dip between 50° and 84° to the northeast and southwest (Fig. 13b). Generally, the stratigraphic offsets of the faults are relatively small (<120 m) (400 ft) (Plates 2a and 2b). The faults are fairly evenly distributed throughout the domain.

Nine high-angle normal faults in domain 1 strike northeast-southwest (Fig. 13c; Plate 1). These faults are typically cut by north- to northwest-striking faults, and they generally cut east-striking faults (Fig. 12). The faults dip steeply, between 66° and 82°, most to the south (Fig. 13c). All northeast-striking faults are planar and result in stratigraphic separations up to 180 m (590 ft) although most have significantly less offset (<20 m) (65 ft) (Plates 2a and 2b).

Nine high-angle normal faults within domain 1 strike east-west, dipping between 71° and 82° (Fig. 13d, Plate 1). All but one dip to the south (Figs. 9 and 13d; Plate 1). These faults are generally cut by faults of the north- to northwest- and northeast-striking sets (Fig. 12). Faults in this set are mostly planar and resulted in minor (<120 m) (<400 ft) stratigraphic offset.

Domain 2 High-Angle Fault Sets

Few cross-cutting relationships exist in domain 2 but one example of inconsistent timing is shown in Figure 14. The figure shows faults labeled A, B, and C located within the large hill of volcanic rocks in the west-central portion of the area. Here, northwest-striking fault B cuts fault A, while the north-striking fault C cuts B but is also cut by A (Fig. 14). Since no consistent cross-cutting patterns among domain 2 faults were observed, faults are grouped by similar strike only.

Sixteen north-striking faults are evenly distributed throughout domain 2. These faults dip to the east and west between 68° and 81° (Fig. 15b). The faults are planar and have mostly minor stratigraphic offset (<~30 m) (100 ft). Some north-striking faults that occur within the intensely faulted Blackrock hanging wall near the mouth of Silver Spring Canyon (Fig. 12; Plate 1) may have larger amounts of offset, up to several hundred

meters. However, these faults are exposed for only 30 to 200 m (100-650 ft) between thin, complexly deformed slices of rock, making the amount of offset uncertain.

Nine faults strike east-west and dip between 63° and 87° to the north and south (Fig. 15c). Most of these faults are planar although one fault that separates the Tertiary Windous Butte Formation from the rhyolite of the White Pine Range south of Plane Crash Canyon bends to the northeast along strike (Plate 1). Stratigraphic separation on this fault is between ~190 and ~800 m (620 and 2600 ft), although most east-west-striking faults have significantly less offset (<20 m) (<65 ft).

Six northwest-striking faults were documented in domain 2. These faults are planar and dip between 66° and 89° northeast and southwest (Fig. 15d). Three of them are concentrated within the complex hanging-wall block west of the mouth of Silver Spring Canyon (Fig. 12; Plate 1). As discussed earlier, faults in this area are poorly exposed making it difficult to calculate stratigraphic offset. The other three faults have less than 45 m (150 ft) of offset.

Only a single pair of faults, occurring within 300 m (1000 ft) of one another in the west-central part of the domain, strike to the northeast (Fig. 12, Plate 1). They are both planar and dip ~85° to the southeast (Fig. 15e). Stratigraphic offset appears to be less than 20 m (65 ft), and cross-cutting relationships with other faults were not observed.

Evidence for Quaternary Faulting

About 1 km southwest of the mouth of Plane Crash Canyon, a northwest-striking, southwest-dipping normal fault created a nearly 1/2 km long, 15-20 m (50-65 ft) high scarp (Fig. 4, Plate 1). Being younger than the other high-angle normal faults, this fault is not included within the two domains. The fault separates a footwall of Tertiary Windous

Butte Formation and old Quaternary-Tertiary gravels from younger Quaternary-Tertiary fan deposits in the hanging wall. The northern end of the scarp terminates abruptly at Quaternary stream deposits.

Currant Summit Fault

The generally east-west-striking Currant Summit fault has been calculated to have an average dip of ~87° N, ~2700 m (10800 ft) of strike-parallel slip, and a throw of ~2000 m (6550 ft) just east of the mapped area (Williams 2000; Williams and Taylor, 2002). The westernmost exposure of the Currant Summit fault is less than 1 km east of Crystal Spring where it separates Ordovician units of the Pogonip Group from the Cambrian Windfall Formation (Fig. 4) (Williams, 2000). The westward continuation of the Currant Summit Fault is covered by alluvium but has been suggested to continue westward along the southern margin of the range (Lumsden, 1964; Moores et al., 1968; Williams, 2000) where an apparent structural discontinuity exists. This structural discontinuity is located between the Paleozoic rocks of the southwestern margin of the White Pine Range and the low hills of volcanic rocks immediately to the south. Alternatively, the fault may project between the hills of volcanic rocks and Devonian carbonate rocks at Dell Hill (Fig. 4; Plate 1).

Folds

Field mapping revealed folds that are both pre- and either syn- or post-extension. As discussed above, small to mesoscale folds occur profusely in the thin-bedded limestones and shales directly beneath the bedding-parallel faults. A large range-scale anticline

dominates the geometry of bedding in the area and several smaller, low-amplitude, possible parasitic folds deform Cambrian rocks and locally, the Silver Spring fault.

Map-Scale Folds

The Cambrian strata composing the southern part of the White Pine Range are deformed into a broad south-plunging, east-vergent anticline, named the White Pine anticline by Lumsden (1964). The anticline has non-planar limbs that change dip about north-south trending kink-style hinges (Figs. 4b and 9; Plates 1 and 2b). The Silver Spring fault conforms to the general shape of this anticline. Near the stocks, the western limb of the fold dips about 20° WSW. Eastward, across a north-south trending kink axis, the western limb dips at a shallower 14° WSW (Plate 1, Plate 2a). East of White Pine Peak, strata dip gently eastward at about 8° across an anticlinal axis. On the eastern side of the range, mapping by Lumsden (1964) and Williams (2000) shows that the eastern limb steepens to 50° to 70° E (Fig. 4).

The Lower Cambrian strata near Currant Gap and south of the Currant Summit fault are similarly folded into a broad, open anticline with an axis that plunges and trends ~6°, 085°. The Currant Gap fault conforms to the shape of this anticline. The western limb near the fold axis dips ~25° WSW until it is cut by the Ragged Ridge fault. The eastern limb dips about 30° E. Lumsden (1964) and Williams (2000) show that the eastern limb composes the northern Horse Range where strata dip up to 75° to the east-southeast (Fig. 4).

Several other smaller folds, labeled A through D on Figure 9, with axes less than 1 km in length are exposed in the Cambrian units in the southern White Pine Range. Fold A is a tight, upright, outcrop-scale anticline that deforms the Cambrian Windfall Formation

in the upper plate of the Silver Spring fault near the Railroad stock (Fig. 9; Plate 1). The fold is distinct from the others in that it is the only fold that occurs exclusively in the hanging wall of the Silver Spring fault, and it has very steep limbs (dips between 40°-50°). The plunge and trend of the fold axis are 30°, 210°. The fold can be followed for a few hundred meters until it is truncated by the Silver Spring fault on the north.

The south-plunging (~3°) Anticline B, in exposures, folds the Cambrian Dunderberg Shale and Upper Lincoln Peak Formation (Fig. 9; Plates 1 and 2b). The axis trends north-northeast and appears to be cut to the south by the Silver Spring fault. The western and eastern limbs dip gently 12° SW and 15° SE, respectively.

In exposures, syncline C folds the Cambrian Windfall Formation and underlying Dunderberg Shale as well as the Silver Spring fault that separates the two formations (Fig. 9; Plates 1 and 2b). The fold axis trends to the north-northeast and plunges 6° S.

Fold D is a south-plunging (~6°), north-south trending anticline that deforms Lower and Middle Cambrian strata along with the surface of the Silver Spring fault (Fig. 9; Plates 1 and 2b). Although the axial trace is poorly exposed, it is geometrically required in cross-sections and is evident on the structure contour map of the Silver Spring fault (Fig. 11; Plate 2b).

Mesoscale Folds

Numerous, consistently-oriented, mesoscale folds occur in the mechanically weak shales and thin-bedded limestones that make up the footwalls, and locally, the hanging walls, of the Silver Spring, Bristlecone, and Currant Gap faults. Although they occur near all three faults, mesoscale folding is most prominent beneath the Silver Spring fault. The abundance of these folds increases near the slip planes of the faults. Also, the consistency

of the orientations of the folds diminishes with increasing distance from the faults. No consistently oriented folds were observed near the limited exposures of the Blackrock Fault.

Most of these folds are gently plunging, recumbent to inclined, parallel, and have chevron geometries (Fig. 16). The fold wavelength is highly variable and is a function of the thickness and competency of individual beds (Fig. 16). Thin beds (<2 cm) typically have a shorter wavelength (~3-8 cm) and thicker beds (3–25 cm) have wavelengths of up to two meters. Some of the tighter folds are faulted along their hinges. Both the amplitude and the consistency in orientation of the folds decrease with increasing distance from the faults.

Undercutting of the more competent upper plate rocks by the weathering of the weaker shale and thinly bedded limestone of the lower plate commonly results in colluvial cover over these mesoscale folds. Therefore, good exposures of the folds were sparse except where the bedding-parallel faults occurred near narrow canyons and gullies where occasional floods clear the fault zone of debris. For example, where the Silver Spring fault occurs near the narrow mouths of both Plane Crash and Silver Spring Canyons, the orientations of 165 mesoscale folds were recorded. In contrast, the orientations of only 30 folds were documented elsewhere along the entire trace of the fault.

Stereoplots of the fold axes and vergence (recorded as poles to axial planes) of the mesoscale folds beneath the Silver Spring fault show their consistent orientations (Fig. 17). The average fold axis orientations for these plots are as follows: 22°, 300° in Plane Crash Canyon; 18°, 325° in Silver Spring Canyon; 06°, 280° east of Plane Crash Canyon;

and 11°, 330° west of Silver Spring Canyon. The average fold axis for all folds measured beneath the Silver Spring fault is 17°, 294°. Axial planes have average orientations of 302°, 17° NE and 301°, 18° NE for Plane Crash and Silver Spring canyons; 300°, 07° NE east of Plane Crash Canyon and 334°, 15° NE west of Silver Spring Canyon (Fig 16). The average attitude of all axial planes is 304°, 16° NE.

Only five mesoscale folds were visible beneath the colluvium-covered Bristlecone fault. The average axis orientation of these folds is 24°, 321° and the average axial plane orientation is 316°, 17° NE (Fig. 17).

Mesoscale near-fault folds are exposed in the footwall of the Currant Gap fault, although they are not as abundant as in the footwall of the Silver Spring fault. The average orientation of 22 measured fold axes is 05°, 074° (Fig. 17). A plot of axial planes shows that the average orientation is 275°, 23° N (Fig. 17).

Sub-Tertiary Unconformity

A single exposure of the sub-Tertiary unconformity occurs on the eastern slopes of Dell Hill where the Oligocene Currant Tuff lies slightly discordantly on top of limestone of the Devonian Guillmette Formation (Plate 1). Here, the Currant Tuff has an average dip of ~20° E and the Guillmette dips ~32° SE. Removing post-volcanic extension shows that the Paleozoic strata would have dipped ~10° E prior to the Oligocene (Plate 2c). Elsewhere, Tertiary volcanic rocks are separated from nearby Paleozoic strata by faults that may have significantly tilted the volcanic rocks relative to the Paleozoic section.

CHAPTER 6

STRUCTURAL INTERPRETATIONS

Field data constrain the relative timing of the White Pine anticline, bedding-parallel faults, large-scale detachment faults, high-angle normal faults, and other major structures. The placement of these deformation events into a viable structural evolution model allows the determination of the relative significance of each structure in the uplift of the range relative to Railroad Valley. Comparison of the timing and structural style documented in the southern White Pine Range to those in nearby ranges reveals whether a single model of evolutionary history can be applied for the development of Railroad Valley.

Mesozoic Contraction

Folding of strata in east-central Nevada has been linked to (1) Mesozoic shortening in the central Nevada thrust belt (Bartley et al., 1993; Taylor et al., 1993; Langrock, 1995; Taylor et al., 2000; Williams, 2000; Gilbert, 2002), (2) Tertiary extension (Lund et al., 1991; Camilleri, 1992; Lund et al., 1993) or (3) intrusive doming (Lumsden, 1964; Walker et al., 1992, Francis and Walker, 2001). Based on structural and stratigraphic data from this study, it is interpreted that major folding including the White Pine anticline in

the southern White Pine Range occurred in the Mesozoic, before the onset of Tertiary extension and plutonism.

Evidence of pre-volcanic deformation in the southwestern White Pine Range includes the angular discordance between the Tertiary Currant Tuff and underlying Devonian Guillmette on Dell Hill (Plate 2c). This discordance indicates the uplift, tilting, and erosion of several hundreds of meters of Mississippian and Pennsylvanian strata prior to the deposition of the tuff. Also, the Rhyolite of the White Pine Range normally crops out beneath the Currant Tuff but is absent at this exposure of the unconformity. The rhyolite does crop out ½ km to the northwest of Dell Hill indicating that it was likely deposited in the immediate area (Plate 1). These relationships can be interpreted to indicate that a paleobasin margin may have existed near Dell Hill, and that younger normal faults brought small blocks of underlying rhyolite to the surface (Plate 2c).

These relationships and others nearby are interpreted to indicate that much of the area near the southern White Pine Range and northern Horse Range underwent deformation, erosion, and had significant topography prior to volcanism. Williams (2000) documented a similar relationship on the east side of the Horse Range where a 22° east-dipping ash-fall tuff unconformably overlies 40°-50° east-dipping Devonian rocks. North of the study area, Langrock (1995) reports folds in Paleozoic units that are covered by undeformed Oligocene volcanic rocks.

Significant uplift and subsequent erosion of the Paleozoic section prior to the late Eocene is also supported by $^{40}Ar/^{39}Ar$ K-feldspar data from the Railroad stock. Poor duplication of lower temperature isothermal pairs in the step heating data as well as poor correlation between the age spectrum and log r/r_o plot indicate that the sample does not

conform to the assumptions of multi-diffusion domain theory (Appendix A; Figs. 18, 19, Table 1) (McDougall and Harrison, 1999). As discussed in Appendix A, one important underlying assumption is that cooling of the K-feldspar was slow and monotonic (McDougall and Harrison, 1999). However, the failure to model the K-feldspar, the similarity of the large domain ages (the highest temperature steps that form a relatively flat age spectrum at ~33 Ma) to the U/Pb crystallization ages (Taylor et al., 1996), and field evidence for shallow emplacement all support the interpretation that the stock was emplaced at shallow crustal levels and cooled relatively quickly. A shallow intrusion is also supported by the relatively small grain size of the stocks and the thin, low-grade metamorphic contact aureole surrounding the stocks.

The uplift, tilting, and paleorelief near the southern White Pine Range could have been created by either large-scale normal faulting, thrust faulting, or folding prior to Oligocene volcanism. No large-displacement normal faults of this age are documented in the region. There is, however, abundant evidence that the region did undergo significant contractional deformation associated with the Mesozoic Eureka-central Nevada thrust belt. Northwest of the study area, in the Duckwater Hills and Pancake Range, a range-scale syncline and several smaller-scale folds and thrusts are documented (Fig. 8) (Carpenter et al., 1993; Perry and Dixon, 1993; Dobbs et al., 1994; Gilbert, 2002). Bartley and Gleason (1990) mapped two thrust faults in the northern Quinn Canyon Range and southern Grant Range that strike north to northeast and verge to the east. Fryxell (1988) documented an overturned north-trending east-vergent anticline in the central Grant Range that is cut by Mesozoic granite. Major Mesozoic deformation in the northern Grant Range is indicated by metamorphism, foliation, and minor east-vergent

folds found in the lower Paleozoic section there (Camilleri, 1992; Lund et al., 1993). North of the study area, in the central and northern White Pine Range, several north-trending folds in the Illipah fold belt are attributed to the Mesozoic central Nevada thrust belt (Hose and Blake, 1976; Taylor et al., 1993; Langrock, 1995).

Like many of these folds, the White Pine anticline, exposed in the southwestern White Pine Range is a broad east-vergent fold with a north-trending axis. These similarities in geometry as well as the position of the southern White Pine Range in the central Nevada thrust belt strongly indicate that prevolcanic folding, uplift, and subsequent erosion are a result of Mesozoic contraction.

Geometric and other similarities between the White Pine anticline and the anticline at Currant Gap indicate that they are the same fold that was displaced by the left-lateral Currant Summit transverse fault. Both are broad and upright folds with axes that trend roughly north-south. Both folds influence bedding-parallel faults. The limbs of the fold at Currant Gap have steeper dips, but deeper structural levels are exposed here and tighter folding near the core of the fold can be expected. The equivalency of these folds was also postulated by Williams (2000).

Regional cross-sections constructed across Railroad Valley show that two to three major thrust faults exist beneath Railroad Valley (Langrock, 1995; Gilbert, 2002). One of these, the White Pine thrust, crops out in the Horse Range and has been interpreted to underlie much of the western White Pine Range (Langrock, 1995; Gilbert, 2002). The White Pine thrust cuts across an open and upright anticline in the Horse Range that is equivalent to the White Pine anticline. Gilbert (2002) speculates that the anticline may be a fault-bend fold above an unnamed out-of-sequence thrust in the footwall of the White

Pine thrust. If correct, this would directly link the White Pine anticline to Mesozoic thrusting.

Because the smaller folds B, C, and D are sub-parallel to the White Pine anticline (Fig. 9), these folds are all interpreted to be a result of pre-Tertiary deformation associated with the central Nevada thrust belt for the following two reasons. (1) Their axes are sub-parallel to the trend of the White Pine anticline, suggesting a possible genetic link between them. (2) No Tertiary deformation event documented in the area can account for the folds. The >30° angular difference in trend between anticline A and the other folds, as well as its distinctive tightly folded geometry, indicate that anticline A developed under different stress conditions. One possibility is that anticline A may be an extensional fold produced by drag along the Silver Spring fault.

Cenozoic Extension

Bedding-Parallel Faults

In addition to fault geometry and, where possible, fault striations, the slip direction on the bedding-parallel faults can be constrained by the orientations of the mesoscale folds that formed close to the faults. The spatial relationship between the consistently-oriented mesoscale folds and the fault surfaces can be interpreted to represent a genetic link between the two. Two orientations of systematically oriented fold axes are possible within fault (shear) zones; fold axes can be parallel or perpendicular to transport direction. Mancktelow and Pavlis (1994) analyzed fold-fault relationships for two different detachment systems associated with metamorphic core complexes and conclude that the axes of some fault-related folds in certain tectonic environments, can parallel

extension direction. However, the folds related to the Silver Spring fault don't appear to fit this model. The axial planes of the folds observed by Mancktelow and Pavlis (1994) have moderate to steep dips indicating a near horizontal direction of the XY plane of the finite strain ellipse and maximum compression that is subparallel to the strike of the fault. In contrast, folds near the Silver Spring fault have nearly horizontal to gently dipping axial planes indicating subvertical directions of the XY plane of the finite strain ellipse and maximum compression.

Two different explanations of these folds are possible. Perhaps differences in rheology (ductilely deformed mylonites of metamorphic core complex vs. folding of thin strata near the Silver Spring fault) could account for the different folding styles observed. Another possibility is that folds near the Silver Spring fault are indicative of relatively low strain and folds near the metamorphic core complexes are products of high strain. Hudleston (1986) suggests a progressive continuum of folding where fold axes are perpendicular to slip direction in early phases of shear (low strain) and later rotate and cluster parallel to slip direction in later phases of shear (high strain).

I interpret that mesoscale folds near the bedding-parallel faults are a result of drag or a local stress field produced by movement of the upper plate along a low-angle fault with relatively low strain. In this interpretation, it follows that the folds would verge in the same direction that the upper plate moved and fold axes would generally be oriented perpendicular to the slip direction. Because this fault-related fold zone lacks any signs of metamorphism or plastic deformation, it is interpreted that they formed dominantly in a brittle regime. The mechanical weakness of the shales and thin-bedded limestones is exhibited in the disharmonic nature of the folding, where thinner-bedded material is

folded more intensely than the thick beds. Therefore, flexural slip and some small-scale ductile processes contributed to the folding.

While attenuation of the mechanically weak shaly units appears to have involved some ductile strain, ubiquitous outcrop-scale high-angle normal faults in the hanging walls of the Silver Spring and Bristlecone faults indicate that thinning of the more competent units was mostly brittle. These high-angle faults sole into the basal fault and break the upper plate into numerous blocks. These blocks have all rotated slightly, collectively extending the plate.

Silver Spring Fault

The northwest-southeast average trend of all fault-related fold axes is interpreted to indicate that the upper plate of the Silver Spring fault moved either to the northeast (~024°) or to the southwest (~204°) (Fig. 17). This is consistent with the single measured fault striation that trends in this same direction (Fig. 17). Fault-related fold vergence and the present geometry of the fault surface can help constrain the slip direction. All but a few of the folds verge to the southwest, providing strong evidence that the slip direction also was to the southwest (Fig. 17). Additionally, the present fault plane dips predominantly to the southwest (Figs. 10 and 11).

Cross-cutting relationships with other units and structures establish the relative timing of movement on the Silver Spring fault. The youngest geologic features cut by the fault are the Tertiary intrusions. U/Pb zircon data (Taylor et al., 1996) as well as $^{40}Ar/^{39}Ar$ cooling ages from large domains in K-feldspar of this study indicate that the stocks were emplaced at 33.17 ± 0.18 Ma (Fig. 18). The youngest feature to overlap the fault is Tertiary to Quaternary alluvial fan deposits surrounding the margin of the range.

Based on these relationships, motion on the Silver Spring fault is loosely bracketed between ~33 Ma and Quaternary.

Map relations suggest that the Silver Spring fault is either cut by the Blackrock Fault or merges with it (Fig. 9, Plates 1, 2a, and 2b). However, since the two faults have different transport directions (southwest vs. west-northwest for the Silver Spring fault and Blackrock fault, respectively), it is inferred that the two faults did not develop at the same time. Thus, it is unlikely that the Silver Spring fault cuts the Blackrock fault. If this were true, the Blackrock fault and its hanging wall of upper Paleozoic and Tertiary volcanic rocks should lie somewhere within the footwall of the Silver Spring fault higher in the range. Because no offset counterpart of the Blackrock fault is exposed in the Silver Spring fault footwall, it is assumed that the Blackrock fault cuts the Silver Spring fault.

A southwest slip direction on the non-planar Silver Spring fault would require an oblique-reverse-sense of slip on some parts of the fault that currently dip eastward (Fig. 9). For example, the northeast end of cross-section A-A' (Plate 2a) shows where the Silver Spring fault dips to the east, thus requiring an apparent thrust motion to the southwest. Given the impossibility of this situation, further explanation for the geometry of the fault is required.

Three explanations for why the Silver Spring fault shares a shape similar to the White Pine anticline are possible. The first possibility is that compressive stresses folded both Cambrian strata and the fault after the fault developed. This would require a late Oligocene or younger deformation event because movement on the fault was post late Eocene. Contractional deformation of this age is not known and as discussed earlier,

evidence supports the interpretation that large-scale folding of Paleozoic rocks in the southern White Pine Range most likely occurred in the Mesozoic.

Another possible explanation for the antiformal shape of the Silver Spring fault is that both fault and strata were folded contemporaneously as part of an arched extensional system associated with major attenuation on a low-angle normal fault. Arching or doming models invoke late-stage warping of the fault surface and underlying strata in response to differential unloading of the footwall of a normal fault (Spencer, 1984; Wernicke and Axen, 1988; Buck, 1988; Axen, 2004). These extensional domes have been documented throughout the Basin and Range in a semicontinuous belt from Canada to Mexico (Coney, 1980; Crittenden et al., 1980; Axen et al., 1993; Axen; 2004), including the northern Grant Range (Camilleri, 1992; Lund et al., 1991; 1993).

Similarities exist between the extensional system in the northern Grant Range and the structures in the southern White Pine Range. Both systems have arched attenuation faults where structurally higher faults appear to be younger. Both systems have range-scale anticlines that deformed Paleozoic strata. The Silver Spring, Bristlecone, and Currant Gap faults are similar to the low-angle attenuation faults at middle structural levels in the Grant Range that are bedding-parallel and bound unique stratigraphic packages (Lund et al., 1993). Due to these similarities, one may hypothesize that folded bedding-parallel faults and strata in the southern White Pine Range formed in a manner similar to the structural dome in the northern Grant Range.

Synextensional doming, however, can be satisfactorily rejected as a valid explanation for the present geometry of Paleozoic strata and the Silver Spring fault for the following reasons. (1) In the northern Grant Range, Oligocene volcanic rocks are concordant with

the underlying deformed Paleozoic section (Lund et al., 1993). This is consistent with the interpretation that doming in the Grant Range is a result of large-displacement on post-volcanic detachment faults. In contrast, as discussed earlier, the angular discordance observed at the sub-Tertiary unconformity near the southern White Pine Range shows that Paleozoic rocks were folded prior to detachment faulting. (2) The Silver Spring fault does not resemble faults that are integral to models of isostatic footwall uplift. The stratigraphic offset on the Silver Spring fault is relatively minor making it highly unlikely that doming could have been induced by slip on the fault itself. Also, in these models, the hanging walls of the detachments typically consist of highly faulted and rotated blocks that lie around the margins of the dome (Axen, 2004). In contrast, the hanging wall of the Silver Spring fault is a mostly continuous uninterrupted structural plate, part of which, remains structurally high in the range (Plate 2a).

One could argue that the Silver Spring fault and Paleozoic strata may have been arched as part of the footwall of the structurally higher and relatively large-scale (heave of >8 km) (26,000 ft) Blackrock fault that more closely resembles detachments in the northern Grant Range extensional model. On the west side of the range, just north of Blackrock Canyon where the Blackrock fault dips ~20° W, the fault bends to the east and continues on to the east side of the range where the fault dips ~10° E (Fig. 8) (Langrock, 1995; Lisenbee and Kieffer Rowe, 1996; W.J. Taylor, unpublished data). If this geometry were a result of doming, one would expect footwall bedding to be similarly domed about an approximate north-south trending axis. However, Lumsden (1964) and Moores et al. (1968) show that the axial trace of the White Pine anticline lies west of this fault bend where it is cut by the Blackrock fault near Sawmill Canyon (Fig. 8). If doming occurred,

the fault bend and anticlinal hinge would be closely aligned. Indeed, farther north near Blackrock Canyon, Langrock (1995) shows that hanging-wall blocks of the west-dipping Blackrock fault lie on top of the eastern limb of the White Pine anticline with no systematic change in footwall dips. This geometric relationship between fault and footwall bedding is inconsistent with the extensional dome in the northern Grant Range where arched attenuation faults share the same geometry as the bedding in their footwalls (Camilleri, 1992; Lund et al., 1993). This led Langrock (1995) to conclude that this bend in the Blackrock fault is primary rather than a product of doming.

Additionally, a reconstruction of cross-section C-C' shows the Ragged Ridge fault, the only nearby detachment fault that could have influenced the development of the White Pine anticline near the Horse Range, to clearly cut the fold (Plate 2c). All these data indicate that the White Pine anticline is older, and not contemporaneous with large-scale detachment faulting as part of a domed extensional system.

The third and preferred interpretation for the present geometry of the Silver Spring fault is that the Silver Spring fault developed following non-planar pre-extensional anisotropies that predominantly dipped to the southwest as part of the western limb of the White Pine anticline. In this interpretation, anisotropies were defined by mechanically strong units of massive carbonate (i.e., the Windfall Formation and the Upper Pole Canyon Limestone) overlying much less-competent shales and thin-bedded limestones (i.e., the Dunderberg Shale and Lower Pole Canyon Limestone). At the onset of major extension, strain could be more easily accommodated by fault development along these pre-existing surfaces of weakness rather than cutting across bedding. Faults would

follow anisotropies that were predominantly dipping to the southwest but in many places were folded.

The Tule Springs detachment in southeastern Nevada is another example of a low-angle fault that localized along a preexisting anisotropy (Axen, 1993; Axen, 2004). The Tule Springs detachment initiated and moved in the Miocene following a 3°-15° west-dipping footwall thrust flat for about 14 km (Axen, 1993). The upper plate consists of strong Cambrian dolomite and the footwall is weak siltstones of the Jurassic Moenave Formation. This mechanical contrast between the two rock types directly controlled the trajectory of the detachment (Axen, 1993; Axen, 2004).

Several other low-angle faults that are sub-parallel to bedding and thin section, commonly called attenuation faults, have been documented throughout much of western Utah and eastern Nevada. Examples include faults near White Horse Pass (Silberling and Nichols, 1994; 2002) and throughout much of the Goshute and Toano ranges (Ketner et al., 1998) in northeastern Nevada, the central Drum Mountains in western Utah (Nutt et al., 1995), and the central Schell Creek Range in eastern Nevada (Drewes, 1967; Walker et al., 1992; Francis and Walker, 2002a). Like the Silver Spring fault, many of these faults occur at or near the contact between units of contrasting competence. The timing of these faults varies from Mesozoic to late Tertiary and have been linked to both contractional and extensional regimes (Hintze, 1978; Nutt et al., 1995; Silberling and Nichols, 2000).

The segments of the Silver Spring fault that presently appear to have a reverse-sense of slip (Fig. 9) can also be reconciled if the range as a whole was tilted to the east during a younger phase of extension. East-tilting of the range is the preferred mechanism for

explaining a similar apparent thrust-sense exhibited on an east-dipping portion of the Blackrock fault discussed earlier (Lisenbee and Kieffer Rowe, 1996). This block tilt is supported by the gently east-dipping volcanic rocks along much of the eastern flank of the White Pine Range indicated by mapping of Moores et al. (1968) and Williams (2000) (Fig. 4). Eastward tilting of the White Pine Range may have been accomplished by large-slip displacement on a west-dipping normal fault located somewhere east of the range. A likely fault is the White River fault that bounds the western margin of much of the Egan Range ~25 km east of the White Pine Range (Fig. 1) (Kellogg, 1964). Kellogg (1964) mapped the White River fault throughout the central and southern Egan Range and showed that the fault had significant Quaternary movement as evidenced by a well-developed scarp in Quaternary alluvium along much of its length and by a 9° rotation in adjacent uppermost Pliocene deposits (Kellogg, 1964; 1978). A similar fault exists along much of the western margin of the northern Egan Range as well, identified by the presence of Quaternary fault scarps and the alignment of springs (Woodward, 1964). Therefore, it seems plausible that the White Pine block may have been tilted to the east as part of the hanging wall of this major west-dipping marginal fault system that is responsible for the delineation of the Egan Range and White River Valley.

Also, although it has been inferred that the White Pine anticline is a product of Mesozoic shortening, some degree of extensional doming cannot be ruled out as a mechanism for eastward rotation of the White Pine Range. In fact, some doming in the footwall of a detachment fault with considerable attenuation such as associated with the Blackrock fault is possible. But because the pre-detachment Paleozoic strata were

previously deformed, it is difficult to estimate what amount of the strain may have been caused by synextensional doming.

Bristlecone Fault

The present attitude of the fault (Fig. 10) along with the orientations of five fault-related folds (Fig. 17) suggest that the slip direction on the Bristlecone fault was to the southwest (~231°). This direction is similar to that of the Silver Spring fault.

The Bristlecone fault is absent near Plane Crash Canyon, apparently, being cut out by the structurally higher and younger Silver Spring fault. Alternatively, the faults could merge together indicating that they were active synchronously. Outcrop patterns (Plate 1) and cross-sections (Plate 2a, 2b) show the Bristlecone fault to have a geometry similar to the segment of the Silver Spring fault that lies structurally above.

In a similar manner to the development of the Silver Spring fault, the Bristlecone fault appears to have formed along the mechanical anisotropy between the massive Upper Lincoln Peak and the subjacent mechanically weak shale of the lower portion of the Lincoln Peak Formation.

Currant Gap Fault

The axes of fault-related mesoscale folds, coupled with the fold vergence suggest that upper plate movement on the Currant Gap fault was to the south (164°) (Fig. 17).

The Currant Gap fault shares similarities with the Silver Spring and Bristlecone faults in that it also occurs between a massive limestone unit and thin-bedded unit, and it conforms to the shape of the White Pine anticline. These similarities led Lumsden (1964) to hypothesize that the Currant Gap fault is equivalent to the Silver Spring fault. The proposed equivalency would require the fault to cut down section in the footwall from the

top of the Middle Cambrian Dunderberg Shale at the southern end of the range to the top of the Lower Pole Canyon Limestone at Currant Gap, some 610 m (2000 ft) in stratigraphic thickness. Two lines of evidence support the interpretation that these are distinct faults: (1) they have different slip directions (south and southwest) and (2) neither fault was observed to cut significantly across section along their entire exposed traces.

Large-Displacement Detachment Faults

Blackrock Fault

This research indicates that the detachment surfaces that juxtapose highly faulted blocks of Pennsylvanian and Mississippian strata against the Cambrian Windfall Formation (Plate 1) are the southern continuation of the Blackrock fault. Evidence supporting this interpretation includes the following. (1) The two faults have similar offset magnitudes. Langrock (1995) reports 7.6 km (25,000 ft) of heave on the Blackrock fault a few kilometers north of this area of study. Minimum slip restorations in this study of cross-section A-A' shows at least 8 km (26,000 ft) of heave on the Blackrock fault (Plate 2a). (2) Along the western margin of the southern White Pine Range (Fig. 8), Langrock (1995) documents the Blackrock fault with an upper plate of Pennsylvannian Ely Limestone and Tertiary volcanic rocks of the Garrett Ranch Group over a lower plate of Cambrian Windfall Formation. This is the same relationship as in this area. (3) The detachment documented in the southwestern White Pine Range has an average dip of 15°-30° similar to the dip magnitude reported by Langrock (1995) for the north-striking segment of the Blackrock fault, although the detachment in this study dips to the southwest. Changes in geometry along the fault are expected, however, as the attitude of

the fault was shown to vary along strike (Lumsden, 1964; Moores et al., 1968; Langrock, 1995; Lisenbee and Kieffer Rowe, 1996; Francis and Walker, 2001).

Exposures of the Blackrock fault in the map area are extremely small with only one exposure being more than 200 m (660 ft) long. Fault orientation alone is not adequate to interpret a possible slip direction, and due to the lack of exposure, no kinematic features for calculating the sense of slip on the Blackrock fault were exposed.

The intermittent trace of the Blackrock fault ends at the southern tip of the range very near the projected strike of the Currant Summit fault (Figs. 4 and 9; Plate 1). Three possible relationships between the Blackrock and Currant Summit faults exist: (1) the Blackrock fault cuts and displaces the Currant Summit fault; (2) the Currant Summit fault cuts and displaces the Blackrock fault so that a counterpart of the detachment exists to the south of the Currant Summit fault; or (3) the Blackrock fault terminates at the Currant Summit fault, transferring strain onto the left-lateral structure. The first option is invalidated by evidence that strongly suggests that the Blackrock fault cannot be younger than the Currant Summit fault. Williams (2000) documented fault scarps in Quaternary sediments along the Currant Summit fault to the east (Fig. 4). Conversely, the Blackrock fault is lapped by Quaternary-Tertiary sediments, indicating that at least some slip on the Currant Summit fault post-dates slip on the Blackrock fault. Similarities between the Blackrock fault and the Ragged Ridge fault to the south (Fig. 4) fuel speculation that the two faults are offset counterparts. But a few key differences, which will be discussed in the next section, show that option 2 is an unlikely scenario. The third option above is the preferred interpretation. Mapping by both Moores et al. (1968) and Williams (2000) show that low-angle normal faults consistently terminate at the Currant Summit fault (Fig. 4).

A detailed study by Williams (2000) categorizes the Currant Summit fault as a barrier transfer fault that prohibits normal fault propagation, allowing low- and high-angle normal faults to transfer slip onto the transfer fault (Fig. 7). Therefore, the preferred scenario is that the Blackrock fault terminates at and has transferred strain, in the Tertiary, onto the Currant Summit fault.

Ragged Ridge Fault

The Ragged Ridge fault shares some similarities with the Blackrock fault indicating a possible correlation between the two. Plate 2c shows at least 6 km (19,000 ft) of heave on the Ragged Ridge fault, comparable to the observed horizontal separation on the Blackrock fault. Both faults generally dip gently (~30°) to the west. If these faults were the same, it could be interpreted that a single fault was cut and displaced eastward by the left-lateral Currant Summit fault.

However, some observations would require explanation. First, Horse Camp Basin deposits are widely distributed and well exposed throughout the hanging wall of the Ragged Ridge fault, but are not found within the hanging wall of the Blackrock fault. It is possible, however, that deposits equivalent to the Horse Camp sediments do exist above the Blackrock fault, but have been buried by younger Tertiary and Quaternary deposits.

Another apparent problem with a Blackrock-Ragged Ridge fault correlation is the spatial relationship between the faults and the axial plane of the White Pine anticline. In the southern White Pine Range, the trace of the Blackrock fault lies 5-2½ km west of the axial trace of the anticline (Fig. 4a). Near Currant Gap, the Ragged Ridge fault occurs less than ½ km west of the axial trace (Fig. 4a). This is despite the fact that the area near Currant Gap has been eroded down to a lower structural level; a west-dipping fault plane

is expected to crop out increasingly to the west at lower structural levels. These spatial relationships are inconsistent with a simple oblique left-lateral offset of a single west-dipping fault, therefore I suggest that the two faults are not an offset single fault.

The preferred interpretation is that these two faults developed with similar geometries and kinematics under the same stress regime, but that they developed independently from one another. In this scenario, both faults would be roughly the same age, would be the main contributors in the delineation of the Horse and White Pine ranges with significant horizontal separation (>6 km) (19,000 ft), would cut older bedding-parallel faults (i.e., the Silver Spring and Currant Gap faults), and would both terminate at and transfer strain onto the Currant Summit fault. This slip transfer implies a change in the magnitude of offset along the Currant Summit fault west of the intersections of the Blackrock and Ragged Ridge faults.

High-Angle Normal Faults

Cross-cutting relationships between the three sets of faults in domain 1 suggest that this domain experienced up to three different episodes of high-angle normal faulting. These are an early period of north-south extension, followed by northwest-southeast extension, followed by northeast-southwest extension. Significant differences in fault strike among temporally distinct sets may indicate periodic rotation of the regional stress field (e.g., Taylor and Switzer, 2001). Regional paleostress reconstructions in the Great Basin indicate a northeast-southwest extension direction in the early to middle Miocene followed by northwest-southeast extension in the late Miocene (Best, 1988; Zoback, 1989). The temporal timing relationships observed here do not agree with those

interpreted for the Great Basin as a whole and likely represent the history of a local stress field, an aberration in the regional stress field or pre-Miocene extension.

The local stress field history of domain 1 is similar to the stress field history interpreted by Williams (2000) west of the study area. Williams (2000) reports northwest-southeast extension followed by a period of east to northeast extension. He concluded that a local rather than regional stress field was responsible for the different fault sets.

Analyzing cross-cutting relationships within high-angle normal faults of domain 2 failed to establish consistent timing patterns among faults. Inconsistent timing patterns of faults may indicate that the faults were active at the same time. Langrock (1995) reported similar inconsistencies among apparently randomly oriented high-angle faults within the hanging wall of the Blackrock Fault near Blackrock Canyon (Fig. 8). She showed that these faults display an orthorhombic symmetry and were active at about the same time (Langrock, 1995). Synchronous faults in multiple orientations more likely form in three-dimensional (3-D) strain fields (Reches and Dieterich, 1983; Langrock, 1995, Lonergan and Cartwright, 1999; Taylor and Novak, in press), in contrast to sub-parallel, temporally discrete fault sets predicted in classical Andersonian fault theory (Anderson, 1951). Although these timing and geometric characteristics can form several different ways, Langrock (1995) favors a model where 3-D strain results from the transport of the Blackrock fault hanging wall over a non-planar footwall. The non-planar geometry of the Blackrock fault is evident from Langrock's mapping, which reveals that the fault near Blackrock Canyon consists of both north- and east-striking segments that connect across a sharp bend. She also documented a large pronounced corrugation extending ~1 km to

the northwest that occurs in part of the north-striking segment. Translation of the upper plate over this highly irregular footwall results in volume disparities in the hanging wall, causing non-conservative 3-D strain.

Although most of the bedrock in domain 2 is covered by Tertiary-Quaternary alluvium, making it difficult to determine if faults display an orthorhombic pattern, most faults in domain 2 are also interpreted to be the result of 3-D strain created above a non-planar footwall. Within the study area, the Blackrock fault makes a major bend in strike from north-south to roughly east-west as it bends around the southwest margin of the White Pine Range (Fig. 4; Plate 1). The surficial trace of the east-striking segment is very irregular (Fig. 4; Plate 1) indicating that much of the southwest-dipping fault plane is also non-planar. The Ragged Ridge fault also appears to have at least one fault bend within the map area where a north-striking segment intersects a northwest-striking segment northwest of Currant Gap (Fig. 4; Plate 1). Because no domain 2 fault cuts across the Blackrock or Ragged Ridge faults, there is little doubt that the majority of domain 2 faults are related to movement on the detachments. Map patterns show that the detachments are highly non-planar, therefore, domain 2 faults can be reasonably interpreted to be a result of 3-D strain in a manner similar to hanging-wall faults near Blackrock Canyon.

Railroad Valley Fault

A high-angle fault that created a scarp within the fan deposits south of Silver Spring Canyon indicates east-west extension possibly as late as Quaternary time. About 4 km to the south, outside of the map area, another scarp formed where a west-dipping fault separates alluvial deposits from Mississippian units and Tertiary volcanic rocks (Fig. 4).

This and several other generally north-striking scarps documented along the eastern margin of Railroad Valley have been interpreted to be part of the range-bounding Railroad Valley fault (Fig. 8) (Effimoff and Pinezich, 1981; Walker et al., 1992; McCutcheon and Zogg, 1994). Ages and geometries similar to other scarps suggest that the Tertiary-Quaternary scarp mapped in this study is a segment of the Railroad Valley fault.

Currant Summit Fault

The Currant Summit fault is considered to be the main structure responsible for the apparent left-lateral offset of the White Pine and Horse Ranges (Lumsden, 1964; Moores et al., 1968; Williams, 2000). Considered to be the easternmost expression of the Pritchards Station lineament (Fig. 6), the Currant Summit fault likely continues westward across Railroad Valley. Although no surficial expression of the Currant Summit fault occurs within the map area, the strike projection of the fault would place it somewhere along the southern margin of the White Pine Range. A westerly continuation of the fault is also suggested by Bouguer gravity anomaly data that indicate a linear division between two sub-basins within Railroad Valley at the approximate latitude of the Currant Summit fault (Snyder et al., 1984; Saltus 1988).

Two options for the location of the western continuation of the Currant Summit fault are possible (Fig. 4). One possibility is that the fault trace trends to the west by northwest from near Crystal Spring, straddling the narrow region north of the large block of Tertiary volcanic rocks and just south of the range front (Fig. 4). This interpretation agrees best with the documented consistently west-trending trace of the Currant Summit fault. Also, although this narrow area is mostly covered by alluvium, the nearby rocks are

highly fractured and faulted, consistent with two major structures (Currant Summit and Blackrock faults) coming close together.

Another possibility is that the fault bends sharply to the southwest, concealed beneath alluvium, placing a large Tertiary volcanic block on the Devonian carbonate rocks of Dell Hill (Fig. 4). However, it seems unlikely for the consistently east-west-striking fault to take a sudden 45° bend to the southwest.

East of the study area, Williams (2000) shows that a different number of high-angle normal faults occur to the north than to the south of the Currant Summit fault. The northern and southern populations of high-angle faults also have different geometries leading to the interpretation that high-angle normal faults terminated at, rather than were offset by, the Currant Summit fault (Williams, 2000). Therefore, most high-angle normal faults are contemporaneous with and transfer strain onto the Currant Summit fault (Fig. 7) (Williams, 2000). Williams (2000) demonstrated that the Currant Summit fault is a transfer fault following the classification system of Faulds and Varga (1998). This transfer fault model consists of a transverse fault that is parallel to the extension direction and has sets of extension-parallel normal faults that terminate at the transfer fault (Faulds and Varga, 1998). Dip-slip motion on these normal faults is transmitted onto the transfer fault as predominantly strike-slip or perhaps oblique slip (Fig. 7). This model allows varying magnitudes of extension on either side of the transfer fault (Faulds and Varga, 1998). Despite widespread alluvial cover, it appears that this model is consistent with data from this study. No high- or low-angle normal fault was observed to propagate across the inferred trajectory of the Currant Summit fault. Nor can any two faults

terminating at and on opposite sides of the Currant Summit fault be correlated across the transverse fault as a single offset structure.

The relationship between the Currant Summit fault and the range-bounding Railroad Valley fault is uncertain. The north-south inferred trajectory of the Railroad Valley fault along the southwestern margin of the range appears to be displaced about 1 km to the east at the latitude of the Currant Summit fault (Fig. 4; Plate 1), although the Railroad Valley fault may simply bend to the east without being offset.

It appears that the Currant Summit fault had a complex and protracted history. The Currant Summit fault accommodated strain from various structures throughout a period spanning from at least an incipient extensional phase involving bedding-parallel faults up to later-stage high-angle normal faulting, possibly including the Quaternary Railroad Valley fault. This composite history makes it impossible to quantify an amount of relative offset for the entire length of the fault. For example, the 3000 m (9800 ft) of strike-slip and 2000 m (6500 ft) of dip-slip calculated from the offset White Pine anticline by Williams (2000) is only valid for the area between the offset fold axis. A few thousand meters to the west of the anticlinal axis, both the Blackrock and Ragged Ridge faults terminate at and transfer their strain onto the Currant Summit fault, undoubtedly changing the amount of net slip on the transverse fault.

The apparent complex history of the Currant Summit fault may help explain a perplexing problem involving the northern margin of the Horse Camp basin. The Currant Summit fault is considered to be the northern margin of the Horse Camp Basin, facilitating much of the uplift in the southern White Pine Range that led to rapid sediment accumulation in the basin in the early Miocene (Horton and Schmitt, 1998). This implies

that the northern block of the Currant Summit fault was topographically high during this time. This is inconsistent with the ~2000 m (6500 ft) of down-to-the-north net slip currently observed along much of the exposed trace of the Currant Summit fault (Williams, 2000). This apparent inconsistency can be explained by assuming a composite history on the Currant Summit fault where, for example, in Miocene time slip was up-to-the-north, perhaps as a product of uplift of the Blackrock footwall. Later, motion on a younger generation of low- and/or high-angle faults that transferred strain onto the Currant Summit fault resulted in the presently observed left-lateral down-to-the-north slip.

Regional Implications

Timing of Extension

Early Cenozoic extension and basin formation in east-central Nevada are marked by the deposition of continental deposits of the Paleocene to Eocene Sheep Pass Formation (Fouch et al., 1979). These sediments unconformably overlie deformed Paleozoic rocks as old as Devonian and were deposited in local basins that do not coincide with the modern margins of basins, including Railroad Valley (Kellogg, 1964; Francis and Walker, 2001). In the Pancake Range, Sheep Pass Formation overlies the Cretaceous Newark Canyon Formation (Fouch et al., 1979; Perry and Dixon, 1993). Sheep Pass deposits do indicate that basin formation occurred in Paleocene to Eocene time.

In and around Railroad Valley, volcanic rocks of the Garrett Ranch Group were deposited prior to the onset of major extension and modern basin formation (Moores et al., 1968; Peterson, 1994). A crude unroofing sequence found in early valley fill

sediments indicates that the volcanic rocks were present where the ranges are currently positioned (McCutcheon and Zogg, 1994).

Early Horse Camp Basin deposits rest unconfomably on 26 Ma tuff of the Shingle Pass Formation indicating that major extension and infilling of synextensional sediments into the early modern basins began after the late Oligocene (Taylor et al., 1989; Horton and Schmitt, 1996). A Barstovian age camel skull found in the lower portion of the deposits further constrain major basin development to have begun in the middle Miocene (T. Fouch, quoted in Horton and Schmitt, 1998). Using provenance studies, the distribution of sedimentary facies, and soft sediment deformation, Horton and Schmitt (1998) show that a significant portion of the sediment source during middle to late Miocene Horse Camp Basin formation was from the northern and southern margins of the basin. This relationship was interpreted to indicate that the initial major uplift of the southern White Pine Range to the north and the Grant Range to the south occurred in the mid-Miocene (Horton and Schmitt, 1998).

The timing of uplift of the northern Grant Range indicated by Horse Camp deposits agrees well with the conclusions of Lund et al. (1993) who favor a middle to late Miocene age for maximum extension there. Also, the west-dipping detachment faults responsible for the major uplift of the central and southern Grant Range were active in the middle to late Miocene (Fryxell, 1988; Bartley and Gleason, 1990).

A model by Lumsden (1964) proposes that contemporaneous uplift and extension of the southern White Pine Range was triggered by the emplacement of the Silver Spring and Railroad stocks. In a similar model, Walker et al. (1992) envision the stocks as hot diapirically-rising granite or possibly as reheated and vertically remobilized Mesozoic

plutons that directly spurred the domal uplift of the southern White Pine Range. The timing of these models involving active intrusive arching of the range, however, is hard to reconcile with the stratigraphic record of the Horse Camp basin. The crystallization age of the plutons is late Eocene to early Oligocene, while Horse Camp Basin sediments indicate that major uplift of the southern White Pine Range did not start until the Middle Miocene, more than ~15 m.y. after the emplacement of the plutons (Horton and Schmitt, 1996, 1998). Post-plutonism extension and uplift is supported by the fact that low-angle normal faults clearly cut the stocks and their contact metamorphic aureoles.

The major uplift of the southern White Pine Range, indicated by the Horse Camp basin deposits, was most likely accommodated by movement on the Blackrock fault. The Blackrock fault has >8 km (26,000 ft) of heave and has been shown to extend >20 km along the western margin of the range (Fig. 8). Data from this study show that the Blackrock fault continues along much of the southern margin of the range as well. Therefore, the Blackrock fault is considered to be the main factor in the uplift of the range throughout the Miocene. Because the Silver Spring fault is cut by the Blackrock fault, slip on the bedding-parallel faults is interpreted to have occurred sometime between ~33 Ma (age of stock cut by the Silver Spring fault) and the mid Miocene, prior to the delineation of the White Pine Range. Because synextensional sediments or other evidence for basin formation before the mid Miocene are not known, slip on the bedding-parallel faults is interpreted to have accommodated extension at depth, resulting in little topography at the surface.

K-feldspar $^{40}Ar/^{39}Ar$ data from the Railroad stock may provide constraints on the timing of motion along the bedding-parallel faults. As discussed in a previous section,

these data support intrusion of magma into the relatively shallow Cambrian section at ~33 Ma. Shallow emplacement resulted in very rapid cooling through ~350° C (upper closure interval for K-feldspar) (McDougall and Harrison, 1999) (Fig. 18; Appendix A). The interval of the age spectrum showing a shallow age gradient from ~32 to ~29 Ma (Fig. 18) may indicate relatively rapid cooling due to tectonic denudation, here, interpreted to be a result of slip on the Silver Spring fault and other bedding-parallel faults. The inflection to a steeper age gradient in the spectrum from ~29 Ma to ~18 Ma (Fig. 18) may indicate a transition to slower cooling during thermal reequilibration of the crust following the cessation of denudation along the bedding-parallel faults.

In light of field structural data, the distribution of synextensional sediments, and $^{40}Ar/^{39}Ar$ thermochronology data, I suggest that the initial attenuation of the crust near the present southern White Pine Range was directed to the southwest and began in the early Oligocene. This initial attenuation contributed very little to the delineation of the modern Railroad Valley, occurring at depth along bedding-parallel attenuation faults that developed along southwest-dipping stratigraphic anisotropies. In this interpretation, major uplift of the White Pine Range did not occur until the mid Miocene motion along the Blackrock fault.

A Proposed Regional Detachment

Similar timing and structural styles documented in the southern White Pine and Grant ranges make it tempting to hypothesize that a single structural model can be applied to the entire eastern margin of Railroad Valley. Francis and Walker (2001) proposed a unifying model where they interpret that attenuation on a regional detachment, extending from the central White Pine Range southward throughout the Grant Range, is responsible

for the formation of Railroad Valley. They suggest that this detachment, called the White Pine detachment, occurs almost exclusively at the position of the weak Mississippian Chainman Shale. In some places, they explain, the Chainman Shale along with much of the Paleozoic section have been completely attenuated so that rocks as young as the Pennsylvanian Ely Limestone lie on top of rocks as old as Cambrian (Walker et al., 1992; Francis and Walker, 2001). Therefore, they expand their definition to include post-Chainman rocks that structurally lie on top of pre-Chainman rocks. Using this criterion, they attempt to correlate the Blackrock fault to other detachments throughout the Horse and Grant ranges (Francis and Walker, 2002a). They also produced a structure contour map that indicates a continuous fault surface throughout the ranges and Railroad Valley (Francis and Walker, 2001; 2002a).

Comparison of available structural data for the ranges illustrates the difficulties in applying a model involving a single regional detachment. Many major detachment faults exposed throughout these ranges do not meet the criterion to represent a segment of the White Pine detachment as defined by Francis and Walker (2001). While one of the several stacked detachments mapped by Lund et al. (1993) does place post-Chainman rocks on Devonian and Silurian rocks, the remaining detachments do not. The major range-forming west-dipping faults mapped by Fryxell (1988) in the central Grant Range clearly did not follow any single stratigraphic horizon, cutting downsection in both the footwalls and hanging walls. Therefore they could not be considered to be equivalent to the White Pine detachment. Perhaps the biggest difficulty with the regional detachment model is the abundant evidence that shows that the Chainman Shale was deformed, faulted, and discontinuous prior to detachment formation (Taylor et al., in press). Folds

and thrusts associated with the Mesozoic central Nevada thrust belt disrupted the Paleozoic section in the White Pine, Horse, and Grant Ranges (Fryxell, 1988; Bartley and Gleason, 1990; Carpenter et al., 1993; Taylor et al., 1993; Langrock, 1995; Williams, 2000) as well as beneath Railroad Valley (Carpenter et al., 1993; Langrock, 1995; Gilbert, 2002). It is therefore difficult to imagine a regional detachment forming along such a deformed and discontinuous stratigraphic horizon.

In addition, the documented slip directions on many of the major detachment faults vary greatly, indicating that each developed independently (Fig. 8). Slip on the Blackrock fault was to the west-northwest (Langrock, 1995). The Silver Spring fault is top-to-the-southwest. Faults in the northern Grant Range slipped due west (Lund et al., 1993). In the central Grant Range, top-to-the-west faults cut top-to-the-east faults (Fryxell, 1988). These differences in extension direction preclude the possibility that these detachments formed as a continuous fault.

Late Miocene to Holocene Extension

A time of tectonic quiescence appears to have existed following major uplift of the southern White Pine Range in the late Miocene. By mid late Miocene, coarse grained facies in the Horse Camp Basin were restricted to the eastern margin of the basin. This indicates that uplift of the northern and southern margins had slowed and that the only source of sediment was from the Horse Range, immediately to the east (Moores, 1968; Horton and Schmitt, 1998). Even more compelling for the argument of tectonic quiescence in the southern White Pine Range are the outcrops of small remnants of highly indurated conglomerate perched along the western wall of Plane Crash Canyon (Plate 1). Lumsden (1964) first recognized this conglomerate, naming it the Broom

Canyon fanglomerate because of other isolated patches of the unit mapped just north of the map area in Broom Canyon. These alluvial deposits are exposed at elevations as high as 2300 m (7600 ft), at least 300 m (1000 ft) higher than the present fan surface surrounding the southwestern margin of the range (Plate 1). These old deposits are interpreted to represent small remnants of a once extensive alluvial fan that accumulated while the uplift of the range slowed dramatically in the late Miocene (Lumsden, 1964). Later uplift and erosion removed much of this fan except for a few isolated patches in the deep canyons.

Starting in the late Miocene, as detachment faulting waned in the southern White Pine Range, a new phase of extension began that involved high-angle normal faulting. Numerous, mostly minor-offset high-angle faults cut and displace the bedding-parallel faults. These faults occur throughout the footwall of the Blackrock and Ragged Ridge faults and their varying strikes indicate that the local stress field had rotated from north-south to northwest-southeast to northeast-southwest.

In the late Miocene, the locus of uplift shifted westward from the Blackrock and Ragged Ridge faults that had controlled major uplift, to the Railroad Valley fault (Lumsden, 1964; Horton and Schmitt, 1998). The White Pine, Horse and Grant ranges along with much of the Horse Camp basin became the footwall of the newly formed Railroad Valley fault (Horton and Schmitt, 1998). Uplift of these ranges continues today along this fault as indicated by fault scarps in Quaternary deposits.

Whereas numerous springs, seeps, and scarps that are aligned with a steep gravity gradient provide strong evidence for the Railroad Valley fault (Lumdsen, 1964; Kleinhampl and Ziony, 1985), the geometry of the fault south of Beaty Canyon in the

northwestern Grant Range is uncertain (Lund et al., 1993). South of Beaty Canyon, the number of springs decreases and gravity gradient is not as steep (Lund et al., 1987; 1993; Blank, 1991; Grow et al., 1992). Seismic reflection profiles across Railroad Valley south of Beaty Canyon have been interpreted to indicate both high- and low-angle range-bounding faults (e.g., Anderson et al., 1983; Effimoff and Pinezich, 1986; Liberty et al., 1994). However, a high-resolution seismic line across the Grant Canyon oil field reportedly shows a gently dipping reflector that can be traced from the valley to surface exposures of west-dipping detachments in the range, without being displaced by a younger high-angle fault (Potter et al., 1991; Lund et al., 1993). Lund et al. (1993) conclude that the west-dipping stack of detachments merge into a single west dipping fault zone that projects beneath the valley and is not cut by the Railroad Valley fault.

Structural Development of Railroad Valley

Figure 20 schematically shows the differences in structural style observed along the eastern margin of Railroad Valley. Tertiary extension and uplift were localized along the present-day trend of the White Pine, Horse, and Grant ranges. However, different extensional systems evolved locally. While major uplift occurred approximately within the same time frame, and primarily by a mode of detachment faulting, fault data show that each domain developed independently. Significant differences in fault geometry and slip direction, amount of extension, and number of faults invalidate structural models that attempt to correlate a regional detachment system.

Transverse faults play an important role in separating some of these structural domains. These structures allow two distinct fault systems with different magnitudes and styles of extension to operate next to one another (Fig. 7). This undoubtedly, is the role

played by the Currant Summit fault which acts as a transfer fault, facilitating differential strain between the more highly extended White Pine Range and the Horse Range (Williams, 2000). Likewise, it appears that the Stone Cabin-Ragged Ridge fault zone serves a similar purpose separating the different structural systems observed in the Horse and Grant ranges (Fig. 20).

The reasons for the development of differing structural styles are many and complex. However, one factor may be the pre-extensional geometries of structures and strata. The trajectory and geometry of the Silver Spring and other bedding-parallel faults was influenced directly by the pre-extensional geometry of alternating stratigraphic sections of strong carbonate and less competent shales as part of a Mesozoic fold. Langrock (1995) suspects that the Blackrock fault might, in part, have followed and reactivated a Mesozoic thrust. Therefore, the distinct structural style observed in the southern White Pine Range may be a product of pre-extensional geometries that were not present in the other ranges.

CHAPTER 7

SUMMARY AND CONCLUSIONS

The structure of the southern White Pine Range records Mesozoic contractile deformation and significant Cenozoic extension. Geologic mapping; retrodeformable cross-sections; regional structural and stratigraphic analyses; $^{40}Ar/^{39}Ar$ thermochronology; and geometric, kinematic, and temporal analysis of structures allow the reconstruction of the structural development of this part of the range. These data show the Oligocene to late Miocene dismemberment of a large-scale Mesozoic fold by two episodes of low-angle normal faulting. Beginning in the late Miocene and continuing to the Quaternary, several episodes of high-angle normal faulting continued to extend and uplift the range. The Cenozoic structural style documented in the southern White Pine Range is similar to but kinematically and temporally distinct from structural styles seen in other ranges bounding the 150 km long Railroad Valley.

Paleozoic strata in the southern White Pine Range are folded into a large asymmetric range-scale fold, the White Pine anticline. The discordance of Tertiary volcanic rocks with the underlying Paleozoic section, significant sub-Tertiary paleorelief, and evidence for shallow emplacement of Oligocene plutons indicate that contractile deformation occurred prior to volcanism. The proximity and similar geometric structure of the White Pine anticline and structures of the late Jurassic to early Cretaceous central Nevada thrust

belt indicate that large-scale folding exhibited in the southern White Pine range is part of this belt and therefore, is Mesozoic in age.

Map relationships and $^{40}Ar/^{39}Ar$ thermochronology show that early extension in the area occurred mainly at depth accommodated by the Silver Spring fault and other bedding-parallel faults beginning in the early Oligocene. However, sediments of the Tertiary Horse Camp basin indicate that maximum extension and uplift via slip on the Blackrock fault occurred during a period from the early to late Miocene (Horton and Schmitt, 1998). The Silver Spring fault generally conforms to the shape of the White Pine anticline. Kinematic analysis of fault-related folds suggests a southwest slip direction. The Silver Spring and other bedding-parallel faults are interpreted to have localized along mechanical anisotropies defined by strong carbonate rocks lying on weak shales and thin-bedded limestone. As part of the southwest-dipping limb of the White Pine anticline, these planar mechanical contrasts were in a favorable geometry to facilitate low-angle fault formation during early extension. The domal shape of the bedding-parallel faults is attributed to the pre-extensional geometry of the anisotropies and later tilting rather than a product of isostatic rebound. Although some eastward tilting of the southern White Pine block by either isostatic rebound or nearby large-scale normal faults is likely.

Bedding-parallel faults are viewed as important components of incipient crustal thinning in the area, although the large-displacement Blackrock fault that bounds much of the western and southern margins of the range is considered to be the principle factor in the uplift of the southern White Pine Range. Randomly oriented and temporally

inconsistent high-angle normal faulting developed in the upper plate of the Blackrock fault as it was transported over a non-planar footwall.

Starting in the late Miocene, high-angle normal faulting played the major role in extension and uplift. At least four distinct episodes of high-angle normal faulting overprint the bedding-parallel faults. East-striking faults are cut by northeast-striking faults, all of which are cut by northwest-striking faults, indicating a rotation of the local stress field through time. The latest episode of faulting cuts Quaternary sediments and is part of the range-bounding Railroad Valley fault system that was responsible for the latest (late Miocene to Holocene) uplift of much of the ranges east of Railroad Valley.

A comparison of the structural model for the southern White Pine range to structural styles observed in other ranges comprising the eastern margin of Railroad Valley shows that several different structural styles contributed to basin development. This contradicts Railroad Valley structural models that require a single regional detachment. While detachment faulting is an important factor in uplift throughout the basin margin, significant differences in geometries and slip direction on documented detachments preclude any attempt to correlate detachments throughout the range as part of a regional model. There appears to be at least four different structural systems responsible for range uplift in the southern White Pine, Horse, northern Grant, and southern Grant-Quinn Canyon ranges. These structural domains are commonly separated by extension-parallel transverse faults. These structures are interpreted to be transfer faults, which separate regions with different magnitudes of extension, by allowing normal faults to transfer strain onto the east-west-striking structures.

APPENDIX A

$^{40}Ar/^{39}Ar$ METHODS

One quartz monzonite sample (RR2) from the Railroad stock was collected for $^{40}Ar/^{39}Ar$ K-feldspar thermochronology. Several kilograms of sample were collected approximately 10 m (30 ft) below the trace of the Silver Spring fault (Fig. 4) and trimmed of weathered surfaces. Thin sections were produced from the sample and inspected for sample quality. The sample was then crushed and sieved to a uniform size. K-feldspar was separated using conventional heavy liquid techniques. Sixty mg of clean and mono-mineralic K-feldspar crystals were handpicked under a binocular microscope. The mineral separation was completed at facilities in the University of Nevada, Las Vegas, Geoscience Department.

The separate was irradiated at the TRIGA type reactor at Oregon State University along with K-glass, Ca-F, and sanidine from the Fish Canyon tuff to monitor the neutron dosage and interfering reactions on potassium and calcium. Following irradiation, the sample was analyzed at the Nevada Isotope Geochronology Laboratory at the University of Nevada, Las Vegas using a double vacuum resistance heated furnace, MAP 215-50 mass spectrometer, and LabView software (written by B. Idelman, Lehigh University).

K-feldspar Modeling

K-feldspars were step heated using a 50-step heating schedule including isothermal duplicates to obtain kinetics information. An age spectrum and Arrhenius plot were then constructed from the step heating data. The form of the age spectrum is a function of geologic cooling of the sample since crystallization. The Arrhenius plot, produced by plotting the natural log of the diffusion coefficients D_o/r^2 (D_o= frequency factor, r= diffusion domain size) against the inverse temperature of the laboratory heating schedule, is a function of the diffusion characteristics of the sample (McDougall and Harrison, 1999). Arrhenius plots of the step heating results show departures from linearity caused by the presence of multiple diffusion domain sizes (Lovera, 1989). The initial low-temperature gas release is produced by smaller domain sizes. Because K-feldspars need to be completely melted in order to degas entirely, the highest temperature data (>~1100° C) typically do not represent volume diffusion information and are excluded from analyses (McDougall and Harrison, 1999).

The next step in the multiple diffusion domain procedure is to model Arrhenius data using computer programs (Lovera et al., 2002). Synthetic Arrhenius plots are produced by applying data ordered according to the lab heating schedule to various combinations of domain sizes until a distribution is found that will reproduce the Arrhenius data determined in the laboratory. A satisfactory domain distribution is expressed in a plot of log r/r_o vs. $\%^{39}Ar$ released (McDougall and Harrison, 1999). A high correlation between the log r/r_o plot, produced during heating in the lab, and the age spectrum, a product of natural geologic cooling, indicates that the same diffusion mechanism operated in the lab as in nature. Well-correlated laboratory and model distributions allow you to use

computer modeling to find thermal histories that reproduce the internal argon distribution determined in the lab.

$^{40}Ar/^{39}Ar$ Results

Step heating data (Table 1) and the associated age spectrum (Fig. 18) for the K-feldspar from the Railroad stock show a large range of ages from ~19 to ~137 Ma during the first 4% of ^{39}Ar released. During this interval, the first steps of the isothermal pairs are much older (~20-108 m.y.), indicating the likelihood of excess argon. The next 18% of ^{39}Ar released shows a variably steep gradient of apparent ages from ~18 to ~29 Ma followed by a more gradual increase from ~29 to ~32 Ma for the following 20% of gas released. The remaining 59% of gas released, excluding the final step, forms a relatively flat age spectrum but falls short of meeting the criteria for a plateau. However, a weighted mean age of 33.17 $\pm$ 0.18 Ma (1σ) calculated for this segment is considered to be the "preferred age" of the stock.

The age spectrum and the Arrhenius plot (Fig. 19) show poor duplication of the isothermal pairs indicating that the K-feldspar sample is not suitable for multi-diffusion domain modeling. In addition, poor correlation of the log r/r_o plot and age spectrum indicate that the sample violates one or more of the assumptions inherent to the multi-diffusion domain modeling technique. Indeed, the computer modeling program of Lovera (2002) failed on each attempt to model the Arrhenius data.

There are several possible reasons for why the modeling failed, such as excess argon from fluid inclusions or abundant deuteritic alteration. However, inspections of thin sections made from the sample as well as the single crystal separate reveal that the

sample was relatively clean and inclusion free. One common violation of the underlying assumptions for multi-diffusion domain modeling is that cooling of the K-feldspar is slow and monotonic (McDougall and Harrison, 1999). As discussed in Chapter 7, field evidence indicates that the Paleozoic section in the southern White Pine Range was uplifted and deeply eroded down as low as to Devonian strata prior to the deposition of the Oligocene volcanic rocks. Therefore, a likely explanation for the failure of the K-feldspar modeling is that the Cambrian section at the time of intrusion was fairly shallow and thus the magma cooled quickly. This interpretation is consistent with the fact that the large diffusion domains from the interval of ~44 to ~100% ^{39}Ar released yield a flat age spectrum at ~33 Ma (Table 1, Fig. 18) which is indistinguishable from the zircon crystallization ages of 33.8 $\pm$ 9.7 and 35.1 $\pm$ 5.7 Ma (Taylor et al., 1996). A shallow intrusion is also supported by the relatively small crystal size of the stocks as well as the thin, low-grade metamorphic contact aureole surrounding the stocks.

Despite the inability to model the thermal history for the sample, the age spectrum can still provide limited but meaningful interpretation and thermal constraints on the K-feldspar. Although most of the age spectrum and log r/r_o plot exhibit poor correlation, steps 17 to 43, constituting ~35% of the ^{39}Ar released, show good correlation between the two. This is interpreted to indicate that this volume of gas was released in the lab by the same boundary and diffusion mechanism as that in nature. Therefore, some thermal constraints can be derived from this portion of the age spectrum.

The age spectrum is interpreted to show crystallization and geologically instantaneous cooling of the intrusion from ~750° C to the closure temperature of Ar in K-feldspar (~350° C) at ~33 Ma. The gradually increasing age pattern from steps 33 to 43 indicates

rapid cooling from ~32 to ~29 Ma (Fig. 18). This can be interpreted to be a result of accelerated crustal denudation due to slip on normal faults. The steep gradient of ages from steps 17 to 31 indicates slow cooling from ~29 Ma to ~19 Ma, most likely due to thermal reequilibration of the intrusion to the ambient crustal temperature during relative tectonic quiescence with only erosional denudation occurring. Interpretations on specific faults that may have influenced this thermal history are discussed in Chapter 7.

APPENDIX B

MESOSCALE FOLD DATA TABLE

Silver Spring Detachment

fold	plunge & trend of axis	strike & dip of axial plane	fold	plunge & trend of axis	strike & dip of axial plane	fold	plunge & trend of axis	strike & dip of axial plane	fold	plunge & trend of axis	strike & dip of axial plane
1	11° 165°	350° 24° E	29	34° 152°	290° 33° N	57	24° 155°	306° 28° N	85	15° 115°	274° 15° N
2	19° 146°	354° 07° W	30	32° 160°	329° 29° E	58	18° 284°	277° 18° N	86	14° 118°	340° 20° E
3	06° 125°	319° 12° E	31	27° 155°	300° 46° N	59	23° 117°	268° 15° N	87	03° 100°	071° 25° N
4	04° 116°	301° 30° N	32	22° 170°	314° 29° N	60	21° 107°	298° 14° N	88	01° 093°	064° 11° S
5	04° 106°	070° 18° N	33	17° 120°	344° 06° E	61	35° 136°	291° 34° S	89	27° 164°	331° 15° E
6	10° 130°	284° 22° N	34	15° 117°	309° 15° N	62	29° 121°	305° 20° S	90	21° 143°	340° 40° E
7	12° 347°	002° 05° E	35	06° 111°	306° 36° N	63	20° 147°	314° 21° N	91	30° 138°	290° 31° N
8	13° 300°	319° 09° E	36	19° 114°	317° 23° E	64	48° 132°	325° 59° E	92	10° 176°	322° 25° E
9	09° 359°	351° 22° E	37	22° 109°	291° 19° N	65	24° 101°	280° 19° N	93	12° 085°	075° 19° N
10	10° 315°	311° 33° N	38	21° 111°	287° 30° N	66	17° 171°	359° 29° E	94	20° 083°	077° 35° N
11	08° 307°	297° 29° N	39	05° 110°	278° 33° N	67	16° 164°	352° 10° E	95	02° 080°	062° 34° N
12	11° 305°	350° 36° W	40	35° 107°	077° 39° N	68	32° 104°	288° 31° N	96	12° 184°	324° 15° E
13	13° 311°	342° 20° E	41	31° 098°	060° 32° N	69	23° 146°	318° 16° E	97	05° 176°	021° 25° W
14	17° 160°	359° 16° E	42	13° 160°	004° 09° W	70	16° 155°	309° 13° N	98	22° 116°	275° 15° N
15	15° 290°	301° 17° N	43	17° 140°	353° 19° E	71	03° 149°	297° 32° N	99	19° 191°	326° 19° E
16	19° 119°	089° 22° N	44	07° 120°	276° 22° N	72	08° 126°	304° 30° N	100	15° 148°	324° 14° E
17	17° 116°	333° 16° E	45	03° 103°	324° 25° E	73	26° 094°	069° 38° N	101	32° 105°	281° 26° N
18	32° 140°	299° 35° N	46	06° 109°	318° 19° E	74	16° 110°	284° 24° N	102	29° 099°	291° 14° N
19	25° 128°	314° 55° N	47	12° 127°	359° 08° W	75	30° 150°	345° 30° W	103	33° 317°	279° 36° N
20	22° 150°	340° 41° E	48	14° 344°	349° 10° W	76	28° 146°	342° 31° E	104	21° 201°	010° 37° E
21	44° 138°	301° 39° N	49	15° 295°	314° 18° N	77	21° 116°	318° 18° E	105	37° 335°	286° 44° N
22	29° 108°	330° 29° E	50	08° 345°	311° 21° N	78	12° 106°	326° 21° E	106	11° 177°	310° 21° N
23	32° 100°	288° 26° N	51	13° 310°	322° 19° E	79	23° 143°	355° 30° E	107	79° 085°	270° 83° N
24	25° 105°	089° 11° S	52	06° 305°	328° 12° E	80	21° 132°	340° 21° E	108	25° 324°	333° 32° E
25	34° 099°	071° 22° N	53	16° 315°	321° 20° E	81	04° 120°	349° 14° W	109	42° 329°	312° 46° N
26	20° 112°	272° 21° N	54	06° 327°	314° 24° E	82	14° 117°	305° 16° N	110	15° 185°	358° 12° W
27	07° 108°	282° 18° N	55	18° 310°	312° 14° N	83	19° 121°	311° 35° N	111	21° 170°	304° 23° N
28	05° 102°	315° 11° E	56	10° 290°	300° 11° N	84	11° 111°	316° 25° E	112	24° 115°	279° 31° N

Table 2. Fault-related fold measurements for the Silver Spring, Bristlecone, and Currant Gap detachments. Folds 1-102 are in Plane Crash Canyon, 103-165 are in Silver Spring Canyon, 166-176 are east of Plane Crash Canyon, and 177-195 are west of Silver Spring Canyon.

Silver Spring Detachment (continued)

fold	plunge & trend of axis	strike & dip of axial plane	fold	plunge & trend of axis	strike & dip of axial plane	fold	plunge & trend of axis	strike & dip of axial plane
113	24° 300°	291° 28° N	143	05° 319°	299° 05° N	173	20° 056°	030° 45° W
114	24° 341°	350° 27° E	144	03° 164°	333° 23° W	174	37° 072°	295° 18° N
115	14° 287°	276° 18° N	145	15° 153°	330° 19° E	175	17° 150°	280° 16° N
116	13° 111°	281° 21° N	146	22° 153°	336° 28° E	176	12° 050°	061° 21° S
117	23° 170°	325° 33° E	147	34° 136°	325° 35° E	177	17° 313°	350° 22° E
118	19° 143°	329° 25° E	148	07° 130°	302° 16° N	178	25° 297°	288° 27° N
119	36° 355°	350° 42° W	149	32° 127°	299° 46° N	179	10° 145°	280° 12° N
120	47° 166°	332° 51° E	150	04° 124°	294° 10° N	180	15° 134°	319° 21° W
121	37° 120°	290° 38° N	151	32° 171°	350° 42° W	181	23° 300°	270° 26° N
122	36° 307°	288° 36° N	152	31° 163°	332° 33° E	182	14° 195°	001° 26° W
123	43° 273°	086° 42° N	153	28° 319°	336° 33° E	183	05° 346°	350° 06° E
124	28° 147°	320° 30° E	154	40° 326°	319° 51° W	184	34° 331°	313° 42° E
125	39° 099°	271° 42° N	155	16° 180°	360° 26° W	185	20° 001°	006° 22° E
126	37° 088°	086° 52° N	156	38° 079°	086° 49° N	186	16° 349°	330° 23° E
127	09° 135°	310° 09° N	157	06° 293°	299° 10° N	187	20° 328°	331° 33° E
128	23° 101°	284° 36° N	158	21° 288°	277° 31° N	188	56° 086°	077° 60° S
129	14° 173°	339° 12° E	159	14° 273°	270° 16° N	189	09° 277°	280° 14° N
130	35° 120°	303° 42° N	160	15° 163°	349° 22° E	190	61° 292°	290° 55° N
131	16° 132°	302° 18° S	161	27° 132°	280° 19° S	191	08° 174°	346° 11° E
132	02° 279°	288° 06° N	162	11° 129°	304° 26° N	192	10° 358°	350° 15° E
133	09° 328°	339° 15° E	163	17° 287°	298° 17° S	193	05° 321°	311° 07° N
134	10° 311°	302° 12° N	164	22° 055°	045° 25° E	194	26° 025°	030° 56° E
135	32° 145°	312° 33° N	165	33° 256°	070° 40° N	195	29° 350°	344° 33° E
136	30° 320°	301° 42° N	166	27° 118°	349° 16° E			
137	29° 189°	358° 32° E	167	18° 341°	333° 22° E			
138	29° 329°	333° 29° E	168	32° 091°	087° 34° S			
139	16° 169°	341° 18° E	169	09° 080°	084° 14° N			
140	59° 091°	275° 62° S	170	07° 103°	316° 12° E			
141	48° 288°	280° 50° N	171	17° 255°	279° 24° N			
142	05° 105°	283° 25° N	172	41° 281°	339° 31° E			

Bristlecone Detachment

fold	plunge & trend of axis	strike & dip of axial plane
1	25° 320°	329° 29° E
2	27° 303°	308° 40° N
3	05° 331°	301° 21° N
4	28° 343°	331° 31° E
5	27° 120°	318° 10° W

Currant Gap Detachment

1	11° 030°	022° 69° E
2	20° 040°	035° 40° E
3	10° 041°	042° 81° E
4	14° 227°	056° 37° S
5	21° 084°	272° 32° N
6	23° 255°	086° 23° N
7	13° 112°	297° 9° N
8	13° 281°	290° 28° N
9	29° 301°	306° 24° N
10	25° 281°	275° 55° N
11	24° 101°	278° 18° N
12	7° 096°	273° 15° N
13	16° 077°	070° 40° N
14	32° 091°	089° 33° N
15	17° 263°	086° 51° N
16	23° 243°	060° 27° N
17	10° 050°	047° 44° N
18	39° 047°	040° 39° W
19	8° 291°	297° 19° N
20	29° 269°	280° 42° N
21	21° 076°	081° 25° N
22	16° 087°	270° 21° N

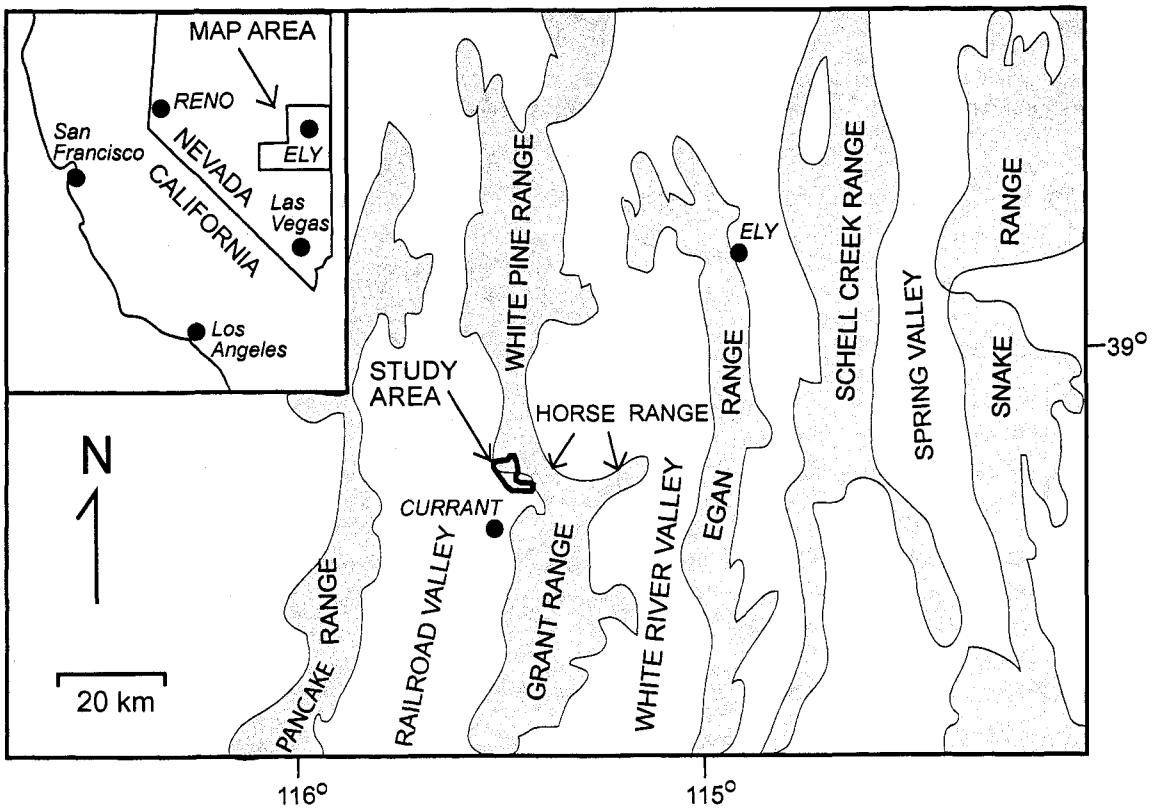

Figure 1. Map showing the location of the study area (modified from Francis and Walker, 2002a).

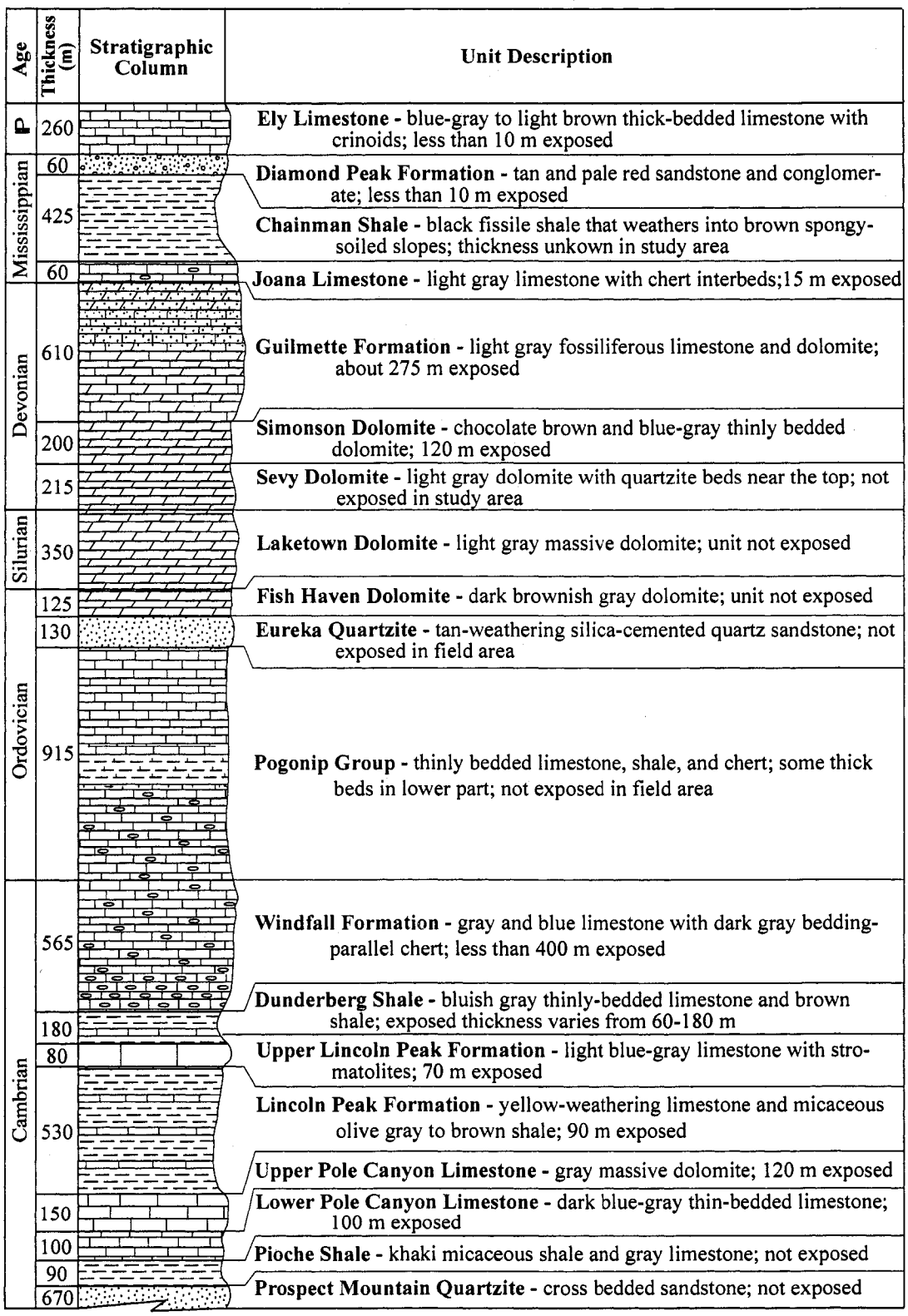

Figure 2. Paleozoic stratigraphy of the southern White Pine Range. Amounts in thickness column are regional thicknesses. Unit descriptions and thicknesses were determined in the field and compiled from Lumsden (1964), Moores et al. (1968), Williams (2000), and Lumsden et al. (2002).

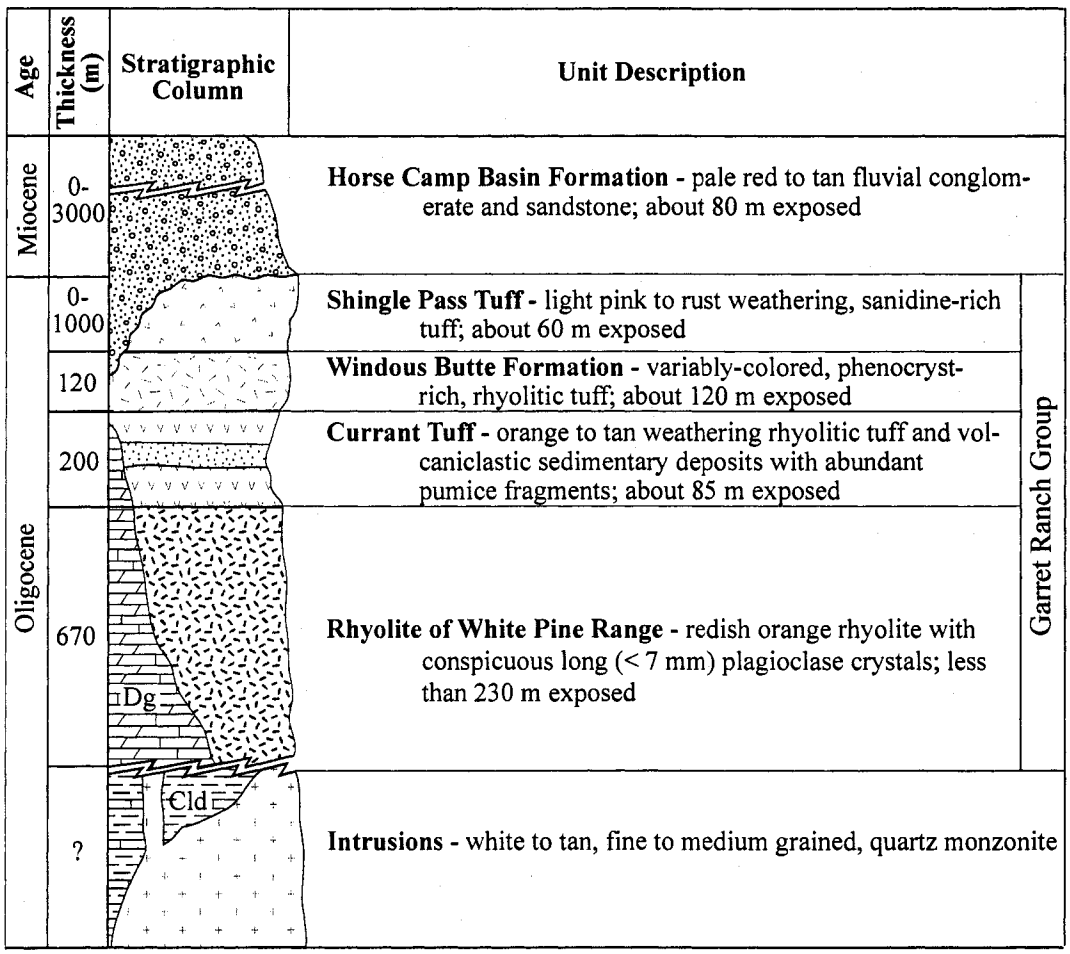

Figure 3. Tertiary units exposed in the southern White Pine Range. Amounts in thickness column are reported regional thicknesses. Unit descriptions and thicknesses were determined in the field and compiled from Lumsden (1964), Moores et al. (1968), Williams (2000), and Lumsden et al. (2002).

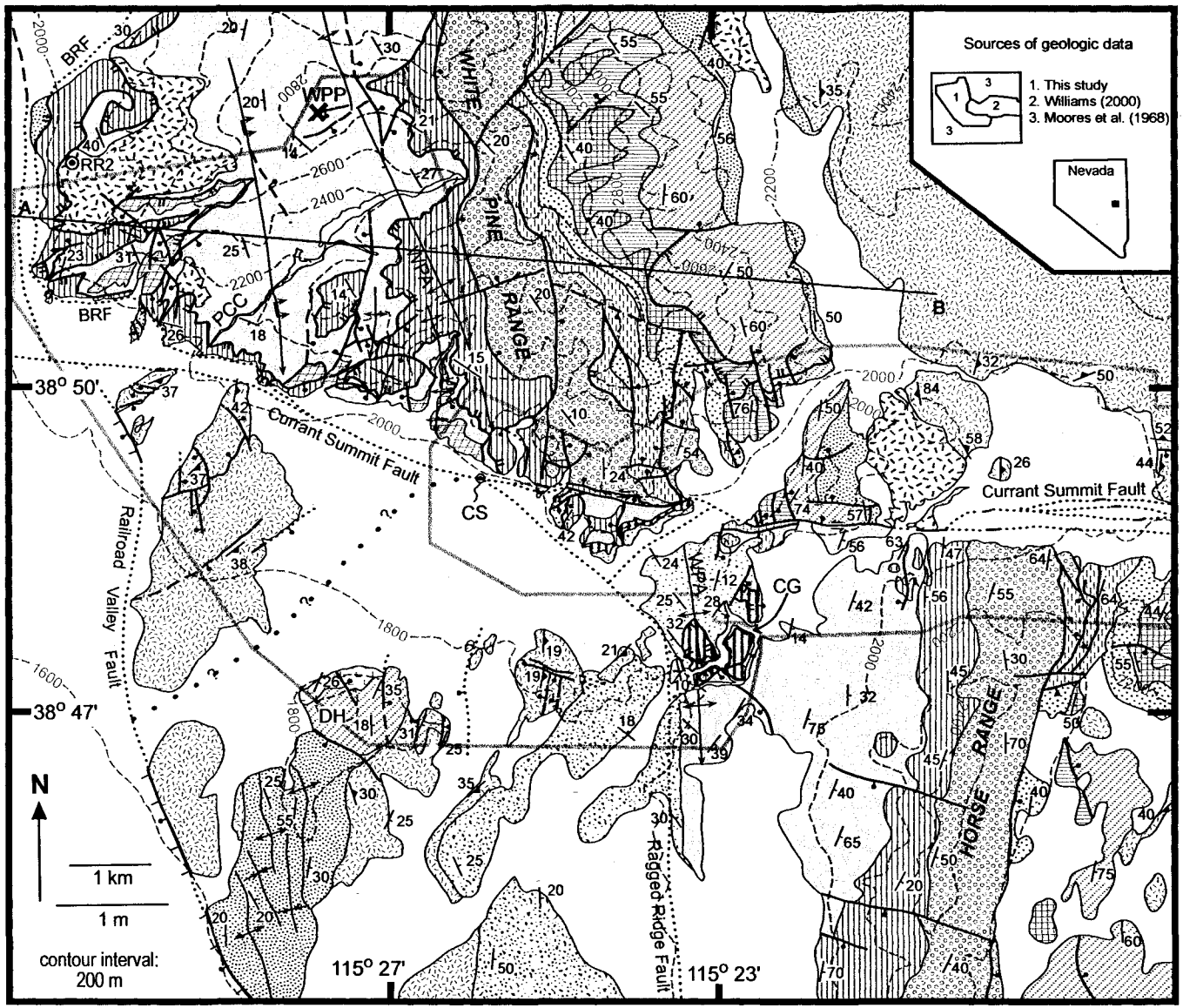

Figure 4a. Simplified geologic map of the southern White Pine and northern Horse ranges. Refer to Figure 4c for geologic units and symbols. Sources shown in inset. BRF - Blackrock Fault, CG - Currant Gap, CS - Crystal Spring, DH - Dell Hill, PCC - Plane Crash Canyon, WPA - White Pine Anticline, WPP - White Pine Peak.

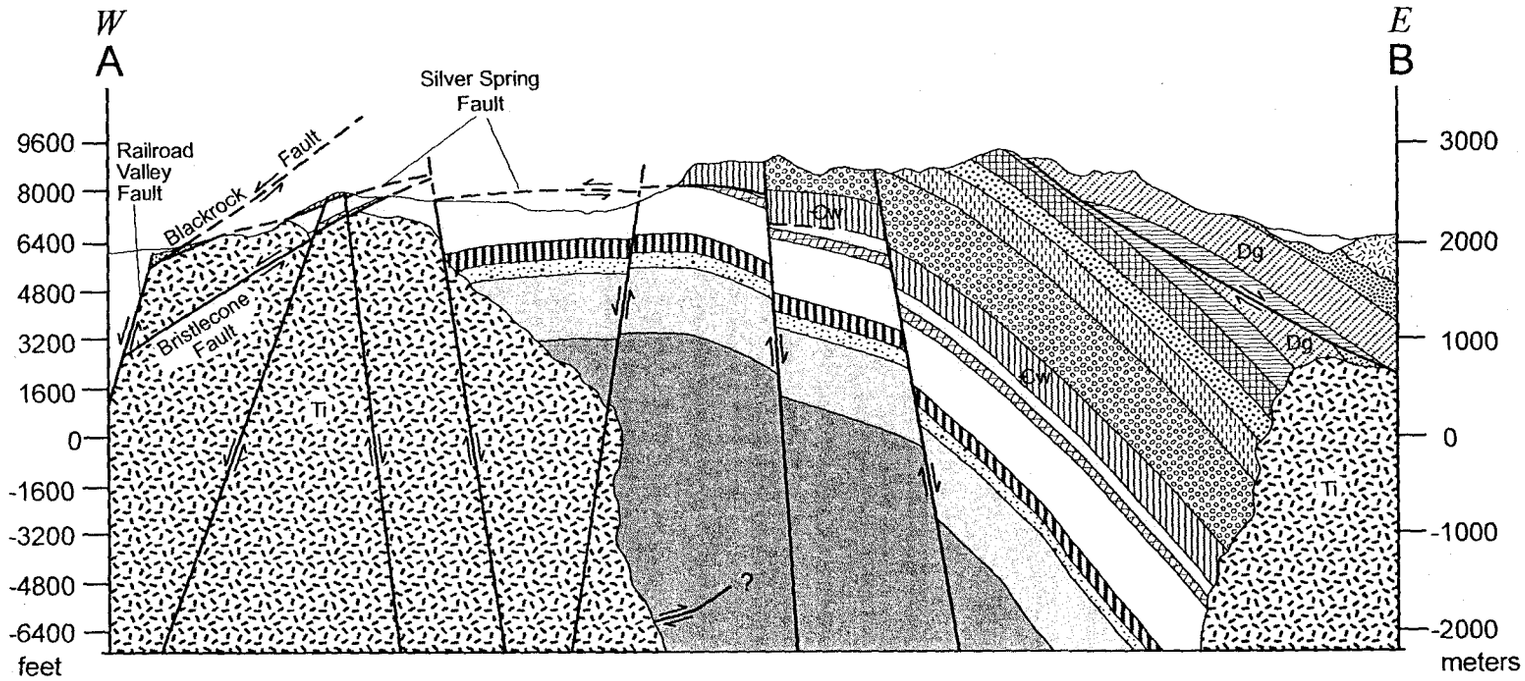

Figure 4b. Geologic cross-section across the White Pine Range. No vertical exaggeration. See Fig. 4a for location, and 4c for unit key. Ti - Tertiary intrusion, Dg - Devonian Guilmette Formation, Cw - Cambrian Windfall Formation. Thrust near base of section is based on the interpretation of Gilbert (2002).

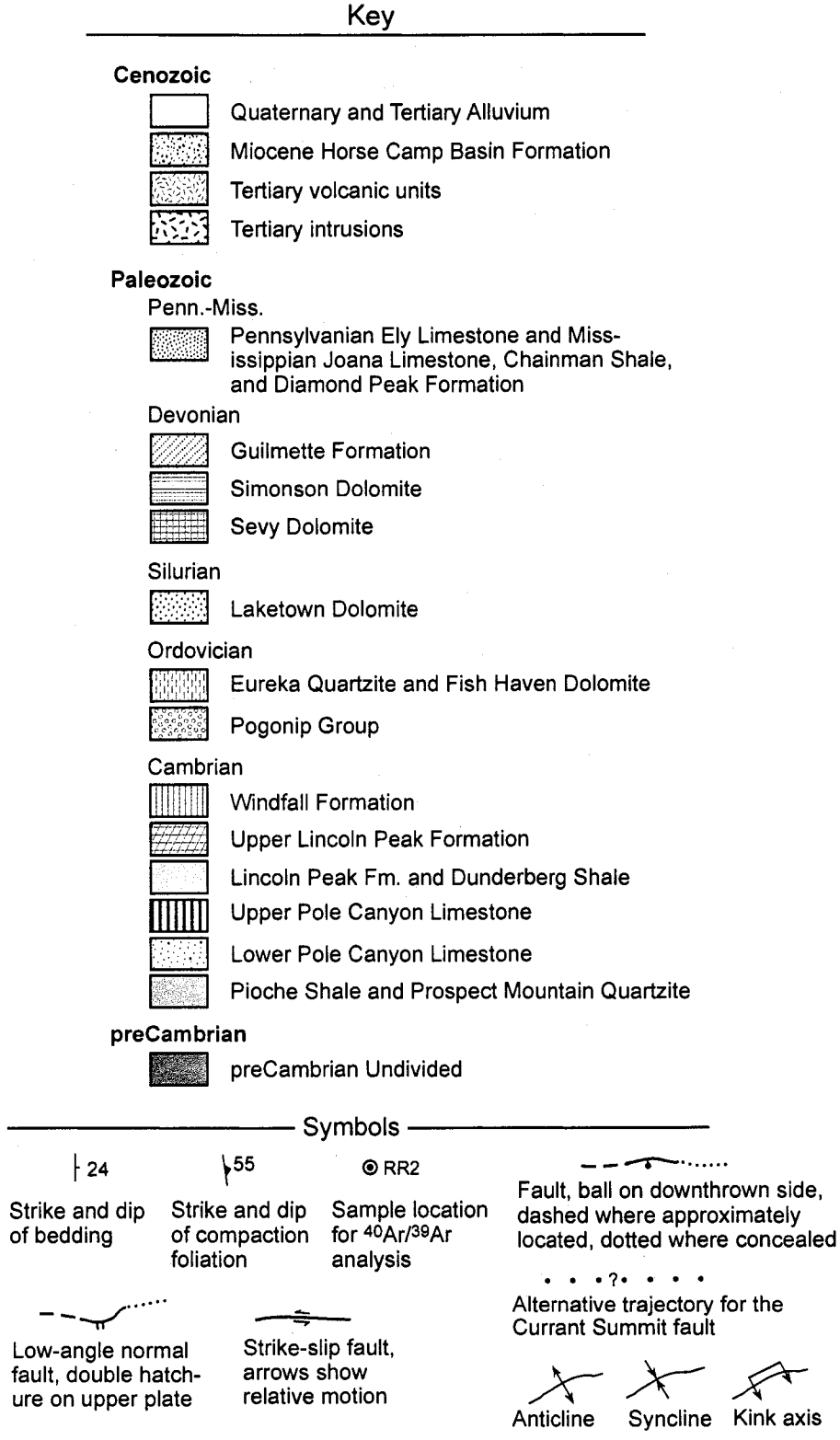

Figure 4c. Key for simplified geologic map and cross-section.

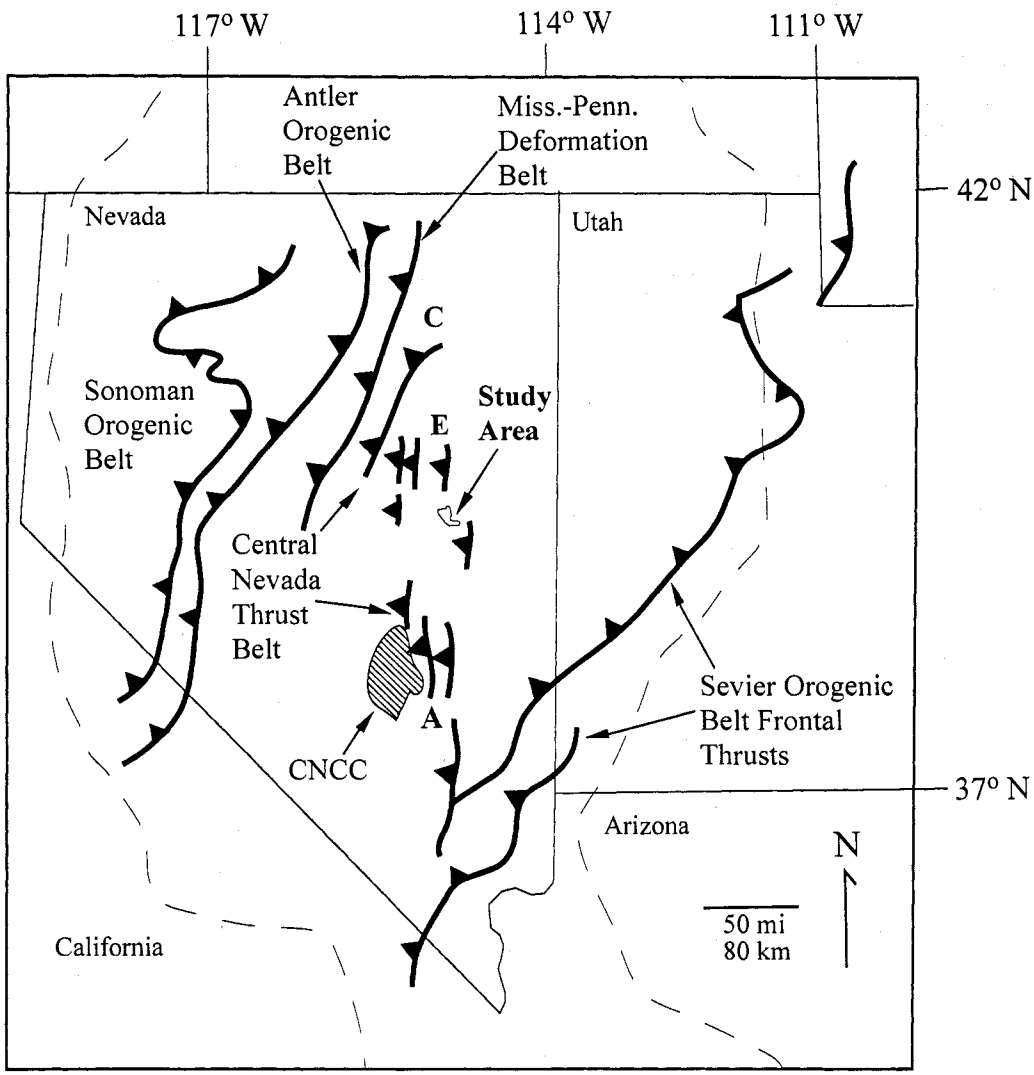

Figure 5. Map showing the locations of major belts of deformation and the central Nevada caldera complex relative to the study area. Limits of the Basin and Range province are shown by dashed line. CNCC - central Nevada caldera complex, A - Alamo, C - Carlin, E - Eureka (Modified from Burchfiel et al., 1992; Taylor et al., 1993; Gilbert, 2002; Trexler et al., 2003).

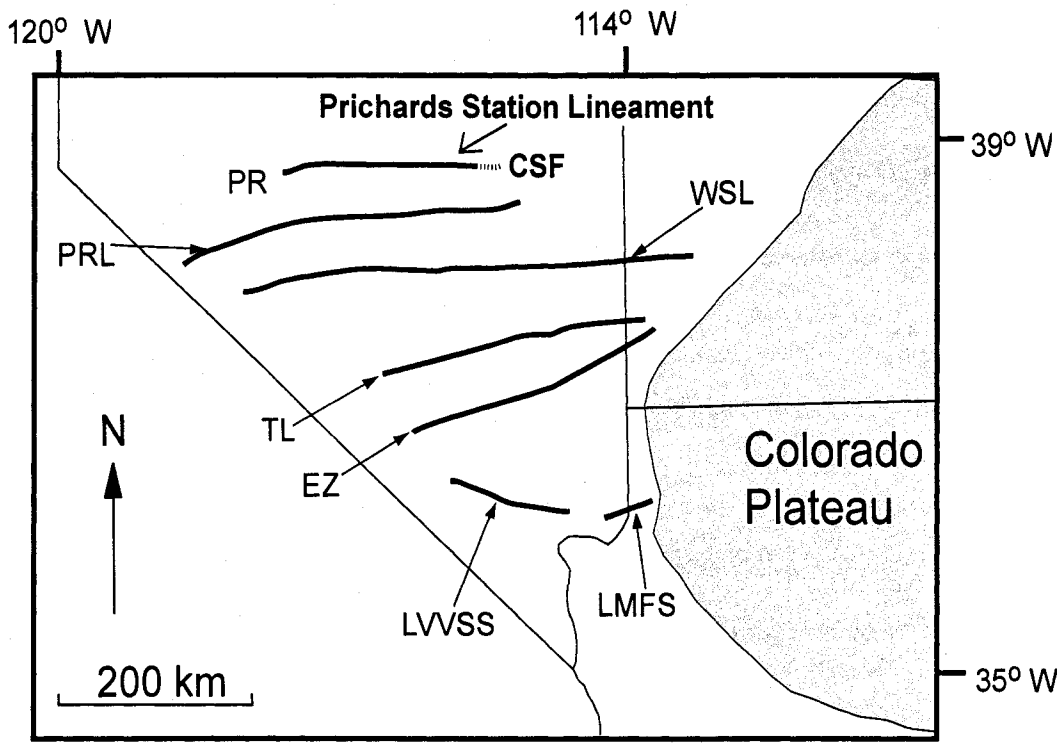

Figure 6. Map of structural lineaments in Nevada and western Utah (modified from Williams and Taylor, 2002). The Currant Summit fault (CSF) is the eastern limit of the Prichards Station lineament. The western limit is near the Paradise Range (PR). Other symbols: PRL - Pancake Range lineament, WSL - Warm Springs Lineament, TL - Timpahute lineament, EZ - Escalante Zone, LVVSS - Las Vegas Valley shear zone, and LMFS - Lake Mead fault system. Location of lineaments from Longwell (1960), Anderson (1973), Ekren et al. (1976), Jayko (1990), and Duebendorfer and Black (1992).

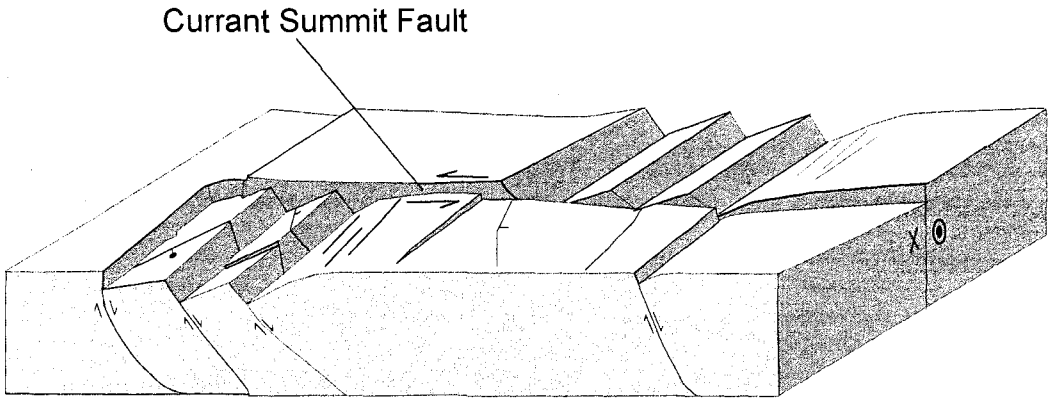

Figure 7. Proposed model for the Currant Summit fault, an oblique-slip transfer fault (from Williams, 2000).

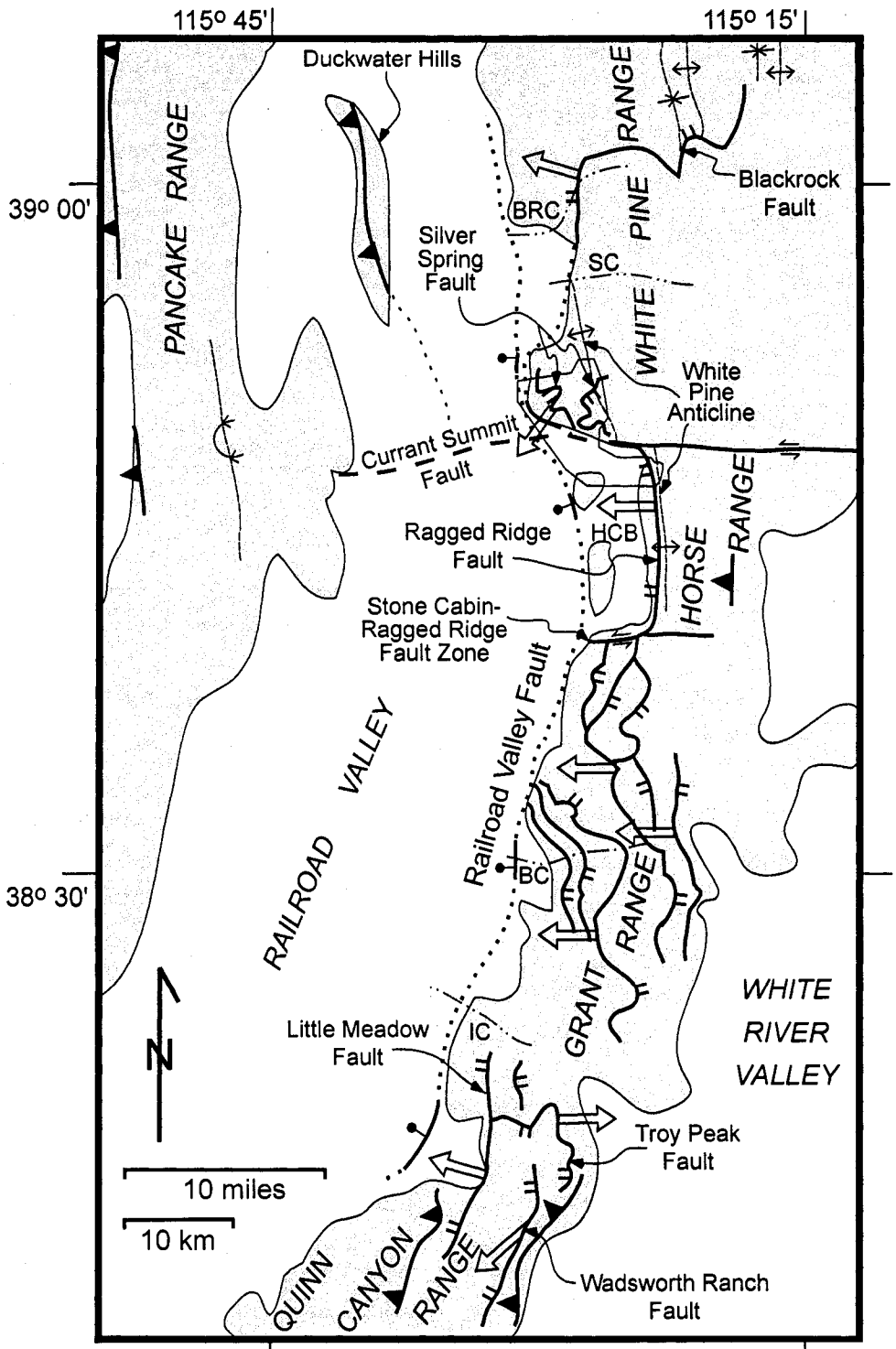

Figure 8. Locations of major low-angle normal faults and select contractile structures near Railroad Valley. Standard geologic symbols used. Hollow arrows indicate interpreted slip vectors of faults. BRC - Blackrock Canyon, SC - Sawmill Canyon, HCB - Horse Camp Basin, BC - Beatty Canyon, IC - Irwin Canyon. Modified from Langrock (1995) and includes map data from Fryxell (1988), Bartley and Gleason (1990), Lund et al. (1993), and Horton and Schmitt (1998).

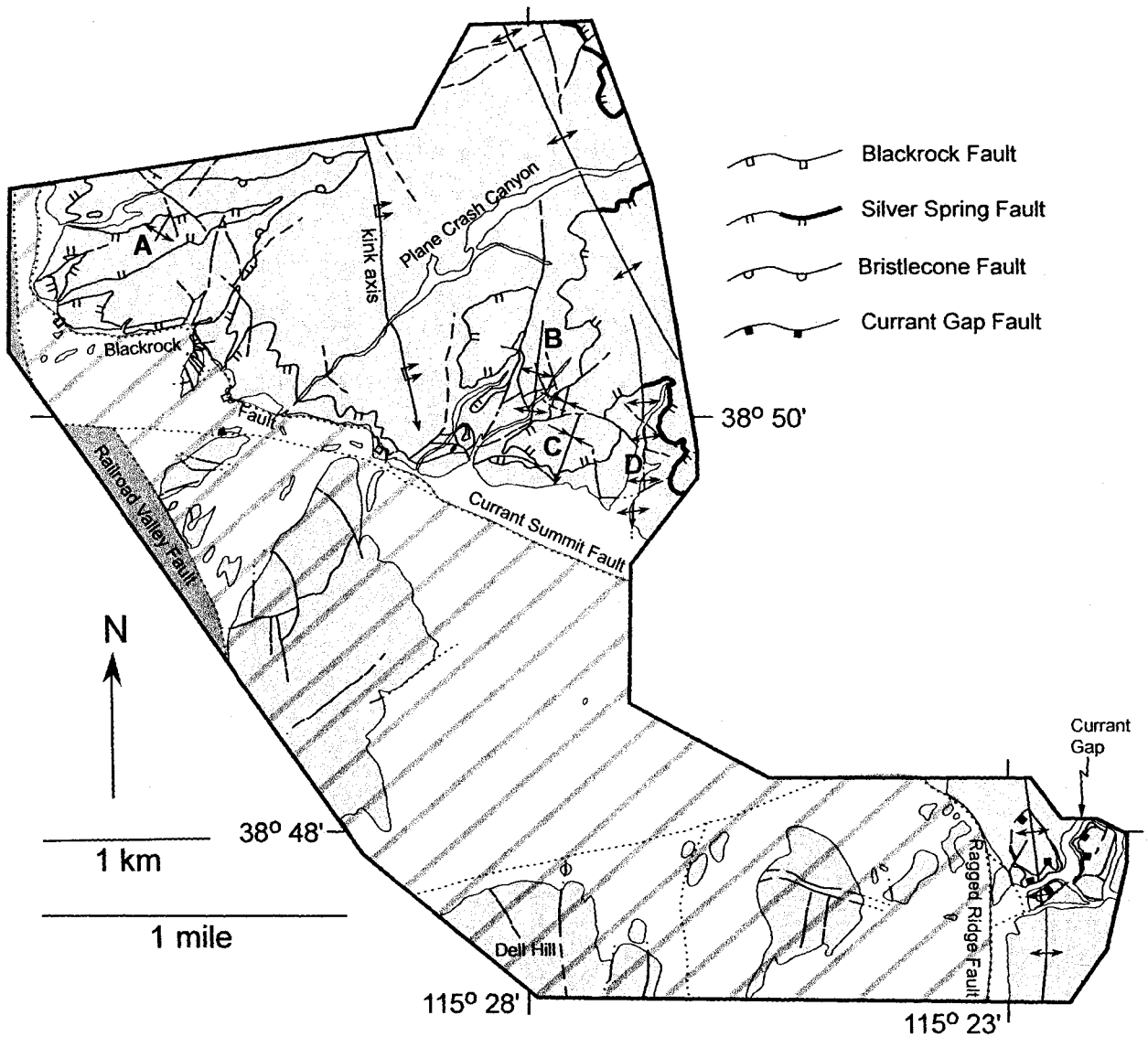

Figure 9. Structure map showing the locations of all faults and folds in the study area. Light gray area is Paleozoic sedimentary rocks and Tertiary volcanic rocks. Area of domain 2 is striped. Dark gray area is an area of faulting younger than domains 1 and 2 and is defined by a possible segment of the Railroad Valley fault. All remaining areas are part of domain 1. Bold segments of the Silver Spring fault denote examples of parts of the fault that presently dip to the east. Letters (A, B, C, and D) label folds discussed in the text.

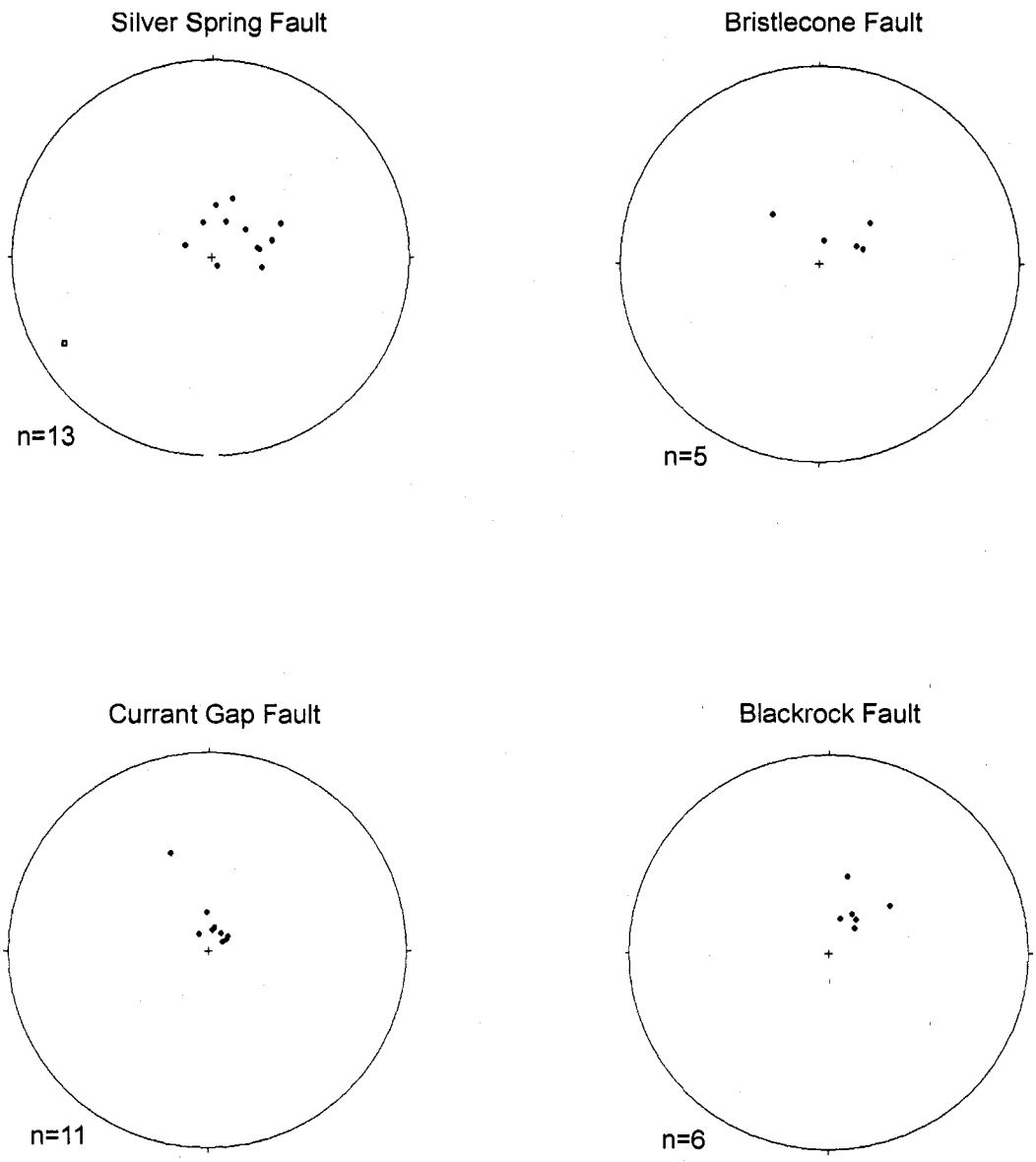

Figure 10. Equal area, lower hemisphere, stereographic projections of poles to measured fault surfaces for all low-angle normal faults. Box on Silver Spring fault plot is a fault striation.

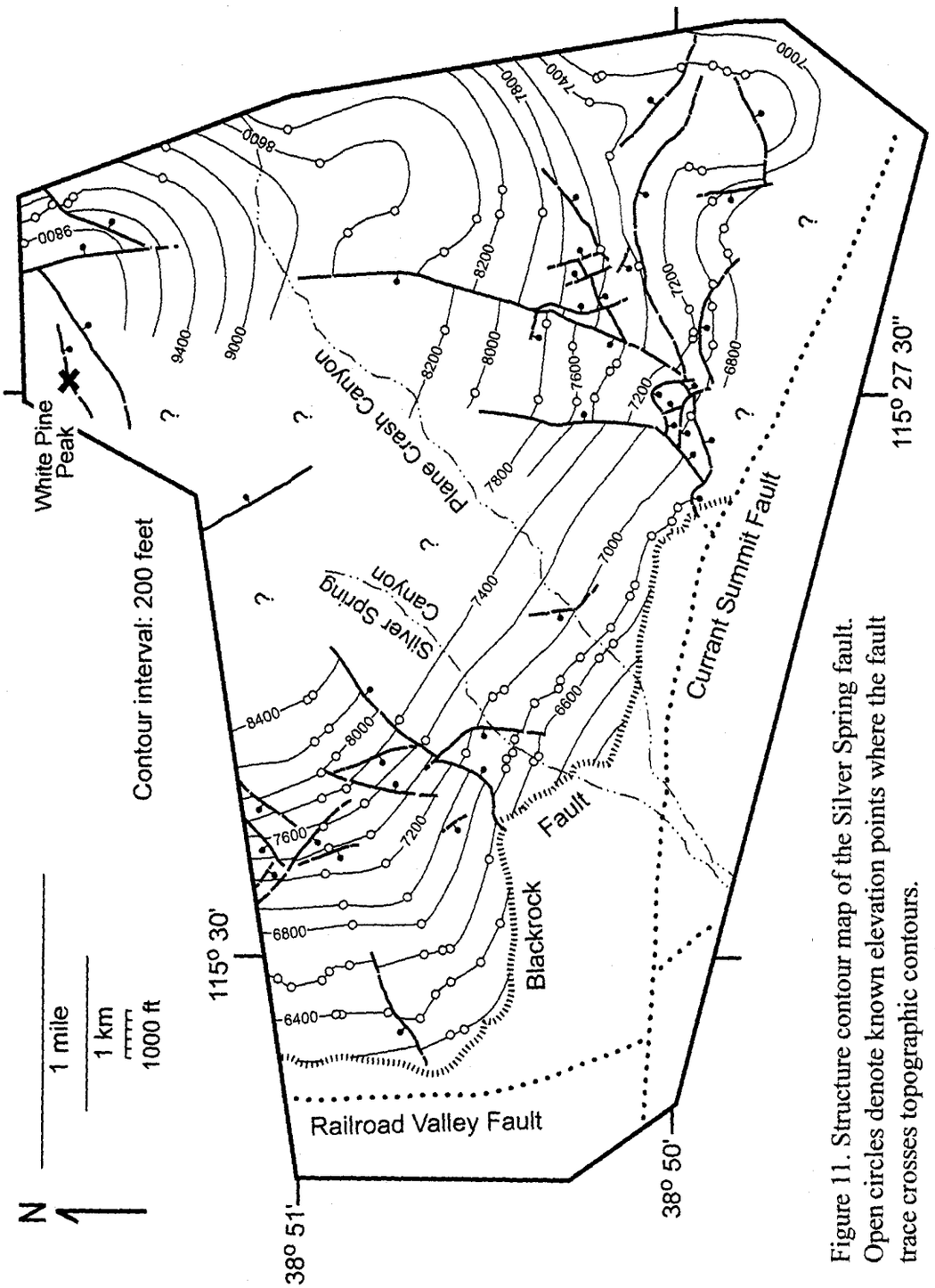

Figure 11. Structure contour map of the Silver Spring fault. Open circles denote known elevation points where the fault trace crosses topographic contours.

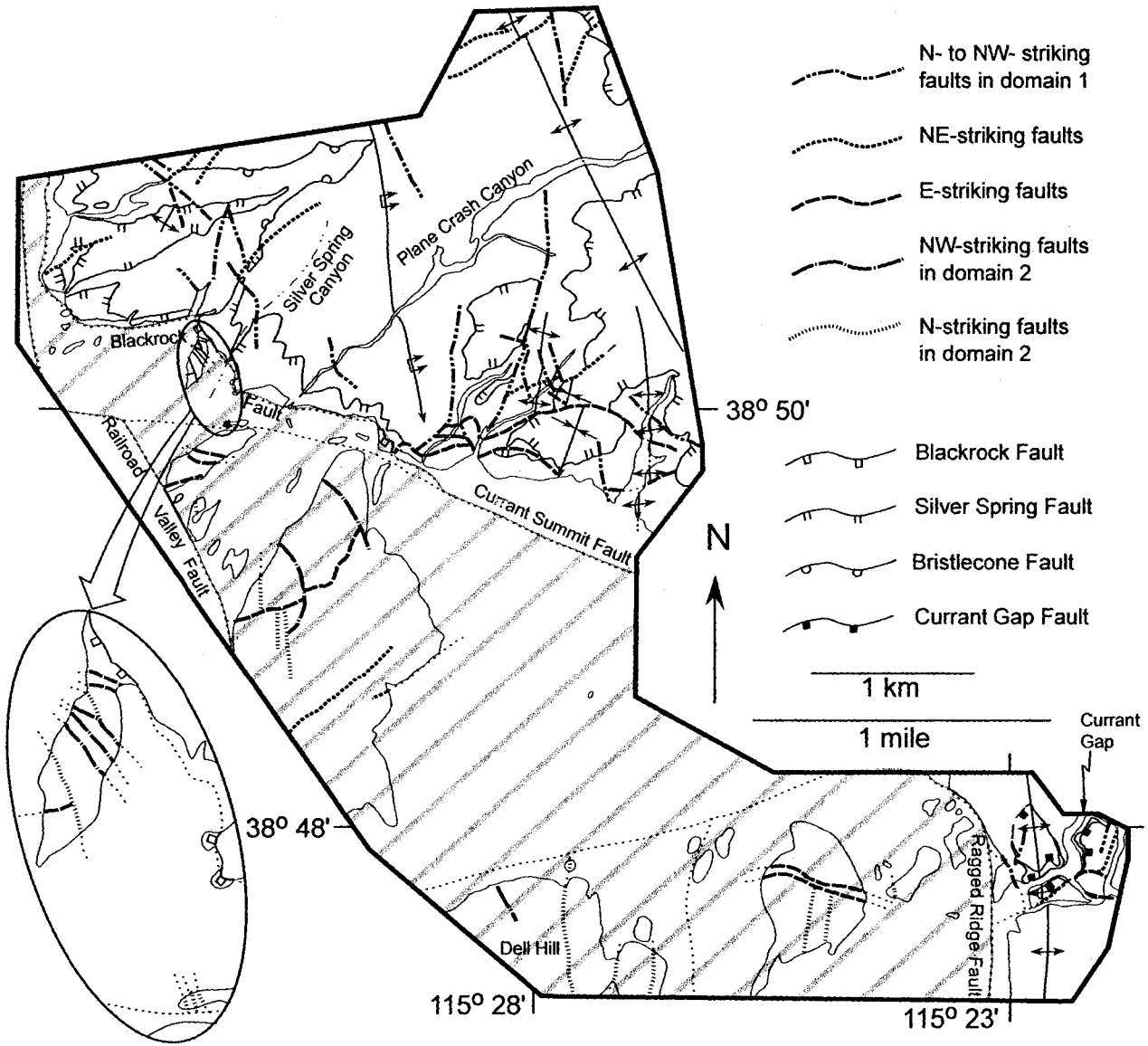

Figure 12. Fault timing map. Area of domain 1 is white and domain 2 is striped. Oval inset shows details of closely spaced and poorly exposed faults near the mouth of Silver Spring Canyon.

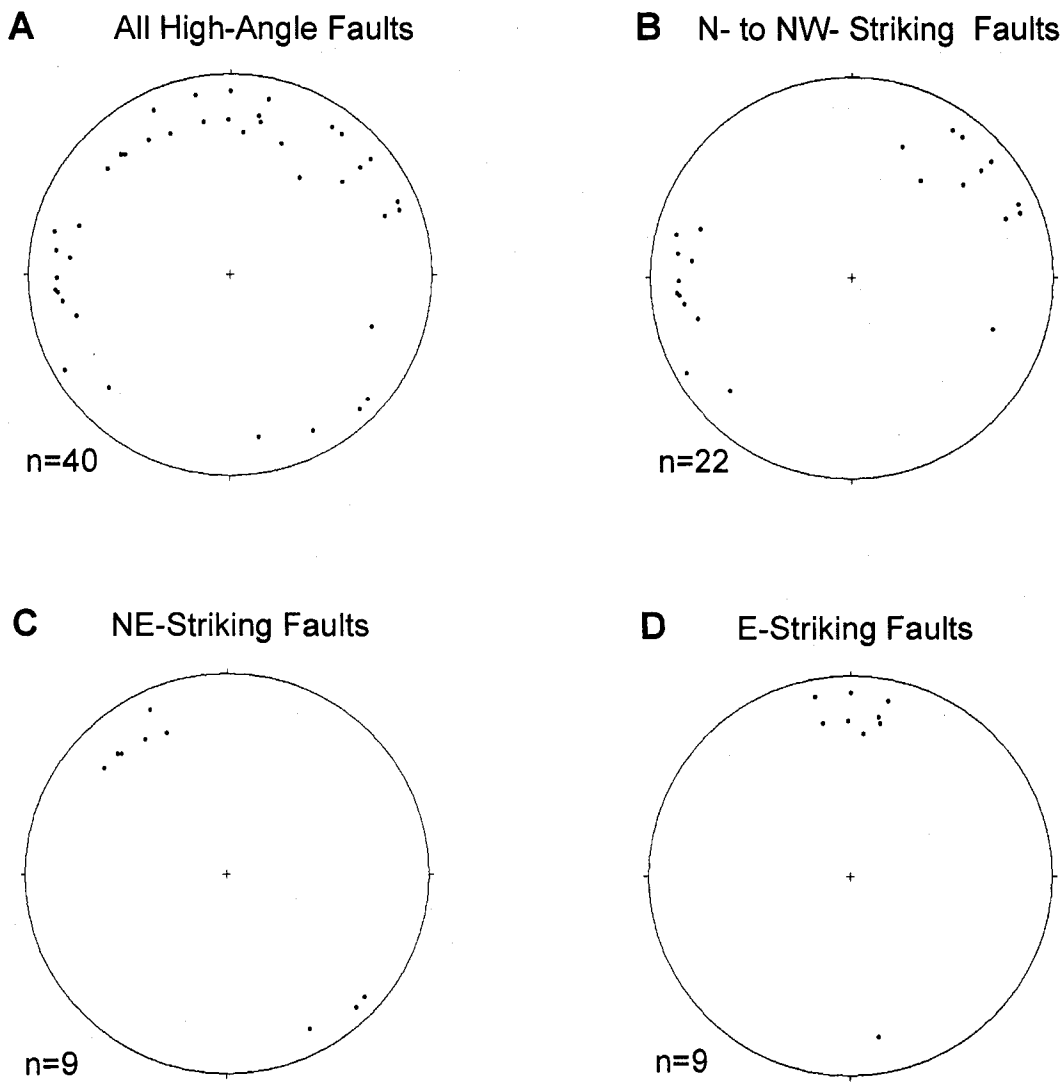

Figure 13. Stereographic projections of poles to high-angle normal faults in domain 1.

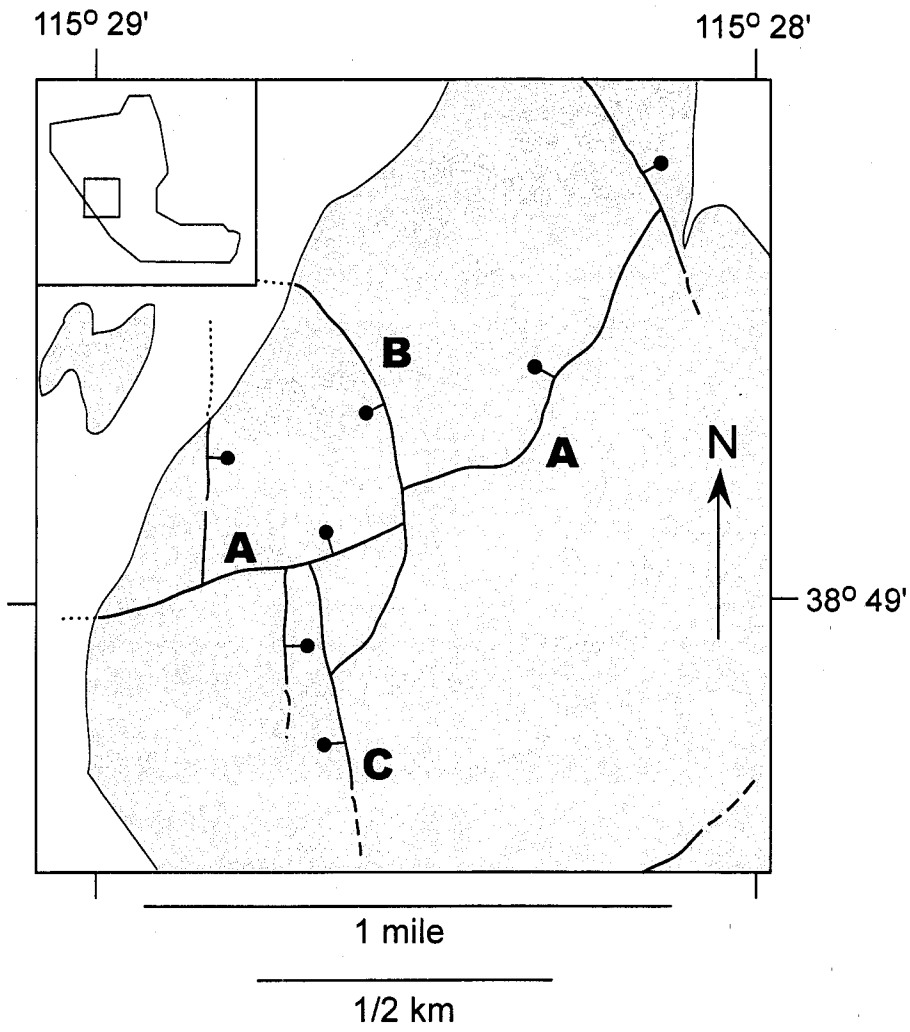

Figure 14. Fault map showing timing inconsistancies within domain 2. Shaded areas are Tertiary volcanic units. See text for explanation. Inset shows location of figure within the map area.

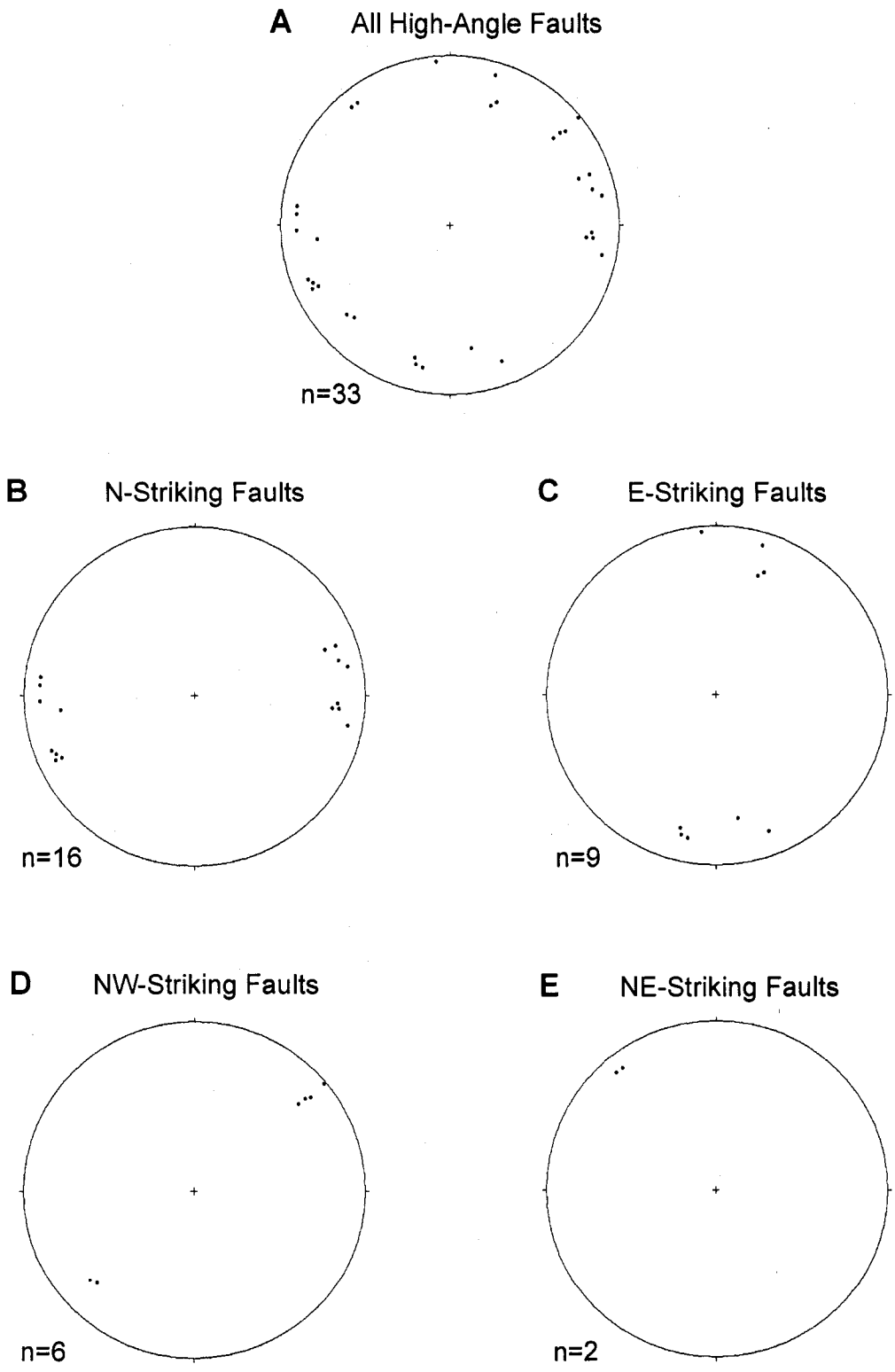

Figure 15. Stereographic projections of poles to high-angle normal faults in domain 2.

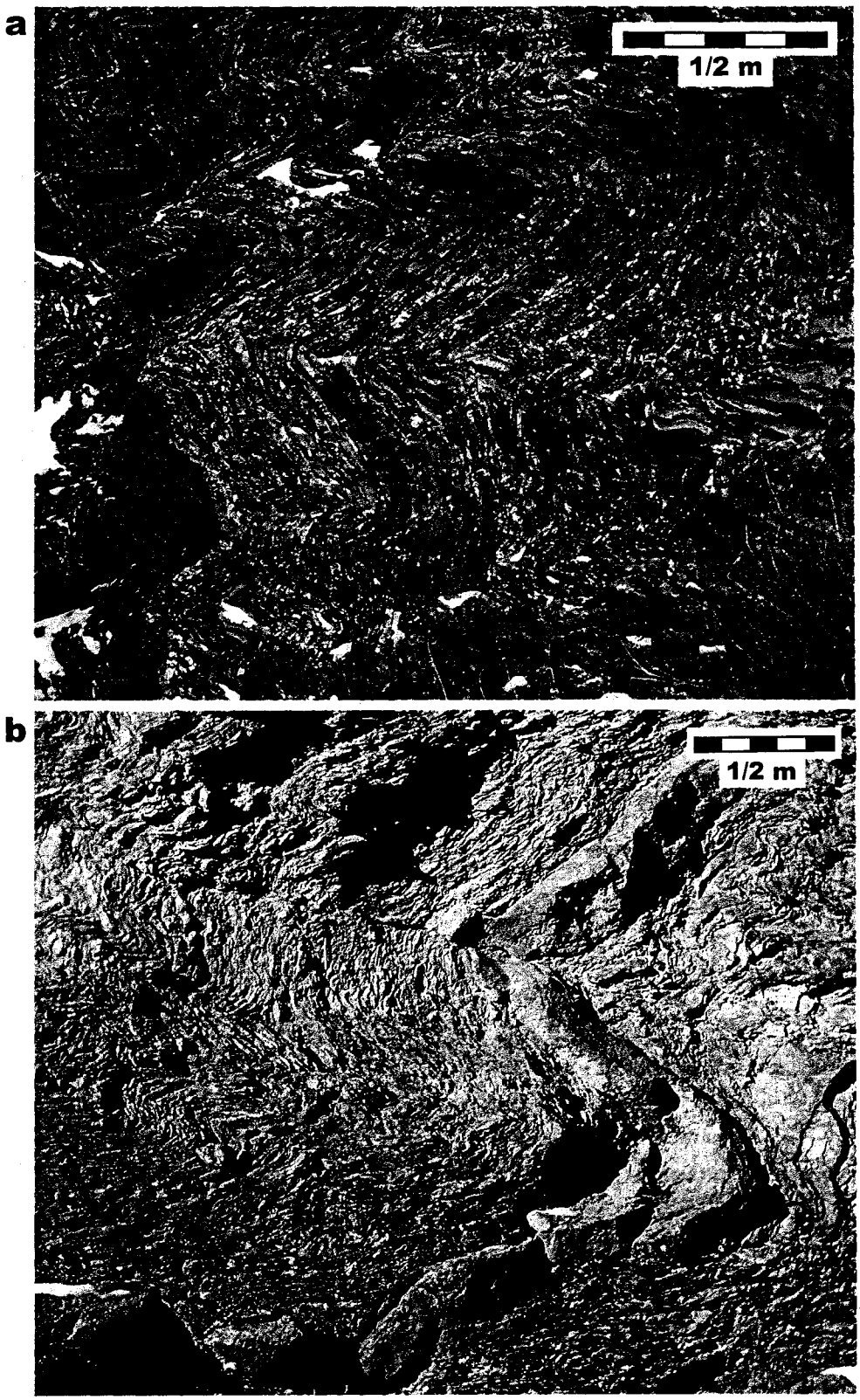

Figure 16. Mesoscale folds in shale and thin-bedded limestone near the Silver Spring fault at the mouth of Plane Crash Canyon. a. Folds are recumbent and have chevron geometries. b. Photo showing disharmonic nature of folding.

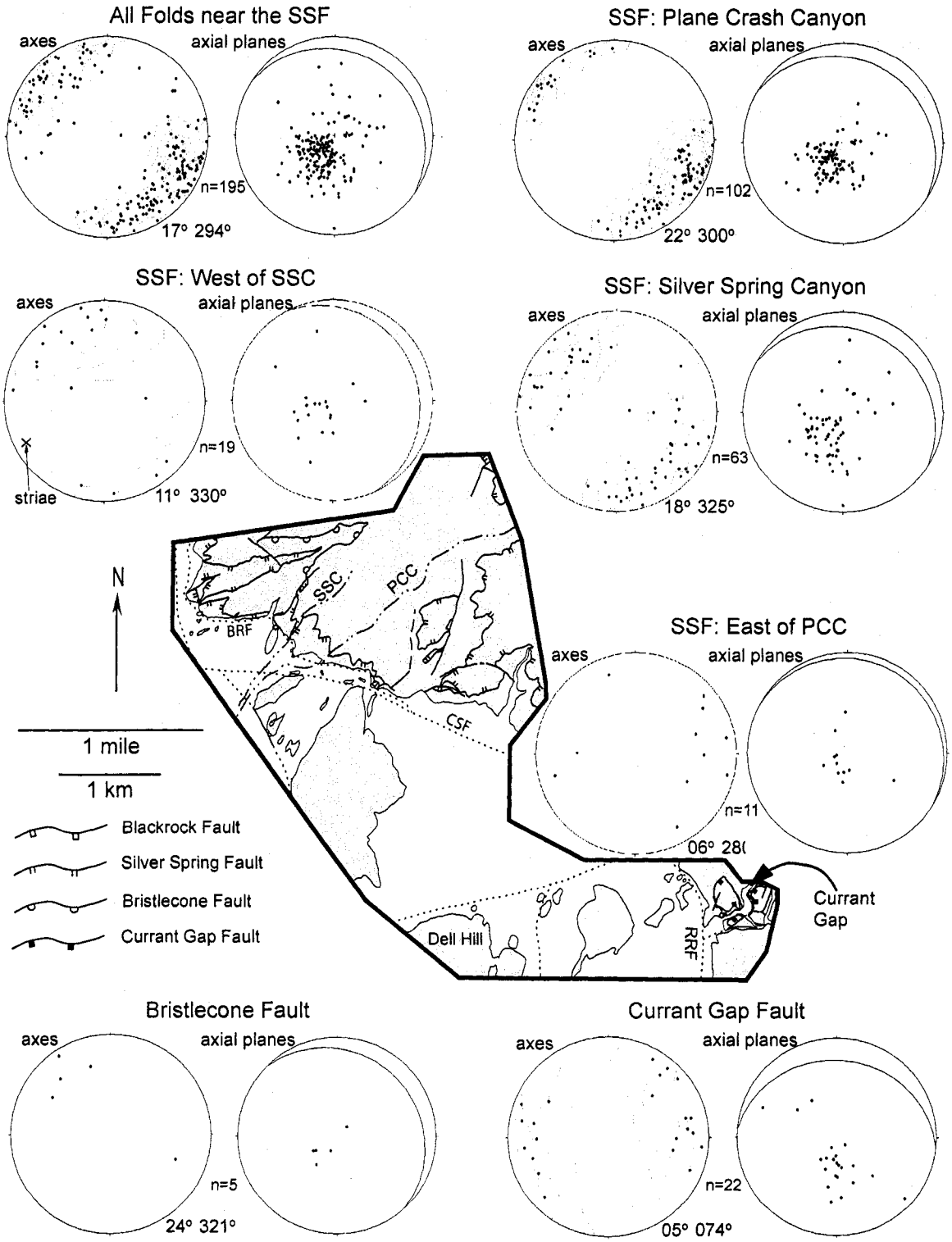

Figure 17. Stereographic projections of mesoscale folds exposed near the bedding-parallel faults. Axes are contoured (C.I. = 2 sigma) where there is sufficient data. Average axis orientation is at lower right of plot. Great circle is the average orientation of axial planes for each location. BRF - Blackrock Fault, CSF - Currant Summit Fault, PCC - Plane Crash Canyon, RRF - Ragged Ridge Fault, SSC - Silver Spring Canyon.

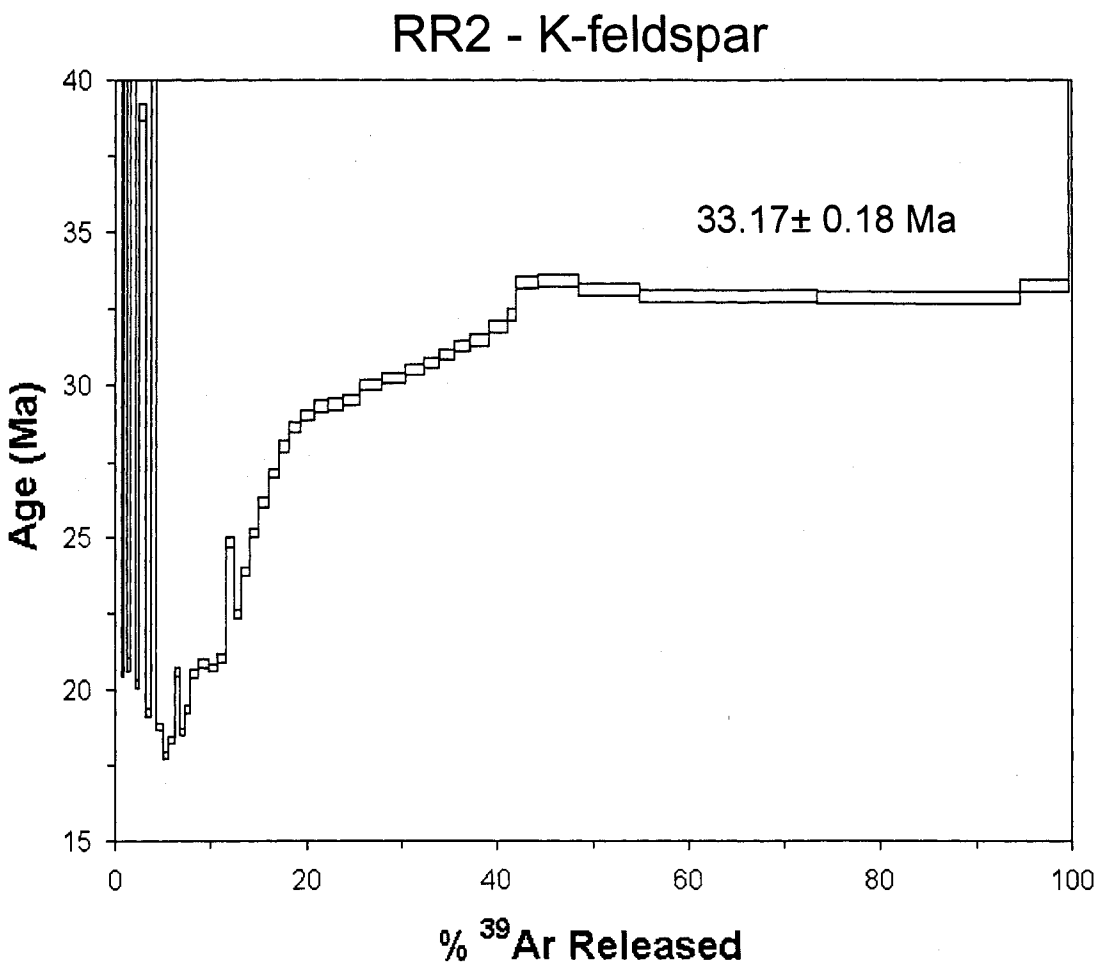

Figure 18. Age spectrum for K-feldspar from the Railroad stock. Errors are 1 sigma.

RR2, K-feldspar, 19.51 mg, J = 0.001526 ± 0.5%

4 amu discrimination = 1.01717 ± 0.22%, 40/39K = 0.0002 ± 0.0003%, 36/37Ca = 0.000272 ± 23.61%, 39/37Ca = 0.000701 ± 1.75%

step	T (C)	t (min.)	^{36}Ar	^{37}Ar	^{38}Ar	^{39}Ar	^{40}Ar	$\%^{40}Ar^*$	% ^{39}Ar released	Ca/K	$^{40}Ar^*/^{39}ArK$	Age (Ma)	1s.d.
1	448	18	3.809	0.043	0.724	1.297	1148.52	3.7	0.0	0.1128798	32.9442	88.49	7.44
2	473	18	2.794	0.057	0.632	7.031	1174.00	31.0	0.1	0.02760161	51.8566	137.40	1.35
3	473	43	1.182	0.055	0.289	4.377	412.773	17.7	0.1	0.04278236	16.1578	43.94	0.70
4	514	18	3.791	0.102	1.001	21.669	2147.620	48.9	0.4	0.01602641	48.5142	128.85	0.91
5	514	43	0.735	0.094	0.253	9.915	287.895	27.7	0.2	0.03227843	7.6310	20.89	0.43
6	555	18	2.227	0.164	0.724	22.434	1332.000	51.7	0.4	0.02488934	30.6875	82.57	0.58
7	555	43	0.624	0.247	0.328	16.167	302.751	42.8	0.3	0.05201724	7.6068	20.82	0.20
8	596	18	1.678	0.413	0.693	28.791	1106.640	56.3	0.5	0.04883966	21.6138	58.54	0.41
9	596	43	0.528	0.571	0.418	24.244	331.647	56.7	0.5	0.08018909	7.3691	20.17	0.15
10	636	18	1.144	0.637	0.661	33.706	812.759	60.4	0.6	0.06434482	14.3012	38.95	0.25
11	638	43	0.362	0.714	0.428	29.396	310.267	67.4	0.6	0.08269776	7.0239	19.23	0.12
12	679	19	0.715	0.675	0.539	31.815	541.823	89.5	0.6	0.0722361	15.1476	41.23	0.24
13	679	44	0.306	0.594	0.513	33.154	315.446	76.0	0.6	0.06100023	6.8503	18.76	0.12
14	720	19	0.397	0.448	0.480	30.980	373.610	64.7	0.6	0.04923524	6.5017	17.81	0.12
15	720	44	0.202	0.428	0.437	32.914	278.364	84.2	0.6	0.0442733	6.6899	18.32	0.12
16	761	19	0.291	0.361	0.436	29.054	301.349	73.4	0.5	0.04230384	7.5098	20.56	0.13
17	761	44	0.147	0.392	0.501	35.849	285.873	90.6	0.7	0.03722947	6.8000	18.62	0.11
18	802	19	0.241	0.344	0.429	28.727	273.277	75.9	0.5	0.04077054	7.0624	19.34	0.13
19	843	19	0.342	0.500	0.669	46.214	445.457	78.7	0.9	0.03683615	7.4940	20.51	0.13
20	884	19	0.467	0.571	0.818	55.986	561.207	76.6	1.0	0.03472436	7.6104	20.83	0.13
21	910	19	0.204	0.418	0.639	46.535	411.024	86.8	0.9	0.03058254	7.5641	20.71	0.13
22	935	19	0.231	0.377	0.623	45.067	412.905	84.9	0.8	0.02848127	7.6777	21.01	0.13

Table 1. $^{40}Ar/^{39}Ar$ step heating data for K-feldspar from the Railroad stock.

RR2, K-feldspar (continued)

step	T (C)	t (min.)	^{36}Ar	^{37}Ar	^{38}Ar	^{39}Ar	^{40}Ar	$\%^{40}Ar^*$	% ^{39}Ar released	Ca/K	$^{40}Ar^*/^{39}ArK$	Age (Ma)	1s.d.
23	961	19	0.265	0.367	0.656	46.635	451.860	85.3	0.9	0.02679357	9.0797	24.83	0.15
24	976	19	0.242	0.308	0.594	41.474	415.111	84.0	0.8	0.02528431	8.2053	22.45	0.14
25	1002	19	0.428	0.349	0.711	48.822	553.794	78.1	0.9	0.02433806	8.7123	23.83	0.14
26	1018	19	0.358	0.305	0.688	48.949	557.445	82.0	0.9	0.02121445	9.1832	25.11	0.16
27	1033	19	0.368	0.294	0.735	50.949	597.970	82.7	1.0	0.01964659	9.5649	26.14	0.16
28	1048	19	0.428	0.317	0.795	56.180	685.204	82.4	1.1	0.01921113	9.9225	27.11	0.16
29	1064	19	0.488	0.328	0.897	63.575	796.371	82.6	1.2	0.01756559	10.2496	28.00	0.17
30	1074	19	0.492	0.348	0.946	65.672	834.394	83.3	1.2	0.01804157	10.4861	28.64	0.17
31	1084	19	0.516	0.353	0.970	69.215	887.925	83.5	1.3	0.017364	10.6253	29.02	0.18
32	1089	24	0.552	0.412	1.140	82.829	1051.70	85.4	1.5	0.01693519	10.7423	29.33	0.17
33	1089	29	0.571	0.421	1.186	84.750	1079.01	85.5	1.6	0.01691288	10.7615	29.39	0.18
34	1089	39	0.582	0.454	1.346	96.159	1211.53	87.0	1.8	0.01607463	10.8132	29.53	0.17
35	1089	59	0.694	0.560	1.727	122.153	1544.74	88.4	2.3	0.01560842	10.9971	30.02	0.18
36	1089	74	0.703	0.586	1.764	126.290	1604.67	89.0	2.4	0.01579806	11.0791	30.25	0.18
37	1089	74	0.560	0.496	1.480	105.800	1347.40	90.0	2.0	0.0159614	11.1781	30.51	0.18
38	1089	74	0.459	0.418	1.272	91.384	1165.71	91.0	1.7	0.01557332	11.2675	30.76	0.18
39	1089	74	0.425	0.386	1.123	80.880	1045.72	90.9	1.5	0.0162488	11.3643	31.02	0.18
40	1089	89	0.451	0.407	1.207	86.815	1127.67	91.6	1.6	0.01596154	11.4656	31.29	0.18
41	1089	119	0.560	0.454	1.430	102.065	1342.24	91.6	1.9	0.01514447	11.5439	31.50	0.18
42	1089	149	0.637	0.486	1.562	109.891	1472.83	91.7	2.1	0.01505737	11.7066	31.94	0.19
43	1141	19	0.336	0.275	0.592	40.932	593.81	84.7	0.8	0.02287419	11.8382	32.30	0.19
44	1200	20	1.039	0.813	1.855	129.941	1899.85	84.5	2.4	0.02130199	12.2440	33.40	0.20
45	1230	20	1.570	1.263	3.254	224.308	3209.38	86.0	4.2	0.01917053	12.2640	33.45	0.20
46	1255	20	2.112	1.763	4.827	338.218	4722.67	87.2	6.3	0.01774724	12.1582	33.17	0.19
47	1300	20	4.601	3.368	1.377	990.568	13256.20	90.0	18.5	0.0115761	12.0675	32.92	0.19
48	1350	20	3.840	1.955	1.573	1128.39	14669.90	92.5	21.1	0.00589877	12.0479	32.87	0.19
49	1400	20	1.119	0.445	3.786	281.383	3756.61	91.6	5.3	0.00538438	12.1959	33.27	0.19
50	1500	20	0.246	0.134	0.244	14.811	365.43	82.1	0.3	0.03080331	19.2570	52.25	0.35
							Cumulative $\%^{39}Ar$ rlsd =		100.0		Total gas age =	31.79	0.13

note: isotope beams in mV, rlsd = released, error in age includes 0.5% J error, all errors 1 sigma (not corrected for decay)

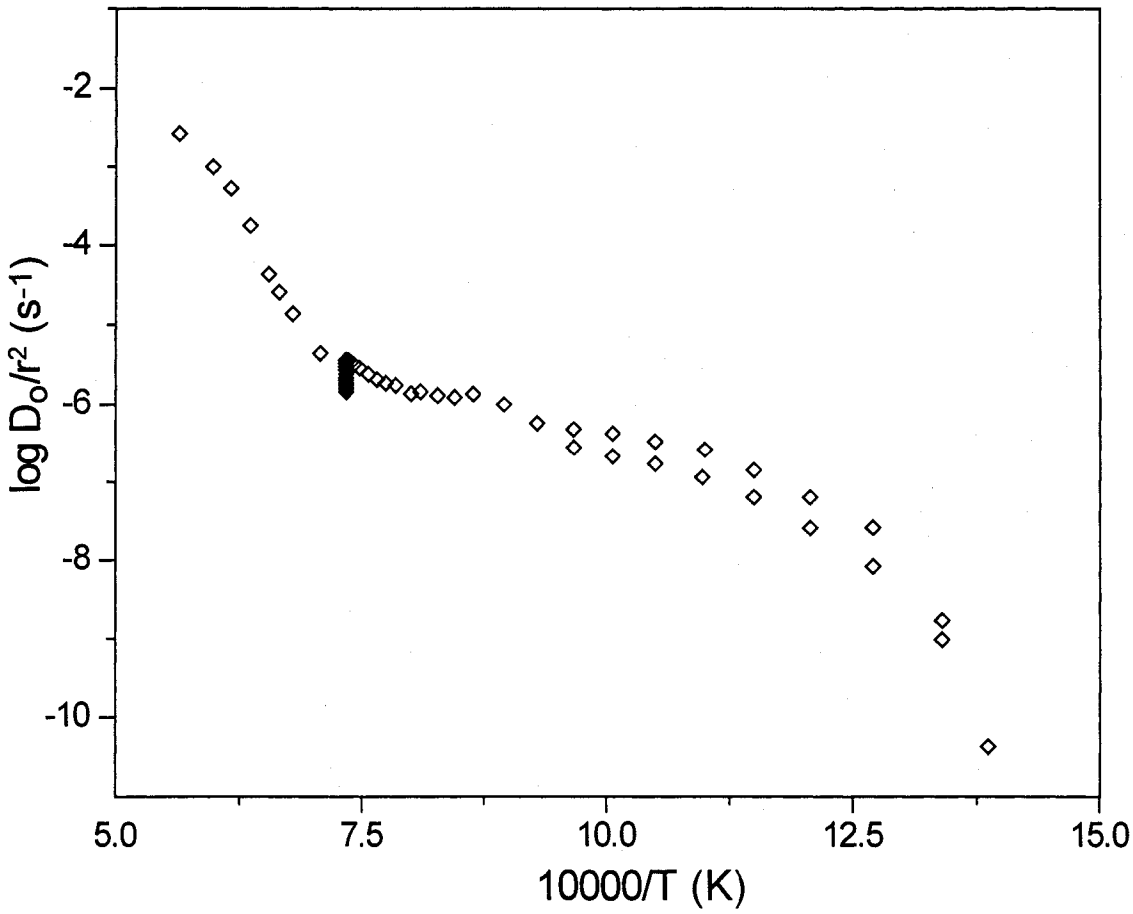

Figure 19. Arrhenius plot for K-feldspar (RR2) from the Railroad stock.

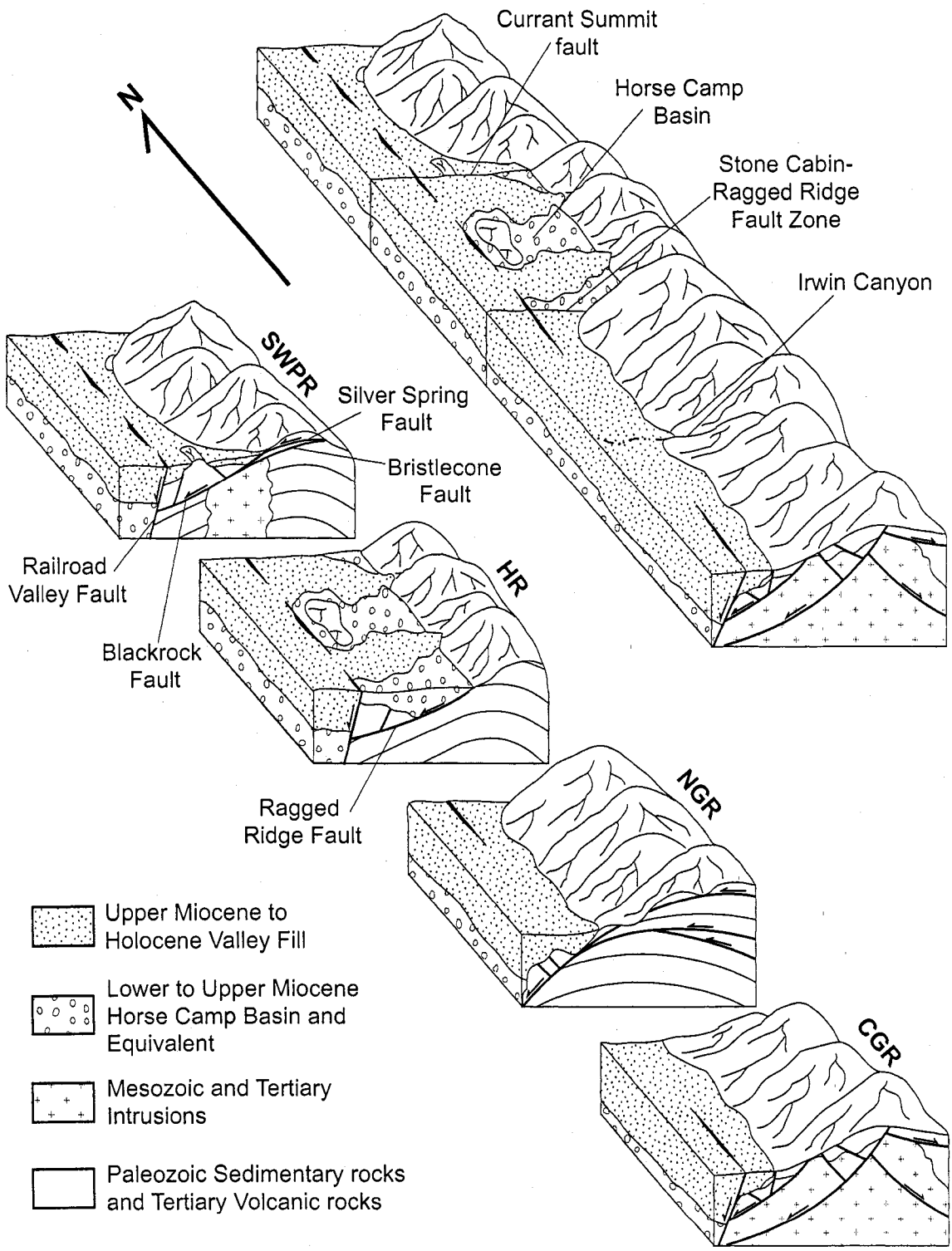

Figure 20. Generalized block model of extensional systems responsible for the structural evolution of Railroad Valley. SWPR= southern White Pine Range, HR= Horse Range, NGR= northern Grant Range, CGR= central Grant Range. Modified from Horton and Schmitt (1998) and includes data from Lund et al. (1993) and Fryxell (1988).

REFERENCES

Anderson, E.M., 1951, The Dynamics of Faulting: Oliver and Boyd, London, 206 p.

Anderson, R.E., 1973, Large magnitude late Tertiary strike-slip faulting north of Lake Mead, Nevada: Geological Society of America Bulletin, v. 82, p. 43-58.

Anderson, R.E., Zoback, M.L., and Thompson, G.A., 1983, Implications of selected subsurface data on the structural form and evolution of some basins in the northern Basin and Range province, Nevada and Utah: Geological Society of America Bulletin, v. 94, p. 1055-1072.

Axen, G.J., 1993, Ramp-flat detachment faulting and low-angle normal reactivation of the Tule Springs Thrust, southern Nevada: Geological Society of America Bulletin, v. 105, p. 1076-1090.

Axen, G.J., 1998, The Caliente-Enterprise zone, southeastern Nevada and southwestern Utah, *in* Faulds, J.E., and Stewart, J.H., eds., Accommodation Zones and Transfer zones: The Regional Segmentation of the Basin and Range Province: Geological Society of America Special Paper 323, p. 181-194.

Axen, G.J. 2004, Mechanics of low-angle normal faults, *in* Karner, G.D., Taylor, B., Driscoll, N.W., and Kohlstedt, D.l., eds., Rheology and Deformation of the Lithosphere at Continental Margins, Columbia University Press, New York, p. 46-91.

Axen, G.J., Taylor, W.J., and Bartley, J.M., 1993, Space-time patterns and tectonic controls of Tertiary extension and magmatism in the Great Basin of the western United States: Geological Society of America Bulletin, v. 105, p. 56-76.

Axen, G.J., Wernicke, B.P., Skelly, M.F., and Taylor, W.J., 1990, Mesozoic and Cenozoic tectonics of the Sevier thrust belt in the Virgin River Valley area, southern Nevada, *in* Wernicke, B.P., ed., Basin and Range Extensional Tectonics at the Latitude of Las Vegas, Nevada: Geological Society of America Memoir 176, p. 123-154.

Bartley, J.M., 1989, Changing Tertiary extension directions in the Dry Lake Valley area, Nevada, and a possible dynamic model, *in* Garside, L.J., and Shaddrick, D.R., eds., Compressional and extensional structural styles in the northern Basin and Range: Seminar Proceedings: Nevada Petroleum Society and the Geological Society of Nevada, p. 35-39.

Bartley, J.M., and Gleason, G.C., 1990, Tertiary normal faults superimposed on Mesozoic thrusts, northern Quinn Canyon and southern Grant Ranges, Nye County, Nevada: *in* Wernicke, B.P., ed., Basin and Range Extensional Tectonics near the Latitude of Las Vegas, Nevada: Geological Society of America Memoir 176, p. 195-212.

Bartley, J.M., Taylor, W.J., Fryxell, J.E., Schmitt, J.G., Vandervoort, D.S., and Walker, J.D., 1993, Tectonic style and regional relations of the central Nevada Thrust Belt: Geological Society of America Abstracts with Programs, v. 25, p. A7.

Best, M.G., 1988, Early Miocene change in direction of least principal stress, southwestern United States: Conflicting inferences from dikes and metamorphic core-detachment fault Terranes: Tectonics, v. 2, p. 249-259.

Best, M.G., Christiansen, E.H., Deino, A.L., Gromme, C.S., McKee, E.H., and Noble D.C., 1989, Eocene through Miocene volcanism in the Great Basin of the western United States: New Mexico Bureau of Mines and Mineral Resources Memoir 47, p. 91-133.

Best, M.G., Scott, R.B., Rowley, P.D., Swadley, W.C., Anderson, R.E., Gromme, C.S., Harding, A.E., Deino, A.L., Christensen, E.H., Tingey, D.G., and Sullivan, K.R., 1993, Oligocene-Miocene caldera complexes, ash-flow sheets, and tectonism in the central and southeastern Great Basin: *in* Lahren, M.M., Trexler, Jr., J.H., and Spinosa, C., eds., Crustal Evolution of the Great Basin and Sierra Nevada: Cordilleran/Rocky Mountain Section, Geological Society of America Guidebook, Department of Geological Sciences, University of Nevada, Reno, p. 285-311.

Blank, H.R., 1991, Aeromagnetic and gravity data for the Lund 1° X 2° quadrangle, Nevada and Utah- an overview: *in* Flanigan, D.M.H., Hansen, M., and Flanigan, T.E., eds., Geology of White River Valley, the Grant Range, eastern Railroad Valley and western Egan Range: Nevada Petroleum Society 1991 Fieldtrip Guidebook, p. 55-58.

Bortz, L.C., 1994, Petroleum geology of the Eagle Springs oil field, Nye County, Nevada, *in* Schalla, R.A., and Johnson, E.H., eds., Oil Fields of the Great Basin: Nevada Petroleum Society, p. 289-298.

Brooks, W. E., and Snee, L.W., 1996, Timing and effect of detachment-related potassium metasomatism on $^{40}Ar/^{39}Ar$ ages from the Windous Butte Formation, Grant Range, Nevada: U.S. Geological Survey Report B2154, 25 p.

Brown, C.L., and Schmitt, J.G., 1991, The Horse Camp Formation: Record of Miocene-Pliocene extensional basin development, northern Grant Range, Nevada, *in* Flanigan, D.M.H., Hansen, M., and Flanigan, T.E., eds., Geology of White River

Valley, the Grant Range, Eastern Railroad Valley and Western Egan Range: Nevada Petroleum Society 1991 Fieldtrip Guidebook, p. 7-13.

Buck, R.W., 1988, Flexural rotation of normal faults: Tectonics, v. 7, p. 959-974.

Burchfiel, B.C., Cowan, D.S., and Davis, G.A., 1992, Tectonic overview of the Cordilleran orogen in the western United States, *in* Burchfiel, B.C., Lipman, P.W., and Zoback, M.L., eds., The Cordilleran Orogen: Conterminous U.S.: Geological Society of America, The Geology of North America, v. G-3, Boulder, p. 407-480.

Camilleri, P.A., 1992, Extensional geometry of a part of the northwestern flank of the northern Grant Range, Nevada: Inferences on its evolution: The Mountain Geologist, v. 29, no. 3, p. 75-84.

Cebula, G.T., Kunk, M.J., Mehnert, H.H., Naeser, C.W., Obradovich, J.D., and Sutter, J.F., 1986, The Fish Canyon Tuff, a potential standard for the $^{40}Ar/^{39}Ar$ and fission-track dating methods: Terra Cognita, v. 6, p. 139-140.

Carpenter, D.G., Carpenter, J.A., Dobbs, S.W., and Stuart, C.K., 1993, Regional structural synthesis of Eureka fold-and-thrust-belt, east-central Nevada, *in* Gillespie, C.W., ed., Structural and Stratigraphic Relationships of Devonian Reservoir Rocks, East-Central Nevada: Nevada Petroleum Society 1993 Field Conference Guidebook, p. 59-72.

Compton, R.R., 1985, Geology in the field, John Wiley & Sons, Inc., 398 p.

Coney, P.J., 1980, Cordilleran metamorphic core complexes: an overview, *in* Crittendon, M.D., Coney, P.J., and Davis, G.H., eds., Cordilleran Metamorphic Core Complexes: Geological Society of America Memoir 153, p. 7-31.

Crane, R.C., 1987, Use of fault cut-offs and bed travel distance in balanced cross-sections: Journal of Structural Geology, v. 9, p. 243-246.

Crittenden, M.D., Jr., Coney, P.J., and Davis, G.H., eds., 1980, Cordilleran metamorphic core complexes: Geological Society of America Memoir 153, 490 p.

Dahlstrom, C.D.A., 1969, Balanced cross sections: Canadian Journal of Earth Sciences, v. 6, p. 57-71.

Davis, G.H., 1983, Shear zone model for the origin of metamorphic core complexes: Geology, v. 11, p. 342-347.

Dickinson, W., 2002, The Basin and Range Province as a composite extensional domain: International Geology Review, v. 44, p. 1-38.

Dobbs, S.W., Garbee, J.J., Stuart, C.K., and Nelson, S., 1994, Integrated geological and geophysical interpretation in the Newark Valley area, Eureka fold-and-thrust belt, east-central Nevada: *in* Dobbs, S.W., and Taylor, W.J., eds., Structural and stratigraphic investigations and petroleum potential of Nevada, with a special emphasis south of the Railroad Valley producing trend, 1994 Field Conference Guidebook, Nevada Petroleum Society, p. 241-253.

Drewes, H., and Palmer, A.R., 1957, Cambrian rocks of the southern Snake Range, Nevada: Geological Society of America Bulletin, v. 69, p. 221-240.

Drewes, H., 1967, Geology of the Connors Pass Quadrangle, Schell Creek Range, east-central Nevada: U.S. Geological Survey Professional Paper 557, 93 p.

Duebendorfer, E.M., and Black, R.A., 1992, Kinematic role of transverse faults in continental extension: An example from the Las Vegas Valley shear zone, Nevada: Geology, v. 20, p. 1107-1110.

Effimoff, I., and Pinezich, A.R., 1981, Tertiary structural development of selected valleys based on seismic data: Basin and Range province, northeastern Nevada: Philosophical Transactions of the Royal Society of London, v. 300, p. 435-442.

Effimoff, I., and Pinezich, A.R., 1986, Tertiary structural development of selected basins: Basin and Range province, northeastern Nevada: Geological Society of America Special Paper, v. 208, p. 31-42.

Ekren, E.B., Bucknam, R.C., Carr, W.J., Dixon, G.L., and Quinlivan, W.D., 1976, East-trending structural lineaments in central Nevada: U.S. Geological Survey Professional Paper 986, 16 p.

Elison, M. W., 1991, Intracontinental contraction in western North America; continuity and episodicity: Geological Society of America Bulletin, v. 103, p. 1226-1238.

Faulds, J.E., and Varga, R.J., 1998, The role of accommodation zones and transfer zones in the regional segmentation of extended terranes, *in* Faulds, J.E., and Stewart, J.H., eds., Accommodation Zones and Transfer Zones: The Regional Segmentation of the Basin and Range Province: Geological Society of America Special Paper 323, p. 1-46.

Foster, N.H., 1979, Geomorphic exploration used in the discovery of the Trap Spring oil field, Nye County, Nevada, *in* Newman, G.W., and Goode, H.D., eds., Basin and Range Symposium and Great Basin Field Conference: Rocky Mountain Association of Geologists and Utah Geological Association Guidebook, p. 477-486.

Fouch, T.D., Hanley, J.H., and Forester, R.M., 1979, Preliminary correlation of Cretaceous and Paleogene lacustrine and related nonmarine sedimentary and

volcanic rocks in parts of the eastern Great Basin of Nevada and Utah: *in* Newman, G.W., and Goode, H.D., eds., Basin and Range Symposium and Great Basin Field Conference: Rocky Mountain Association of Geologists and the Utah Geological Association, p. 305-312.

Francis, R.D., and Walker, C.T., 2001, The role of attenuation in the formation of the Railroad Valley structural basin, east-central Nevada: Detachment control of petroleum reservoirs: American Association of Petroleum Geologists Bulletin, v. 85, p. 1153-1182.

Francis, R.D., and Walker, C.T., 2002a, Cenozoic detachments and attenuation in east-central Nevada in Ehni, W., and Faulds, J., eds., Detachment and attenuation *in* eastern Nevada and its application to petroleum exploration: Nevada Petroleum Society Field Trip Guidebook, p. 73-95.

Francis, R.D., and Walker, C.T., 2002b, The Currant Summit fault: strike slip or a detachment?, *in* Ehni, W., and Faulds, J., eds., Detachment and attenuation in eastern Nevada and its application to petroleum exploration: Nevada Petroleum Society Field Trip Guidebook, p. 115-127.

Fryxell, J.E., 1984, Structural development of the west-central Grant Range, Nye County, Nevada [Ph.D. thesis]: Chapel Hill, University of North Carolina, 139 p.

Fryxell, J.E., 1988, Geologic map and descriptions of stratigraphy and structure of the west-central Grant Range, Nye County, Nevada: Geological Society of America Map and Chart Series MCH064.

Fryxell, J.E., Taylor, W.J., Schmitt, J.G., French, D.E., Camilleri, P.A., Hulen, J., and Langrock, H., 1996, Field trip guide to the Cenozoic structure and stratigraphy of central Nevada, *in* Taylor, W.J., and Langrock, H., eds., Cenozoic Structure and Stratigraphy of Central Nevada: Nevada Petroleum Society Inc., Reno, p. 111-122.

Fryxell, J.E., 1998, Detachment and thrust faults of the Grant Range and Railroad Valley: Age, origin, and relationship to the structural development of Railroad Valley, *in* French, D.E., and Schalla, R.A., eds., Hydrocarbon habitat and special geologic problems of the Great Basin: Nevada Petroleum Society Inc., Reno, p. 67-68.

Gilbert, J.J., 2002, Cenozoic extension superimposed on a Mesozoic thrust belt, central Nevada [M.S. thesis]: University of Nevada, Las Vegas, 77 p.

Giles, K.A., and Dickinson, W.R., 1995, The interplay of eustasy and lithospheric flexure in forming stratigraphic sequences in foreland settings: an example from the Antler foreland, Nevada and Utah: Society for Sedimentary Geology Special Publication, v., 52, p. 187-211.

Grabb, R.F., 1994, Extensional tectonics and petroleum accumulations in the Great Basin, *in* Schalla, R.A., and Johnson, E.H., eds., Oil Fields of the Great Basin: Nevada Petroleum Society, p. 41-56.

Groshong, R.H., 1989, Half-graben structures: Balanced models of extensional fault-bend folds: Geological Society of America Bulletin, v. 101, p. 96-105.

Grow, J.A., Blank, H.R., Potter, C.J., Jr., and Miller J.J., 1992, Constraints on extensional fault geometries in eastern Railroad Valley, Nevada, based on seismic reflection and gravity data: Geological Society of America Abstracts with Programs, v. 24, p. 16.

Hague, A., 1883, Abstract of report on the geology of the Eureka district, Nevada: U.S. Geological Survey Third Annual Report, 1881-1882, p. 237-290.

Hintze, L.F., 1978, Sevier orogenic attenuation faulting in the Fish Springs and House Ranges, western Utah: Brigham Young University Geology Studies, v. 25, p. 11-24.

Hood, K.C., 1985, Depositional environments and biostratigraphy of the Lower Middle Cambrian, White Pine Range, Nevada [PhD dissertation]: University of Kansas, 71 p.

Horton, B.K., and Schmitt, J.G., 1996, Sedimentology of a lacustrine fan-delta system, Miocene Horse Camp Formation, Nevada, USA: Sedimentology, v. 43, p. 133-155.

Horton, B.K., and Schmitt, J.G., 1998, Development and exhumation of a Neogene sedimentary basin during extension, east-central Nevada: Geological Society of America Bulletin, v. 110, p. 163-172.

Hose, R.K., and Blake, M.C., Jr., 1976, Geology and mineral resources of White Pine County, Nevada: Nevada Bureau of Mines and Geology, Bulletin 85, 105 p.

Hudleston, P.J., 1986, Extracting information from folds in rocks: Journal of Geological Education, v. 34, p. 237-245.

Humphrey, F.L., 1960, Geology of the White Pine Mining District, White Pine County, Nevada: Nevada Bureau of Mines, Bulletin 57, 119 p.

Janecke, S.U., Vanderburg, C.J., and Blankenau, J.J., 1998, Geometry, mechanisms and significance of extensional folds from examples in the Rocky Mountain Basin and Range province, U.S.A.: Journal of Structural Geology, v. 20, p. 841-856.

Jayko, A.S., 1990, Shallow crustal deformation in the Pahranagat area, southern Nevada, *in* Wernicke, B.P., ed. Basin and Range extensional tectonics near the latitude of

Las Vegas, Nevada: Geological Society of America Memoir 176, p. 213-236.

Kellogg, H.E., 1963, Paleozoic stratigraphy of the southern Egan Range, Nevada: Geological Society of America Bulletin, v. 74, p. 685-708.

Kellogg, H.E., 1964, Cenozoic stratigraphy and structure of the southern Egan Range, Nevada: Geological Society of America Bulletin, v. 75, p. 949-968.

Kellogg, H.E., 1978, Tertiary structural development of the southern Egan Range, Nevada: American Association of Petroleum Geologists Bulletin, v. 62, p. 886.

Ketner, K.B., Day, W.C., Elrick, M., Vaag, M.K., Zimmerman, R.A., Snee, L.W., Saltus, R.W., Repetski, J.E., Wardlaw, B.R., Taylor, M.E., and Harris, A.G., 1998, An outline of tectonic, igneous, and metamorphic events in the Goshute-Toano Range between Silver Zone Pass and White Horse Pass, Elko County, Nevada: A history of superposed contractional and extensional deformation: U.S. Geological Survey Professional Paper 1593, 12 p.

Kleinhampl, F.J., and Ziony, 1985, Geology of northern Nye County, Nevada: Nevada Bureau of Mines and Geology Bulletin 99A, 172 p.

Langrock, H., 1995, Tectonic denudation of Mesozoic contractile structures by a low-angle normal fault and associated faults, southern White Pine Range, Nevada [M.S. thesis]: University of Nevada, Las Vegas, 109 p.

Lawson, A.C., 1906, The copper deposits of the Robinson mining district, Nevada: University of California Department of Geology Bulletin 4, p. 287-357.

Liberty, L.M., Heller, P.L. and Smithson, S.B., 1994, Seismic reflection evidence for two-phase development of Tertiary basins from east-central Nevada: Geological Society of America Bulletin, v.106, p. 1621-1633.

Lisenbee, A., and Kieffer Rowe, B., 1996, The White Pine detachment, Blackrock and Freeland Canyons area, White Pine Range, Nevada, *in* Taylor, W.J., and Langrock, H., eds., Cenozoic Structure and Stratigraphy of Central Nevada: Nevada Petroleum Society Field Conference Volume, p. 93-99.

Lister, G.S., and Davis, G.A., 1989, The origin of metamorphic core complexes and detachment faults formed during Tertiary continental extension in the Colorado River region, U.S.A.: Journal of Structural Geology, v. 11, p. 65-93.

Lonergan, L., and Cartwright, J.A., 1999, Polygonal faults and their influence on deep water sandstone reservoir geometries, Alba Field, United Kingdom central North Sea: American Association of Petroleum Geologists Bulletin, v. 83, p. 410-432.

Longwell, C.R., 1960, Possible explanation of diverse structural patterns in southern

Nevada (Bradley volume): American Journal of Science, v. 258-A, p. 985-990.

Lovera, O.M., 1989, $^{40}Ar/^{39}Ar$ thermochronometry; implications of having samples with a distribution of diffusion domain sizes [Ph.D. dissertation]: Chicago, University of Chicago, 140 p.

Lovera, O.M., Grove, M., and Harrison, T.M., 2002, Systematic analysis of K-feldspar $^{40}Ar/^{39}Ar$ step heating results II: Relevance of laboratory argon diffusion properties to nature: Geochimica et Cosmochimica Acta, v. 66, p. 1237-1255.

Lumsden, W.W., Jr., 1964, Geology of the southern White Pine Range and northern Horse Range, Nye and White Pine Counties, Nevada [Ph.D. dissertation]: University of California, Los Angeles, 249 p.

Lumsden, W.W., Walker, C.T., and Francis, R.D., 2002, The Precambrian and Paleozoic stratigraphy of the White Pine, Grant and Schell Creek ranges in eastern Nevada: the key to interpreting structures formed by extension and attenuation *in* Ehni, W., and Faulds, J., eds., Detachment and Attenuation in Eastern Nevada and its Application to Petroleum Exploration: Nevada Petroleum Society Field Trip Guidebook, p. 33-72.

Lund, K., Beard, H.R., Blank, H.R., Jr., and Tuftin, S.E., 1987, Mineral resources of the Blue Eagle wilderness study area, Nye County, Nevada: U.S. Geological Survey Bulletin 1731-D, 19 p.

Lund, K., Beard, L.S., and Perry, W.J., 1991, Structures of the northern Grant Range and Railroad Valley, Nye County, Nevada: implications for oil occurrences, *in* Flanigan, D.M., Hansen, M., and Flanigan, T.E., eds., Geology of the White River Valley and Grant Range, Eastern Railroad Valley and Western Egan Range, Nevada: Nevada Petroleum Society Fieldtrip Guidebook, p. 1-6.

Lund, K., Beard, L.S., and Perry, W.J., 1993, Relation between extensional geometry of the northern Grant Range and oil occurrences in Railroad Valley, east-central Nevada: American Association of Petroleum Geologists Bulletin, v. 77, p. 945-962.

Manktelow, N.S., and Pavlis, T.L., 1994, Fold-fault relationships in low-angle detachment systems: Tectonics, v. 13, p. 668-685.

McCutcheon, T.J., and Zogg, W.D., 1994, Structural geology of the Grant Canyon-Bacon Flat field area, Nye County, Nevada: implications for hydrocarbon exploration in the Great Basin, *in* Schalla, R.A., and Johnson, E.H., eds., Oil Fields of the Great Basin: Nevada Petroleum Society, p. 201-226.

McDougall, I., and Harrison, M.T., 1999, Geochronology and thermochronology by the $^{40}Ar/^{39}Ar$ method, Oxford University Press, New York, 270 p.

Miller, E.L., Miller, M.M., Stevens, C.H., Wright, J.E., and Madrid, R., 1992, Late Paleozoic paleogeographic and tectonic evolution of the western U.S. Cordillera: *in* Burchfiel, B.C., Lipman, P.W., and Zoback, M.L., eds., The Cordilleran Orogen: Conterminous U.S.: Geological Society of America, The Geology of North America, v. G-3, p. 57-106.

Moores, E.M., 1968, Mio-Pliocene sediments, gravity slides, and their tectonic significance, east-central Nevada: Journal of Geology, v. 76, p. 88-98.

Moores, E.M., Scott, R.B., and Lumsden, W.W., 1968, Tertiary tectonics of the White Pine-Grant Range region, east-central Nevada: Geological Society of America Bulletin, v. 79, p. 1703-1726.

Nolan, T.B., 1935, The Goldhill mining district, Utah: U.S. Geological Survey Professional Paper 177, 172 p.

Nolan, T.B., Merriam, C.W., and Williams, J.S., 1956, The stratigraphic section in the vicinity of Eureka, Nevada: U.S. Geological Survey Proffessional Paper 276, p. 1-77.

Nutt, C.J., Thorman, C.H., Snee, L.W., and Hintze, L.F., 1995, Eocene or older attenuate faults in the eastern Great Basin, *in* Coyner, A.R., and Fahey, P.L., eds., Geology and Ore Deposits of the American Cordillera: 1995 Geological Society of Nevada Symposium Proceedings, p. 609-623.

Oldow, J.S., 1984, Tectonic implications of a late Mesozoic fold and thrust belt in northwestern Nevada: Geology, v. 11, p. 542-546.

Perry, W.J., Jr., and Dixon, G.J., 1993, Structure and time of deformation in the central Pancake Range, *in* Gillespie, C.W., ed., Structural and Stratigraphic Relationships of Devonian Reservoir Rocks, East-Central Nevada: 1993 Field Conference Guidebook, Nevada Petroleum Society, p. 123-132.

Peterson, J.A., 1994, Regional geology and paleotectonic development of the Railroad Valley area, *in* Schalla, R.A., and Johnson, E.H., eds., Oil Fields of the Great Basin: Nevada Petroleum Society, p. 15-40.

Potter, C.J., Grow, J.A., Lund, K., Perry, W.J., Miller, J.J., and Lee, M.W., 1991, Comparison of basin geometry and faulting styles along a regional seismic reflection profile from Railroad Valley to Lake Valley, Nevada, *in* Flanigan, D.M.H., Hansen, M., and Flanigan, T.E., eds., Geology of White River Valley, the Grant Range, eastern Railroad Valley and western Egan Range: Nevada Petroleum Society 1991 Fieldtrip Guidebook, p. 59-60.

Reches, Z., and Deiterich, J.H., 1983, Faulting of rocks in three-dimensional strain fields

I. Failure of rocks in polyaxial, servo-control experiments: Tectonophysics, v. 95, p. 111-132.

Rees, M.N., 1986, A fault-controlled trough through a carbonate platform; the Middle Cambrian House Range Embayment: Geological Society of America Bulletin, v. 97, p. 1054-1069.

Roberts, R.J., Hotz., P.E., Gilluly, J., and Ferguson, H.G., 1958, Paleozoic rocks of north-central Nevada: American Association of Petroleum Geologists Bulletin, v. 49, p. 1926-1956.

Rowell, A.J., and Rees, M.N., 1981, Basinal deposits and outer shelf basins in the Cambrian of Nevada and Utah: U.S. Geological Survey Open File Report OF 81-0743, p. 188-192.

Rowley, P.D., 1998, Cenozoic transverse zones and igneous belts in the Great Basin, western United States: Their tectonic and economic implications, *in* Faulds, J.E., and Stewart, J.H., eds., Accommodation Zones and Transfer Zones: The Regional Segmentation of the Basin and Range Province: Geological Society of America Special Paper 323, p. 47-75.

Smith, J.F., and Ketner, K.B., 1977, Tectonic events since early Paleozoic in the Carlin-Pinon Range area, Nevada: U.S. Geological Survey Professional Paper 867-C, 18 p.

Sadlick, W., 1960, Some preliminary aspects of Chainman stratigraphy, *in* Boettcher, J.W., and Sloan, W.W., Jr., eds., Geology of east central Nevada: Intermountain Association of Petroleum Geologists Guidebook, 11th annual Field Conference, p. 81-90.

Saltus, R.W., 1988, Bouguer gravity anomaly map of Nevada: Nevada Bureau of Mines and Geology Map 94A.

Schneyer, J.D., 1984, Tertiary age extension of Leppy Hills area (southwest Silver Island Mountains) near Wendover, Nevada: American Association of Petroleum Geologists Bulletin, v. 68, p. 948.

Silberling, N.J., and Nichols, K.M., 1994, Geometry of Tertiary low-angle detachment faulting controlled by earlier contractional structures, Goshute Range, Nevada: Geological Society of America Abstracts with Programs, v. 26, p. 92.

Silberling, N.J., and Nichols, K.M., 2000, Significance and context of attenuation faults in the Mesozoic structural history of the northeastern Great Basin of Nevada and Utah: Geological Society of America Abstracts with Programs, v. 32, p. 170.

Silberling, N.J., and Nichols, K.M., 2002, Geologic map of the White Horse Pass area,

Elko County, Nevada: Nevada Bureau of Mines and Geology Report 132, 8 p.

Smith, W.S.T., 1925, An apparent-dip protractor: Economic Geology and the Bulletin of the Society of Economic Geologists, v. 52, p. 181-184.

Snyder, D.B., Healy, D.L., and Saltus, R.W., 1984, Bouger gravity map of Nevada, Lund Sheet: Nevada Bureau of Mines and Geology, Map 80.

Sonder, L.J., and Jones, C.H., 1999, Western United States extension; how the west was widened: Annual Review of Earth and Planetary Sciences, v. 27, p. 417-462.

Speed, R.C., 1979, Collided Paleozoic microplate in the western United States: Journal of Geology, v. 87, p. 279-292.

Speed, R.C., Elison, M.W., and Heck, F.R., 1988, Phanerozoic tectonic evolution of the Great Basin: *in* Ernst, W.G., ed., Metamorphism and crustal evolution, western United States: Rubey Volume VII, p. 572-605.

Speed, R.C., and Sleep, N.H., 1982, Antler orogeny and foreland basin: A model: Geological Society of America Bulletin, v. 93, p. 815-828.

Spencer, J.E., 1917, Geology and ore deposits of Ely, Nevada: U.S. Geological Professional Paper 96, 189 p.

Spencer, J.E., 1984, Role of tectonic denudation in warping and uplift of low-angle normal faults: Geology, v. 12, p. 95-98.

Taylor, W.J., Bartley, J.M., Lux, D.R., and Axen, G.J., 1989, Timing of Tertiary extension in the Railroad Valley-Pioche transect, Nevada: constraints from $^{40}Ar/^{39}Ar$ ages of volcanic rocks: Journal of Geophysical Research, v. 94, p. 7757-7774.

Taylor, W.J., Bartley, J.M., Fryxell, J.E., Schmitt, J.G., and Vandervoot, D.S., 1993, Tectonic style and regional relations of the central Nevada thrust belt, *in* Lahren, M.M., Trexler, Jr., J.H., and Spinosa, C., eds., Crustal Evolution of the Great Basin and Sierra Nevada: Cordilleran/Rocky Mountain Section, Geological Society of America Guidebook, Department of Geological Sciences, University of Nevada, Reno, p. 57-96.

Taylor, W.J., Johnson, J.A., and Walker, J.D., 1996, Kinematics and mechanics along a low-angle normal fault, the Silver Spring detachment, central Nevada, *in* Taylor, W.J., and Langrock, H., eds., Cenozoic Structure and Stratigraphy of Central Nevada: Nevada Petroleum Society Field Trip Guidebook, p. 101-109.

Taylor, W.J., Bartley, J.M., Martin, M.W., Geissman, J.W., Walker, J.D., Armstrong, P.A., and Fryxell, J.E., 2000, Relations between hinterland and foreland

shortening, Sevier orogeny, central North American Cordillera: Tectonics, v. 19, p. 1124-1143.

Taylor, W.J., and Novak, H.L., accepted, Three-dimensional strain above low-angle normal faults: a kinematic model and example from Nevada, USA: Journal of Structural Geology.

Taylor, W.J., and Switzer, D.D., 2001, Temporal changes in fault strike (to 90°) and extension directions during multiple episodes of extension: an example from eastern Nevada: Geological Society of America Bulletin, v. 113, p. 743-759.

Taylor, W.J., Gilbert, J., Fryxell, J.E., Williams, N.D., and Novak, H., in press, Discussion on the role of attenuation in the formation of the Railroad Valley structural basin, east-central Nevada: Detachment control of petroleum reservoirs: American Association of Petroleum Geologists Bulletin.

Trexler, J. H., Jr., Cashman, P. H., Cole, J. C., Snyder, W. S., Tosdal, R. M., and Davydov, V. I., 2003, Widespread Effects of Mid-Mississippian Deformation in the Great Basin of western North America: Geological Society of America Bulletin, v. 115, p. 1278-1288.

Walker, C.T., Francis, R.D., Dennis, J.G., and Lumsden, W.W., 1992, Cenozoic attenuation detachment faulting: A possible control on oil and gas accumulation in east-central Nevada: American Association of Petroleum Geologists Bulletin, v. 76, p. 1665-1686.

Walker, C.T., and Francis, R.D., 2002, Tectonic styles associated with extension and attenuation in the Grant, Schell Creek and White Pine Ranges, in Ehni, W., and Faulds, J., eds., Detachment and Attenuation *in* Eastern Nevada and its Application to Petroleum Exploration: Nevada Petroleum Society Fieldtrip Guidebook, p. 97-114.

Wernicke, B.P., and Axen, G.J., 1988, On the role of isostasy in the evolution of normal fault systems: Geology, v. 16, p. 848-851.

Wernicke B., 1992. Cenozoic extensional tectonics of the U.S. Cordillera, *in* Burchfiel, B.C., Lipman, P.W., and Zoback M.L., eds., The Cordilleran Orogen: Conterminous U.S.: Boulder, Colorado, Geological Society of America, The Geology of North America v. G-3, p. 553-81.

White, N., 1992, A method for automatically determining normal fault geometry at depth: Journal of Geophysical Research, v. 97, p. 1715-1733.

Williams, N.D., 2000, A transverse fault in an extended terrane, the Currant Summit fault, Nevada [M.S. thesis]: University of Nevada, Las Vegas, 104 p.

Williams, N.D., and Taylor, W.J., 2002, Extensional oblique-slip barrier transfer fault: the Currant Summit fault, east-central Nevada *in* Ehni, W., and Faulds, J., eds., Detachment and Attenuation in Eastern Nevada and its Application to Petroleum Exploration: Nevada Petroleum Society Field Trip Guidebook, p. 149-163.

Woodward, L.A., 1964, Structural geology of the central northern Egan Range, Nevada: Bulletin of the American Association of Petroleum Geologists, v. 48, p. 22-39.

Wyld, S.J., Rogers, J.W., and Wright, J.E., 2001, Structural evolution within the Luning-Fencemaker fold-thrust belt, Nevada: progression from back-arc basin closure to intra-arc shortening: Journal of Structural Geology, v. 23, p. 1971-1995.

Wyld, S.J., Rogers, J.W., and Copeland, P., 2003, Metamorphic evolution of the Luning-Fencemaker fold-thrust belt, Nevada: illite crystallinity, metamorphic petrology, and $^{40}Ar/^{39}Ar$ geochronology: Journal of Geology, v. 111, p. 17-38.

Zoback, M.L., 1989, State of stress and modern deformation of the northern Basin and Range Province: Journal of Geophysical Research, v. 94, p. 7105-7128.

VITA

Graduate College
University of Nevada, Las Vegas

Tyler R. Knudsen

Local Address:
1290 West Horizon Ridge PKWY #822
Henderson, Nevada 89012

Home Address:
4398 North Droubay Road
Erda, Utah 84074

Degree:
Bachelor of Science, Geology, 2002
University of Utah, Salt Lake City, Utah

Special Honors and Awards:
University of Nevada, Las Vegas Geoscience Department scholarship, 2003, 2004
University of Nevada, Las Vegas Graduate Student Association Grant, 2003
American Association of Petroleum Geologists Grants-in-Aid recipient, 2003
Cooper-Hansen Foundation Scholarship recipient, 2002

Thesis Title:
The Silver Spring and Blackrock faults, east-central Nevada: kinematics, timing, and role of low-angle normal faulting in the development of Railroad Valley

Thesis Examination Committee:
Chairperson, Dr. W.J. Taylor, Ph.D.
Committee Member, Dr. M.L Wells, Ph.D.
Committee Member, Dr. A.D. Hanson, Ph.D.
Graduate Faculty Representative, Dr. K.A. Robins, Ph.D.